

State of Global Water Resources 2023 Report

WEATHER CLIMATE WATER



WORLD
METEOROLOGICAL
ORGANIZATION

WMO-No. 1362



Give us your feedback!

<https://forms.office.com/e/P2kn2nDKwX>



Interactive version of the report

<https://storymaps.arcgis.com/stories/c56d4a08c1ce4b05b900d3f5852a52af>

WMO-No. 1362

© World Meteorological Organization, 2024

The right of publication in print, electronic and any other form and in any language is reserved by WMO. Short extracts from WMO publications may be reproduced without authorization, provided that the complete source is clearly indicated. Editorial correspondence and requests to publish, reproduce or translate this publication in part or in whole should be addressed to:

Chair, Publications Board
World Meteorological Organization (WMO)
7 bis, avenue de la Paix
P.O. Box 2300
CH-1211 Geneva 2, Switzerland

Tel.: +41 (0) 22 730 84 03
Email: publications@wmo.int

ISBN 978-92-63-11362-7

Cover illustration from WMO 2020 Calendar Competition: "Reality is an illusion" by Rajit Banerjee, Pangong Lake, Ladakh, India.

NOTE

The designations employed in WMO publications and the presentation of material in this publication do not imply the expression of any opinion whatsoever on the part of WMO concerning the legal status of any country, territory, city or area, or of its authorities, or concerning the delimitation of its frontiers or boundaries.

The mention of specific companies or products does not imply that they are endorsed or recommended by WMO in preference to others of a similar nature which are not mentioned or advertised.

The findings, interpretations and conclusions expressed in WMO publications with named authors are those of the authors alone and do not necessarily reflect those of WMO or its Members.

Contents

Acknowledgements	ii
List of abbreviations	v
Executive summary	vi
Foreword	ix
Introduction.	1
The backdrop: overview of climatic conditions in 2023	3
Data sources	4
Anomaly calculation	5
River discharge	6
Reservoirs.	10
Inflow into selected reservoirs	10
Reservoir storage.	11
Lakes	12
Groundwater levels	13
Soil moisture	16
Observed soil moisture from the International Soil Moisture Network	16
Modelled soil moisture.	17
Evapotranspiration.	19
Terrestrial water storage	21
Case study on the water storage situation in Central Europe during 2023	22
Snow cover and glaciers.	24
Snow water equivalent.	24
Peak snow mass in North American basins	25
Glaciers	25
Glacier contribution to seasonal river runoff.	25
The year 2023 in context.	27
High-impact hydrological events	30
Flooding in Libya	30
Flooding in Democratic Republic of the Congo and Rwanda	30
Flooding in the Horn of Africa	30
Flooding in Mozambique and Malawi.	30
Drought in Central America and the southern United States	32
Drought in Argentina, Uruguay and Brazil	32
Drought in Peru	32
Flooding on the North Island of New Zealand	33
Flooding in China and the Philippines.	33
Flooding in Italy	33
Synthesis	34
Endnotes	38
Annex. Technical annex	45

Acknowledgements

WMO is grateful to the following contributors.

WMO MEMBER STATES AND TERRITORIES THROUGH HYDROLOGICAL ADVISORS AND ASSIGNED FOCAL POINTS FOR THE STATE OF THE GLOBAL WATER RESOURCES REPORT

Argentina; Armenia; Australia; Azerbaijan; Belgium; Belize; Benin; Bhutan; Botswana; Brazil; Bulgaria; Canada; China; Costa Rica; Croatia; Cyprus; Czechia; Denmark; Egypt; El Salvador; Finland; France; Germany; Ghana; Guatemala; Honduras; Hong Kong, China; Hungary; Iceland; India; Iraq; Israel; Japan; Kazakhstan; Kenya; Republic of Korea; Latvia; Lesotho; Malawi; Mauritius; Republic of Moldova; Montenegro; Myanmar; Nepal; New Zealand; Nigeria; Norway; Pakistan; Panama; Paraguay; Peru; Philippines; Poland; Russian Federation; Serbia; Singapore; Slovakia; Slovenia; South Africa; Sri Lanka; Sweden; Switzerland; United Republic of Tanzania; Thailand; Turkmenistan; United Kingdom of Great Britain and Northern Ireland; Uruguay; Uzbekistan; Viet Nam.

Hydrological Advisors and focal points contributed to and supported the preparation of the present report by providing observational data, information about major hydrological events that occurred in 2023 and other relevant information, and participated in the review and validation of the report.

STEERING COMMITTEE MEMBERS

Jan Danhelka (Czechia, Vice-President of INFCOM); Harry Dixon (United Kingdom); Katie Facer-Childs (United Kingdom, HydroSOS Technical Team Lead); Mohamed Housseini Ibrahim (Niger, Chair of Hydrological Coordination Panel); Michel Jean (Canada, President INFCOM); Harry Lins (United States of America); Ian Lisk (United Kingdom, President SERCOM); Ilias Pechlivanidis (Sweden, Research Board); Marcelo Uriburu Quirno (Argentina, Vice-Chair of the Standing Committee on Hydrological Services); Yuri Simonov (Russian Federation, Chair of the Standing Committee on Hydrological Services); Narendra Tuteja (Australia, Chair of the Expert Team on Operational Hydrological Prediction Systems); Andy Wood (United States, Expert Team on Operational Hydrological Prediction Systems).

REGIONAL HYDROLOGICAL ADVISORS

Angela Corina (Regional Association VI), John Fenwick (Regional Association V), Mohamed Housseini Ibrahim, Sung Kim (Regional Association II), Jean-Claude Ntonga (Regional Association I), Fabio Andres Bernal Quiroga (Regional Association III), and Jose Zuniga (Regional Association IV), who contributed to the preparation and review of the report.

WMO EXPERTS

Experts from the Standing Committee Climate, Standing Committee on Hydrological Services, Standing Committee on Services for Agriculture, Study Group on Renewable Energy Transition, and former Joint Expert Team on Hydrological Monitoring, who participated in the preparation and review of the report.



MEMBERS OF THE GLOBAL HYDROLOGICAL MODELLING COMMUNITY

Jafet Andersson (Swedish Meteorological and Hydrological Institute (SMHI)), Berit Arheimer (SMHI), Hasnain Aslam (University of Tokyo), Nishan Kumar Biswas (NASA), Martyn P. Clark (University of Saskatchewan), Chris DeBeer (University of Saskatchewan), Mohamed Elshamy (Environment and Climate Change Canada (ECCC), Global Institute for Water Security (GIWS) (University of Saskatchewan)), Xing Fang (University of Saskatchewan), Angelica Gutierrez (National Oceanic and Atmospheric Administration (NOAA)), Riley Hales (Brigham Young University (BYU)), Shaun Harrigan (European Centre for Medium-range Weather Forecasts (ECMWF)), Kristina Isberg (SMHI), Rohini Kumar (Helmholtz Centre for Environmental Research – UFZ), Sujay Kumar (National Aeronautics and Space Administration (NASA)), Henrik Madsen (DHI), Christopher Marsh (University of Saskatchewan), Jim Nelson (BYU), Wanshu Nie (NASA), Emmanuel Nyenah (Goethe University Frankfurt), John Pomeroy (University of Saskatchewan), Daniel Princz (ECCC, GIWS (University of Saskatchewan)), Oldrich Rakovec (Helmholtz Centre for Environmental Research – UFZ), Robert Reinecke (Johannes Gutenberg University Mainz), Jörgen Rosberg (SMHI), Luis Samaniego (Helmholtz Centre for Environmental Research – UFZ), Hannes Müller Schmied (Goethe University Frankfurt, Senckenberg Leibniz Biodiversity and Climate Research Centre (SBIK-F), Frankfurt), Tricia Stadnyk (University of Calgary), Edwin H. Sutanudjaja (Utrecht University), Niko Wanders (Utrecht University), Albrecht Weerts (Deltares), Kosuke Yamamoto (Japan Aerospace Exploration Agency), Kei Yoshimura (University of Tokyo), and Xing Yuan (Institute of Atmospheric Physics, Chinese Academy of Sciences), who contributed to the initial discussions, report preparation, global modelling and remotely sensed data, feedback and review.

GLOBAL DATA CENTRES AND EXTERNAL EXPERTS

Elie Gerges (International Groundwater Resources Assessment Centre (IGRAC), Elisabeth Lictevout (IGRAC), Simon Mischel (Global Runoff Data Centre (GRDC)), Arnaud Sterckx (IGRAC) and Matthias Zink (International Soil Moisture Network (ISMN)), who supported the preparation of the report. We thank Jan Polcher (École Polytechnique, France) for contributing to the preparatory workshop for this report.

We also thank the research groups of Stefan Kollet (Forschungszentrums, Juelich, Germany) and Nico Sneeuw (University of Stuttgart, Germany) for contributing a case study for the hydrological situation in Central Europe in 2023 and data sets for the extension of in situ river discharge data through satellite observations, respectively. We are grateful to Jiawei Hou (Australian Bureau of Meteorology) for providing lake storage data from the Global Water Monitor.

CONTRIBUTORS AND CO-AUTHORS FOR SPECIFIC CHAPTERS

Groundwater Levels: Elie Gerges (IGRAC), Elisabeth Lictevout (IGRAC), Arnaud Sterckx (IGRAC), who supported the preparation of the report and developed the methodology.

Soil Moisture: Matthias Zink (ISMN), who contributed to the soil moisture chapter with in situ data and supported the drafting of the related section.

Terrestrial Water Storage: Andreas Güntner and Eva Boergens (German Research Centre for Geosciences (GFZ), who provided the terrestrial water storage data which form an important part of the present report.

Snow Cover and Glaciers: Inés Dussaillant (World Glacier Monitoring Service (WGMS), University of Zurich, Switzerland), Lawrence Mudryk (ECCC) and Michael Zemp (WGMS, University of Zurich, Switzerland), who provided results on glacier mass changes. The following experts, who contributed



data and images for case studies shown the chapter: Iulii Didovets (Potsdam Institute for Climate Impact Research, Green Central Asia programme); Abror Gafurov (GFZ); Nikolay Kassatkin (Central Asian Regional Glaciological Centre under the auspices of the United Nations Educational, Scientific and Cultural Organization (UNESCO)); Kabutov Khusrav (Center for Glacier Research of the National Academy of Sciences of Tajikistan); Gulomjon Umirzakov (National University of Uzbekistan); and Ryskul Usabaliev (Central-Asian Institute for Applied Geosciences).

WMO SECRETARIAT LEAD AUTHORS

Sulagna Mishra (Scientific Officer) and Stefan Uhlenbrook (Director, Hydrology, Water and Cryosphere), who were also supported by hydrology colleagues within the Secretariat in producing and reviewing the report.

INDEPENDENT CONSULTANTS

Anastasia Lobanova and Iulii Didovets, who carried out the scientific analysis of the raw data to produce the results for the chapters on River Discharge, Soil Moisture, Evapotranspiration, Reservoirs, Lakes, Snow Cover and Glaciers and High-impact Hydrological Events. They contributed significantly to writing of the report with support from the authors mentioned above. Nilay Dogulu, who reviewed the report and designed the infographics and interactive Web version of the report (ArcGIS StoryMap) that can be found [here](#).



List of abbreviations

AET	actual evapotranspiration
DJF	December–January–February
EW4All	Early Warnings for All initiative
GDP	gross domestic product
GHMS	global hydrological modelling system
GRACE	Gravity Recovery and Climate Experiment
GRanD	Global Reservoir and Dam
GRDC	Global Runoff Data Centre
HydroSOS	Global Hydrological Status and Outlook System
IGRAC	International Groundwater Resources Assessment Centre
IOD	Indian Ocean Dipole
ISMN	International Soil Moisture Network
JJA	June–July–August
MAM	March–April–May
NMHS	National Meteorological and Hydrological Service
SDG	Sustainable Development Goal
SON	September–October–November
SWE	snow water equivalent
TWS	terrestrial water storage
WHOS	WMO Hydrological Observing System

Executive summary

HYDROLOGICAL CONDITIONS AND SIGNIFICANT EVENTS OF 2023

- **Large-scale processes and WMO *State of the Global Climate 2023* (WMO No. 1347):** The year 2023 was marked by unprecedented heat, becoming the hottest year on record at 1.45 °C above pre-industrial levels. The transition from La Niña to El Niño conditions, as well as the positive phase of the Indian Ocean Dipole (IOD) contributed to this extreme heat and diverse weather impacts ranging from heavy rains and floods to droughts.
- **River discharge:** Compared to the historical period, 2023 was marked by mostly drier-than-normal to normal river discharge conditions. Similar to 2022 and 2021, over 50% of global catchment areas showed river discharge deviations from near-normal conditions, predominantly lower than normal, with fewer basins exhibiting above- and much-above-normal conditions.
- **River discharge:** Large territories of North, Central and South America suffered severe drought and reduced river discharge conditions in 2023. The Mississippi and Amazon basins saw record-low water levels. The east coast of Africa experienced above- and much-above-normal discharge. The Horn of Africa, which had suffered five consecutive dry rainy seasons, was affected by flooding. In Asia and Oceania, large river basins – the Ganges, Brahmaputra and Mekong – experienced lower-than-normal conditions over almost their entire basin territories. The North Island of New Zealand and the Philippines exhibited much-above-normal annual discharge conditions. In northern Europe, the entire territory of the United Kingdom and Ireland saw above-normal discharge, as did Finland and southern Sweden.
- **Reservoirs:** The inflows into reservoirs showed a pattern similar to that of global river discharge, with India, North, Central and South America, and parts of Australia experiencing below-normal inflow conditions. The basin-wide reservoir storage varied significantly, reflecting the influence of water management, with much-above-normal levels in basins like the Amazon and Paraná, where river discharge was much below normal in 2023.
- **Lakes:** Lake Coari in the Amazon faced below-normal water levels, leading to extreme water temperatures, and Lake Turkana, shared between Kenya and Ethiopia, had above-normal volumes, following much-above-normal river discharge conditions.
- **Groundwater levels:** In South Africa the majority of wells showed above-normal groundwater levels, following above-average precipitation in recent years; the same was true in India, Ireland, Australia and Israel. Notable depletion in groundwater availability was observed in North America and Europe due to prolonged drought. In Chile and Jordan groundwater levels were also below normal, with the long-term declines due to over-abstraction rather than climatic factors.
- **Soil moisture:** Levels of soil moisture were predominantly below normal or much below normal across large territories globally, with North America, South America, North Africa and the Middle East particularly dry during June–August. In contrast, certain regions, including Alaska, north-eastern Canada, India and parts of the Russian Federation, experienced much-above-normal soil moisture levels. The northern and south-eastern coasts of Australia, along with New Zealand’s North Island, also had above-normal soil moisture due to wetter conditions and flooding.

- **Evapotranspiration:** Central and South America, especially Brazil and Argentina, faced much-below-normal actual evapotranspiration (AET) in September–October–November. Mexico also experienced below-normal AET throughout almost all of 2023, reflecting severe drought conditions.
- **Snow water equivalent:** Most catchments in the northern hemisphere (except those in the northern United States and the Lena catchment far the eastern Russian Federation) had below- to much-below-normal snow water equivalent (SWE) in March, indicating lower-than-normal snow availability and below-normal spring flood potential. Seasonal peak snow mass for 2023 was much above normal in North America and much below normal in Eurasia.
- **Glaciers:** In 2023, glaciers lost more than 600 gigatons (Gt) of water, the largest mass loss registered in the last five decades. Following 2022, 2023 is the second consecutive year in which all glaciated regions in the world reported ice loss. Observed summer mass loss over recent years indicates that glaciers in Europe, Scandinavia, the Caucasus, north-western Canada, western South Asia and New Zealand have passed “peak water” (the threshold of maximum runoff due to melting), while the southern Andes (dominated by the Patagonian region), Russian Arctic and Svalbard seem to still present increasing melt rates.
- **Terrestrial water storage:** Large parts of the continents experienced below-average terrestrial water storage (TWS) conditions in 2023. Notable exceptions were sub-Saharan Africa, the Tibetan Plateau and subregions of India, Australia and northern South America.
- **High-impact hydrological events:** Africa was the most impacted by extreme hydrological events in terms of human lives lost: In Libya where two dams collapsed due to flooding, over 11 000 lives were lost and the event affected 22% of the population. The floods also affected the Horn of Africa, the Democratic Republic of the Congo, Rwanda, Mozambique and Malawi, leading to additional toll of over 1 600 deaths. The southern United States, Central America, Argentina, Uruguay, Peru and Brazil were affected by widespread drought conditions, which led to a 3% loss in gross domestic product (GDP) in Argentina and the lowest levels ever observed in the Amazon River and Lake Titicaca.

KEY IMPROVEMENTS IN THE 2023 REPORT

- **Expanded scope:** The 2023 report includes new chapters and three new hydrological variables (lake volumes, reservoir volumes, snow water equivalent), as well as an extended chapter on glaciers; thus, it provides a more comprehensive view of the global water cycle.
- **Observed data:** The number of river discharge measurement stations increased from 273 in 14 countries to 713 in 33 countries, and the groundwater data collection expanded to 35 459 wells in 40 countries, compared to 8 246 wells in 10 countries in the previous year (Figure 1). However, despite improvements in observational data, Africa, South America and Asia remain underrepresented in hydrological data collection, highlighting the need for improved monitoring and data sharing, particularly in the Global South.
- **Modelled data:** Ten global hydrological modelling systems (GHMSs) (see Table A3 in the Annex) provided substantial input that strengthened the analysis of variables, especially river discharge, evapotranspiration, soil moisture, snow and ice cover, and terrestrial water storage.

- **Model validation:** Modelled river discharge values showed agreement with observed data in over 73% of validated basins, especially in Central and Northern Europe, New Zealand, Australia and selected river basins in India, Myanmar and South America. Still, discrepancies between modelled and observed anomalies were not eliminated. Increased observed data availability is important for validation to properly assess model reliability in different regions around the globe. Intermodel comparison showed agreement in 97% of basins.

REPORT IMPLICATIONS AND FUTURE OUTLOOK

By incorporating new elements, guided by observational data that is improved both in quality and quantity compared to previous editions and modelling outcomes from multiple sources, this report delivers a detailed overview of the state of global water resources for the year 2023. Additional objectives for future editions of the report are to enhance the accessibility and availability of observational data (through both better monitoring and improved data sharing), further integrate relevant variables into the report, and encourage country participation to better understand and report water cycle dynamics. Future reports are anticipated to include even more observational data, supported by initiatives like WMO's Global Hydrological Status and Outlook System (HydroSOS), the WMO Hydrological Observing System (WHOS), and collaboration with global data centres such as the Global Runoff Data Centre (GRDC), International Soil Moisture Network (ISMN), International Groundwater Resources Assessment Centre (IGRAC), GEMS/Water Data Centre and the International Data Centre on Hydrology of Lakes and Reservoirs (HYDROLARE).

Foreword



The release of WMO's State of Global Water Resources Report for 2023 builds on the success of the last two reports in this new annual series, which was introduced in response to global calls for an independent and consistent assessment of water resources to inform policy discussions. The reports have garnered significant attention and endorsement from WMO Member States and Territories, the international community, partners and the media. They provide a clear overview of the status of water resources in major basins, comparing current data to long-term averages across various variables that represent the water cycle (also known as the *hydrological cycle*).

The 2023 edition of the report further expands on its predecessors by including additional variables such as in situ soil moisture data and reservoir storage, an overview of cryosphere components

along with a review of major hydrological disasters that occurred globally in 2023. The report also saw an exponential increase in contributions from WMO Members (through Hydrological Advisors and assigned focal points) in terms of both in situ data and modelled data. The report's preparation also relied heavily on global hydrological and land surface modelling systems, as well as remotely sensed data, ensuring broader global coverage and addressing data gaps. Although data sharing and engagement have increased, achieving a globally uniform report based solely on hydrological observations remains a challenge, necessitating further investments in monitoring and data sharing in line with the [WMO Unified Data Policy](#), and promoted by the WMO Hydrological Observing System (WHOS). The report also highlights the potential of Earth-system-based observations for infilling gaps in observational time series, which can be of great benefit to WMO Members. In the future, WMO is committed to including additional variables such as water quality in the annual reports as well as exploring local trends via regional reports.

Future reports will directly benefit from WMO's Global Hydrological Status and Outlook System (HydroSOS) as it becomes fully operational. The 2023 report illustrates the practical value of an annual synthesis of global water resources, providing essential insights for large-scale decision-making and policy development. It also supports and forms a solid backbone to facilitate the United Nations Secretary-General's vision of a comprehensive early warning system (the Early Warnings for All (EW4All) initiative) and contributes to the achievement of the Sustainable Development Goals (SDGs) related to water and climate. Appreciation is extended to the steering committee, lead authors, and all contributors, including WMO Member National Meteorological and Hydrological Services, global data centres and supporting organizations.

A handwritten signature in black ink, appearing to be 'C. Saulo'.

(Prof. Celeste Saulo)
Secretary-General

Introduction

The State of Global Water Resources report series offers a comprehensive and consistent overview of water resources worldwide, portraying the state of hydrological variables over the course of a year. The report offers a systematic and standardized analysis of water resources at a global scale, which responds to the main outcomes of the UN 2023 Water Conference, which called for an “Operational Global Water Information System to support water, climate and land management for socioeconomic resilience, ecological sustainability and social inclusion by 2030”.¹

The preparation of the 2023 report was made possible through continuous involvement from WMO Members, represented by National Meteorological and Hydrological Services (NMHSs), as well as other organizations, including data centres, the global hydrological modelling community and the Earth observation community. The 2023 report offers advances in methodology and data sources: new chapters and variables have been added, including variables covering lake level, reservoir volumes and snow water equivalent, to present an even more comprehensive overview of the year 2023 water condition globally.

The number of observed data points received from WMO Members, the Global Runoff Data Centre (GRDC) and other partners for river discharge measurements increased significantly, rising from 273 stations in 14 countries in 2022 to 713 stations in 33 countries in 2023. Similarly, for groundwater, data for 35 459 wells from 40 countries were collected in 2023, compared to 8 246 wells in 10 countries in 2022 (Figure 1). The [Soil moisture](#) chapter now includes observed data provided by Members of the International Soil Moisture Network (ISMN), which were used to validate modelled results.

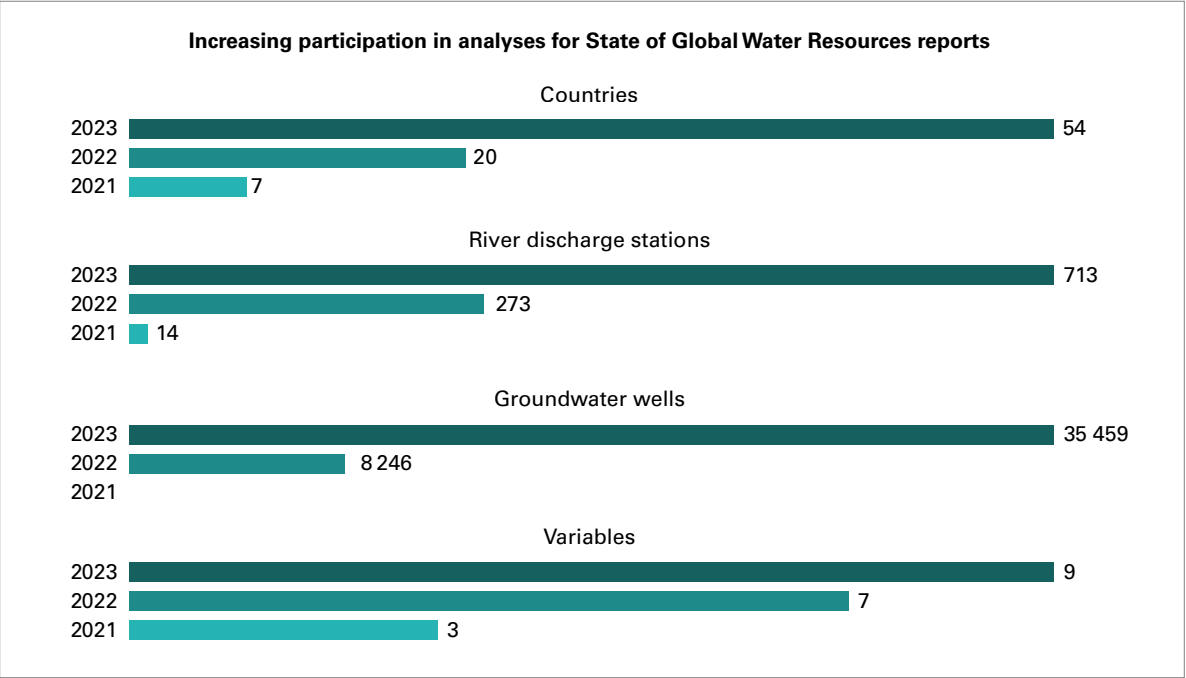


Figure 1. Increase in the number of countries, stations with observed river discharge data (both quality-controlled and not), groundwater wells and variables available for reporting in the years 2021, 2022 and 2023



The global hydrological modelling and Earth observation communities have made substantial contributions to the chapters on evapotranspiration, soil moisture, snow and ice cover, terrestrial water storage, lake levels and reservoir volumes. In total, 16 different modelling and Earth observation-based data products were used for the 2023 report. These contributions have strengthened the analyses, particularly in ungauged or data-sparse regions, and have extended the number of products used, thereby helping to reduce uncertainty in the findings.

The 2023 edition includes chapters on [River discharge](#), [Reservoirs](#), [Lakes](#), [Groundwater levels](#), [Soil moisture](#), [Evapotranspiration](#), [Terrestrial water storage](#) and [Snow cover and glaciers](#), each offering global and/or regional insights. [Snow cover and glaciers](#) focuses on snow water equivalent and the state of major glaciers worldwide. The [High-impact hydrological events](#) chapter provides a global overview of significant hydrological events from 2023, while the final [Synthesis](#) presents the major findings on the overall state of global water resources for the year 2023.

The information presented in the report serves as a valuable resource for policymakers and decision makers, as well as water and disaster risk reduction professionals, contributing to a better understanding of global freshwater status and trends. In future editions, the report will also provide a historical perspective on the state of global water resources, adding to the understanding of regional and global trends.

The present report directly supports the United Nations 2030 Agenda (Sustainable Development Goals (SDGs)), especially SDG 6: Clean Water and Sanitation, as well as other water-related SDGs by providing critical data for sustainable water resources management, addressing water scarcity, overabundance and water quality issues. The report also supports SDG 13: Climate Action, informing strategies to align water resources management with climate change mitigation, by improving understanding of climate-related impacts on water (hydrological) systems. Furthermore, the report's focus on observed and modelled datasets stresses the importance of open data sharing, reinforcing SDG 17: Partnership for the Goals, by building global partnerships and enhancing cooperation across national, regional and global scales.

Improving data sharing and engagement from WMO Members in future editions of the State of Global Water Resources report will advance our understanding of the implications of hydrological processes for water resources, benefiting policymakers and decision makers, water resource managers, water users and the general public, and providing better validation of modelling results for river basins around the globe. These reports are helping to create an extensive global dataset of hydrological variables, which includes observed and modelled data from a wide array of sources. Thus, this work enhances global data sharing efforts, aligning with the focus of the global Early Warnings for All ([EW4All](#)) initiative on improving data quality and access for water-related hazard monitoring and forecasting, and providing early warning systems for all by 2027. It also aligns with WMO's Global Hydrological Status and Outlook System ([HydroSOS](#)) which provides a framework for producing standardized status and outlook indicators to explain the current status and seasonal and sub-seasonal forecasts of hydrological conditions.



THE BACKDROP: OVERVIEW OF CLIMATIC CONDITIONS IN 2023

The year 2023 was characterized by record-breaking temperatures, making it the hottest year on record, with the global mean temperature reaching 1.45 °C ($\pm 0.12\text{ °C}$) above pre-industrial levels.² Concentrations of the primary greenhouse gases – carbon dioxide (CO_2), methane and nitrous oxide – continued to rise throughout 2023, with CO_2 concentrations reaching 419.3 parts per million by the end of the year.³ Also, the decadal average temperature (2014–2023) was $1.20 \pm 0.12\text{ °C}$ above the pre-industrial average, marking this period as the warmest decade on record, with unprecedented monthly temperatures for both oceans and the atmosphere.⁴

Fueled by heat, the year 2023 saw unprecedented extreme events in many parts of the world.⁵ Heatwaves hit Europe, North America and China, while Canada faced its most extreme wildfire season ever recorded, with over 14.9 million hectares destroyed by fire.⁶ In Libya, intense rainfall led to the collapse of three dams, with over 4 700 people losing their lives and 8 000 people considered missing. Climate change likely contributed to increasing the event's rainfall intensity by up to 50%, as well as to increasing the probability of the event.⁷

Following three consecutive years of La Niña that concluded in early 2023, El Niño conditions started to emerge in the tropical Pacific Ocean during the boreal summer. However, the atmospheric response lagged, and it was not until early September that El Niño conditions were fully established in both the ocean and the atmosphere.⁸ This shift to El Niño resulted in varied weather impacts, including heavy rains, floods, droughts and heatwaves. The Indian Ocean Dipole (IOD) showed its first positive phase since 2019, peaking in October, which exacerbated dry and warm conditions in Australia and caused significant flooding in the Horn of Africa. The North Atlantic Oscillation (NAO) experienced an unusual negative phase in June and July, contributing to snow and ice melt in southern Greenland, as well as record-high temperatures across eastern Canada and Europe (Ireland, Belgium and Italy, among others).

As shown in Figure 23 of *State of the Global Climate 2023* (WMO-No. 1347), in 2023, total precipitation exceeded the normal level in several regions, with hotspots in Asia and various parts of Africa, Europe and North America. Significant rainfall deficits were observed in Central and South America, Canada, the Mediterranean region, North Africa and others.

Preliminary data for September 2022–August 2023 show a significant loss in glacier mass that would be the highest on record (1950–2023), with an average balance of -1.2 m of water equivalent. This severe loss is mainly due to extreme melting in western North America and the European Alps, where Switzerland's glaciers have lost about 10% of their remaining volume over the past two years. Snow cover in the northern hemisphere has been decreasing in late spring and summer: in May 2023, the snow cover extent was the eighth lowest on record (1967–2023). For North America the May snow cover was the lowest in the same period.



DATA SOURCES

The data used in the report were gathered from various sources (refer to Box 1 and [Data sources](#) in the Annex), including NMHSs, the Earth observation community (which provided satellite-based observations) and the global modelling community, ensuring a robust, spatially consistent and comprehensive analysis. The [River discharge](#) and [Soil moisture](#) chapters are based on modelled and observed data. Where possible, in situ data were used to validate the modelled results. Global hydrological modelling systems (GHMSs) contributed to obtaining values for additional hydrological variables, in particular soil moisture, reservoir inflows, actual evapotranspiration and terrestrial water storage. The [Groundwater levels](#) chapter is based solely on observed data.

Box 1

DATA SOURCES 2023⁹

- *Observed river discharge data:* National Meteorological and Hydrological Services (NMHSs), the Global Runoff Database Centre (GRDC),¹⁰ enhanced streamflow observations using Earth-system-based products.¹¹
- *Simulated river discharge data:* Ten global hydrological modelling systems (GHMSs).
- *Inflow into selected reservoirs globally:* Three GHMSs.
- *Reservoir volume anomalies:* United States National Aeronautics and Space Administration (NASA).¹²
- *Lake volumes:* Global Water Monitor.^{13,14}
- *Groundwater data:* International Groundwater Resources Assessment Centre (IGRAC) for 40 selected countries.
- *Soil moisture:* Three GHMSs.
- *Observed soil moisture:* Observed data from the International Soil Moisture Network (ISMN).
- *Evapotranspiration:* Five GHMSs.
- *Terrestrial water storage (TWS):* Gravity Recovery and Climate Experiment and the follow-on satellites (GRACE/GRACE-FO),¹⁵ two GHMSs, ParFlow/CLM model for Central Europe.¹⁶
- *Glaciers:* WMO Member States and Territories, World Glacier Monitoring Service (WGMS), Central-Asian Institute for Applied Geosciences (CAIAG), German Research Centre for Geosciences (GFZ), National University of Uzbekistan, Center for Glacier Research of the National Academy of Sciences of Tajikistan and external experts.
- *Snow water equivalent:* Environment and Climate Change Canada (ECCC).^{17,18}
- *High-impact events:* Contributions of WMO Members to WMO State of the Global Climate Report, open data sources such as the EM-DAT database,¹⁹ ReliefWeb and others.



ANOMALY CALCULATION

For each of the variables presented in the chapters, the anomaly²⁰ was calculated by comparing the state in the year 2023 to the annual long-term means obtained from the historical period²¹ (observed and historical, respectively), as described in Box 2.

Further details of the methods (including an overview of all data sources), the GHMSs used in the analysis, the definitions of the indicators used in the report, and additional results are documented in the [Annex](#).

Box 2

The annual mean of each hydrological variable (for example, river discharge, inflow into reservoirs) for a defined reference period of data (modelled or observed) was calculated for each year. The ranking of each respective variable in 2023 falls under categories based on the following definition:

much below normal:	$Q_{2023} \leq 10\text{th percentile}$
below normal:	$10\text{th} < Q_{2023} < 25\text{th percentile}$
normal: ²²	$25\text{th} \leq Q_{2023} \leq 75\text{th percentile}$
above normal:	$75\text{th} < Q_{2023} < 90\text{th percentile}$
much above normal:	$Q_{2023} \geq 90\text{th percentile}$

Where results are obtained from several models, the above-specified rankings were assigned an integer (“much below normal” = 1, “below normal” = 2, “normal” = 3, “above normal” = 4, “much above normal” = 5), and then an average was calculated across the outputs of the ensemble of models for each of the basins. The resulting number was rounded and translated back into one of the categories listed above.

Note that while the reference period for the data varies for the different variables (30 years (1991–2020) for river discharge,²³ 20 years (2004–2023) for groundwater and 19 years (2002–2020) for terrestrial water storage) based on data availability, the classification of the ranking remains the same. For further information on the reference period used for each variable, refer to [Table A2](#) in the Annex. Note that the selection of different reference periods may influence the calculated results.

River discharge

This 2023 edition of the State of Global Water Resources report builds upon the Hydrobasins level 4 delineation adopted by the previous report.²⁴ The proposed delineation represents approximately 986 river basins (with a minimum area threshold of 10 000 km²) around the globe (Figure A1 in the Annex).

The river discharge analysis in the 2023 edition of the report, similar to the 2021 and 2022 editions, is based on in-situ data received from WMO Members represented by NMHSs, mainly obtained via the GRDC database, supplemented with substantial contributions from global hydrological models. The 10 GHMSs listed in the Annex, Table A3 were used for this year's report, and all 10 were used for river discharge calculations. For more information about the models, the input data used and other details, please refer to [Global hydrological modelling systems](#) in the Annex.

The volume of observational data for the year 2023 has substantially increased (Figure 1). Only stations with at least 345 days of data points for 2023 and covering the historical period of at least 20 years (2001–2020) were selected for the analysis. At the time of preparation of this report,²⁵ observed daily river discharge data (covering the entire year 2023) were available from 713 stations (see Figure 2 for gauge locations), in comparison with 273 stations used in the 2022 edition and 38 stations in 2021. Most of these stations are located in Europe (48%)

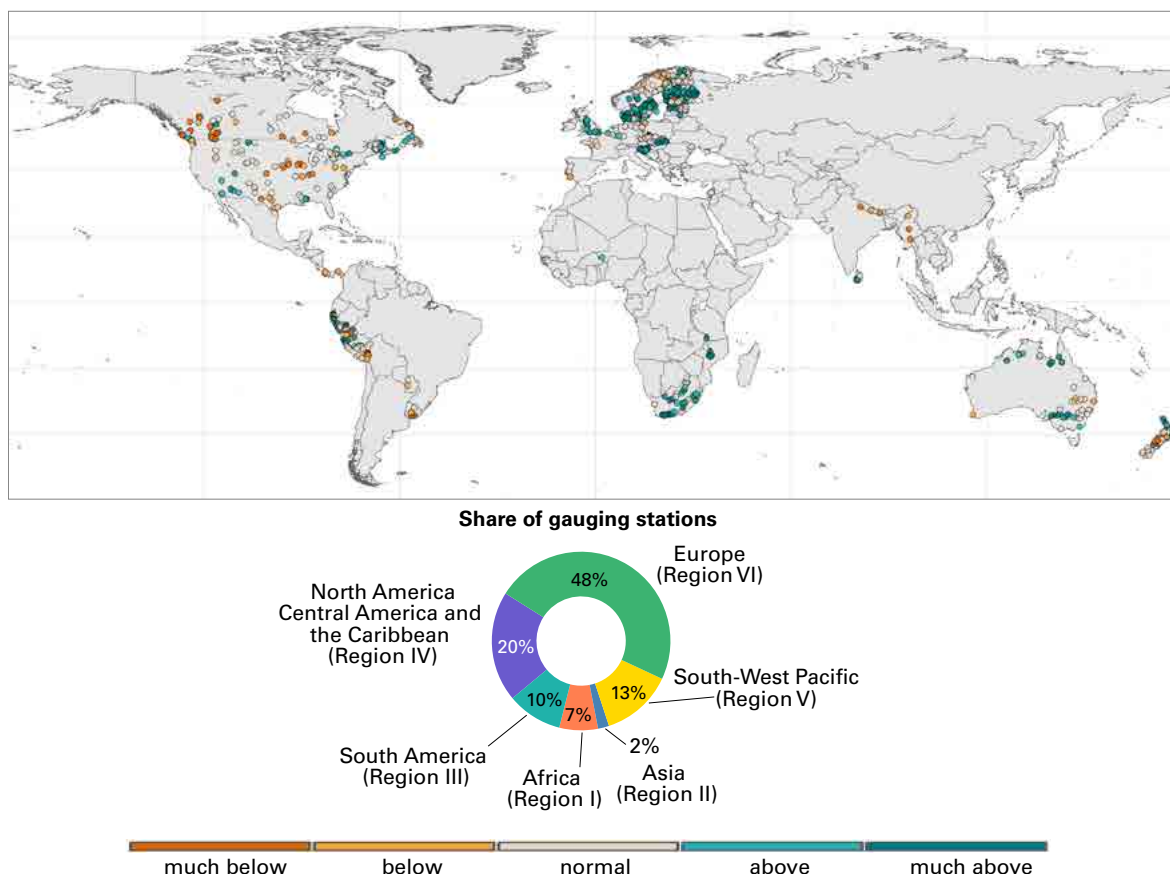


Figure 2. Observed mean river discharge for the year 2023 compared to the period 1991–2020 (for stations with a minimum of 20 years of data availability (2001–2020)); the dots are placed at the gauging station location (that is, the gauged basin outlet). The results presented here were derived from the observed river discharge data, which were obtained from NMHSs and the GRDC database. The results were also used to validate the simulated GHMS results in Figure 3, where the reference period was adjusted to match the available in-situ data (see Figure A7 in the Annex). Regions in the map refer to the WMO regions.

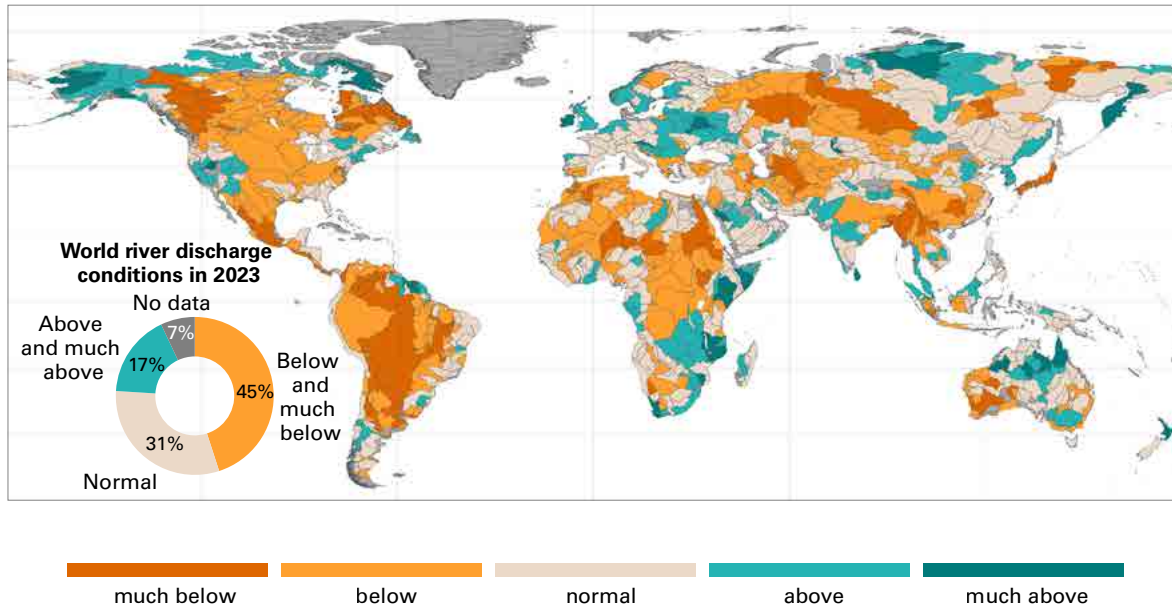


Figure 3. Mean river discharge for the year 2023 compared to the period 1991–2020 (for basins larger than 10 000 km²). The results presented here are derived from the modelled river discharge data obtained from an ensemble of 10 GHMS simulations (see [Methods](#) in the Annex). Inset (bottom left) shows the percentage distribution of the modelled catchment area under the given conditions. Dark gray areas indicate no modelling data. The results were validated against hydrological observations wherever available (see [Figure A6](#) in the Annex).

and North America (20%), while Africa, South America and Australia have a share ranging from 2% to 13%. The smallest proportion of available stations (around 1%) is found in Asia.

For the data obtained from GHMSs and from the observed river discharge stations, the mean annual river discharge for 2023 was compared with historical values from 1991 to 2020 for modelled results, or with at least 20 years (2001–2020) for observed data. The discharge levels were then classified as normal, above normal, below normal, much above normal or much below normal relative to these historical values (refer to [Table A2](#) in the Annex for more details). The [Annex](#) provides details on each of the GHMSs used, together with information on their set-up and calibration with historical data, and on how simulations for 2023 were produced. It also outlines potential sources of uncertainty associated with the modelling framework applied. In basins where observed river discharge data was available, the trends simulated by the GHMSs were validated.

[Figure 2](#) presents the observed mean river discharge for the year 2023 against the selected historical period (1991–2020), and [Figure 3](#) presents the modelled mean river discharge for the year 2023 against the selected historical period (1991–2020). The calculation is based on ensemble results from the GHMSs (see the [Annex](#) for details on the method of calculations). In cases where observation data were available, they were used to validate the model results shown in [Figure 3](#). A detailed presentation of the validation showing basins where the GHMS simulations agreed with the observed data is provided in the Annex, [Figure A6](#).

Validation of modelled results showed good overall agreement²⁶ (>69% of basins) between observed and simulated anomalies (based on multi-model mean) for the year 2023, particularly in Central and Northern Europe, New Zealand, Australia, the upper part of the Paraná River in Brazil and Paraguay, the Ganges in India and the Irrawaddy River in Myanmar. At the same time, modelled anomalies disagreed with observations in South Africa, the upper Amazon

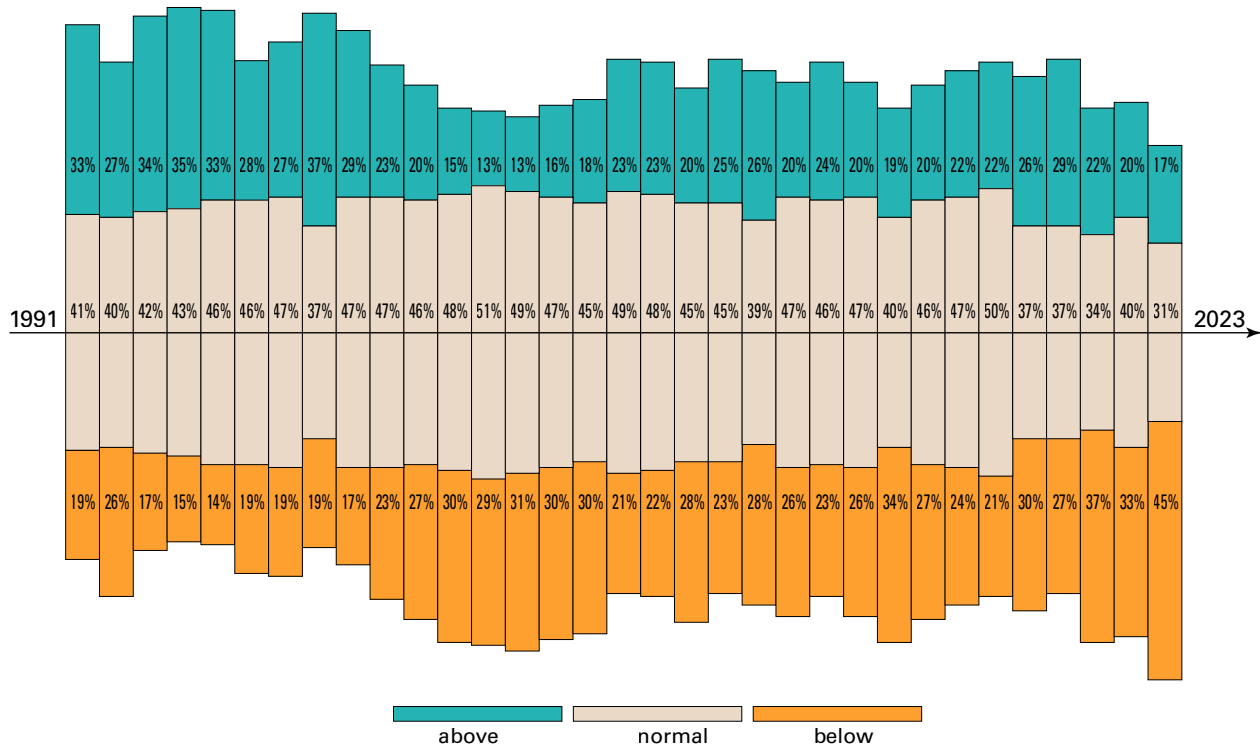


Figure 4. The distribution of the area under different river discharge conditions for the years 1991–2023

basin, the Lule basin (Sweden), the Nelson and upper Mississippi basins in North America, and the Niger River in Africa (for full validation results refer to [Figure A6](#) in the Annex). The location of the gauges with observed river discharge data is critical for reliable model validation, as presented in the Annex, [Figure A5](#); in some locations, such as the Amazon river basin, gauges used for validation were too far away from the modelled outlets, which can undermine the validation results. This underlines the importance of the availability and comparability of the observed data and the modelled data.

With respect to the historical period, the year 2023 was characterized by mostly drier-than-normal to normal conditions (Figure 4). Similarly to 2022 and 2021, in more than 50% of global catchment area river discharge exhibited deviations from normal conditions; it was predominantly lower than normal, with a smaller proportion of basins exhibiting above- and much-above-normal conditions. At the global scale, the river discharge conditions in 2021 and 2022 followed a similar pattern, with more areas experiencing drier-than-usual conditions compared to areas with wetter-than-usual conditions. In 2022, more area globally was under normal conditions than in 2021.²⁷

A comparison of the areas under different river discharge conditions for every year from 1991 to 2023 using a constant historical normal (1991–2020) showed a rising trend in dry areas over time, with 2023 being the driest in the last 33 years, followed by 2021 and 2015. The last five consecutive years showed some of the lowest percentages of area under normal conditions over the past 33 years.

In 2023, below- and much-below-normal conditions prevailed in the Americas: across North America, except for Alaska, 2023 mean discharge was lower to much lower than normal.



The 2023 drought in the Mississippi and Ohio tributary basins, along with reduced groundwater from three consecutive years of drought in the Missouri tributary basin, resulted in record low water levels in the Mississippi River.²⁸ The Yukon river basin in North America experienced above- and much-above-normal discharge conditions.

Below- to much-below-normal conditions gripped almost the entire territory of Central America and South America. On 26 October 2023 water levels in the Amazon river basin at the port of Manaus reached their lowest recorded level since 1902 (12.70 m).²⁹ The transition from La Niña (2022/2023) to El Niño (2023) appears to have been a key climatic driver in this record-breaking dry and warm situation, combined with a widespread anomalous warming over the worldwide ocean.³⁰

The east coast of Africa was characterized by above- and much-above-normal discharge – as in the Limpopo and Zambezi river basins, and coastal catchments in Tanzania, Mozambique and the Horn of Africa. The Horn of Africa, which had suffered five consecutive dry rainy seasons, was affected by flooding, triggered by El Niño conditions.³¹ In Libya the annual discharge conditions were indicated as above normal. The Niger, Lake Chad, Nile and Congo basins were characterized by below-normal discharge conditions.

In Europe, the basins of the Danube and Dnieper were characterized by above-normal conditions. Additionally, central and western Europe saw normal discharge conditions, and in Italy river discharge remained normal. In Northern Europe, the entire territory of the United Kingdom and Ireland saw above-normal discharge, as did southern Sweden, Norway and Finland. In the Russian Federation, the basins in the European part of the country and in Siberia (the Volga, Ob, and Northern Dvina) were characterized by lower-than-normal conditions, while a number of river basins in eastern Siberia and the far eastern part of the country (such as the Lena and Ussuri) and the Kamchatka Peninsula's rivers saw above- and much-above-normal discharge conditions.

Across the Middle East and Central Asia, discharge conditions remained lower than normal. In Asia and Oceania, large river basins such as those of the Ganges, Brahmaputra and Mekong experienced lower-than-normal conditions over almost the entire basin territories. In Australia, basins on the northern coast saw above-normal discharge conditions, while the Murray–Darling basin had predominantly normal conditions. The North Island of New Zealand and the Philippines exhibited much-above-normal annual discharge conditions.

Reservoirs

This chapter presents the state of the reservoirs in 2023 based on data from two sources: modelled inflow into selected reservoirs globally and anomalies in reservoir volume in 2023, obtained from NASA, as a combination of satellite-based products, described in Biswas et al.³²

INFLOW INTO SELECTED RESERVOIRS

The inflow data were obtained from three sources that comprise satellite-based ([Global Water Watch](#)) and GHMSs products, namely, the Wflow_sbm,³³ CaMa-Flood with Dam^{34,35} and World-Wide HYPE (WWH) models³⁶ (more details listed in [Table A3](#) in the Annex). All available reservoirs from the above sources were included for analysis and were identified by their GRanD ID.³⁷ Daily inflow data into the selected GRanD reservoirs were computed from the three GHMS models for the historical period between 1991 and 2020 and for the year 2023. Inflow anomalies were then calculated following the same method as for river discharge (see [Box 2](#)). Results are presented in Figure 5. Water inflow into the reservoirs was selected as an indicator due to its low dependency on water resources management strategies such as reservoir operations.

Inflow into reservoirs in 2023 generally reflected the overall discharge conditions, with the global balance being mostly below normal or normal. Specifically, reservoirs in India, particularly along the west coast, experienced below- and much-below-normal inflows. Similar conditions were observed on the east coast and the South Island of New Zealand. In Australia, the Murray–Darling River also recorded below-normal inflows.

In North and South America, reduced water availability was evident with lower-than-usual inflows into reservoirs, particularly in the Mackenzie River in North America, across the entire territory of Mexico, and in the Paraná River in southern Brazil and Argentina. Across the Middle East and Central Asia, inflows into reservoirs remained lower than usual.

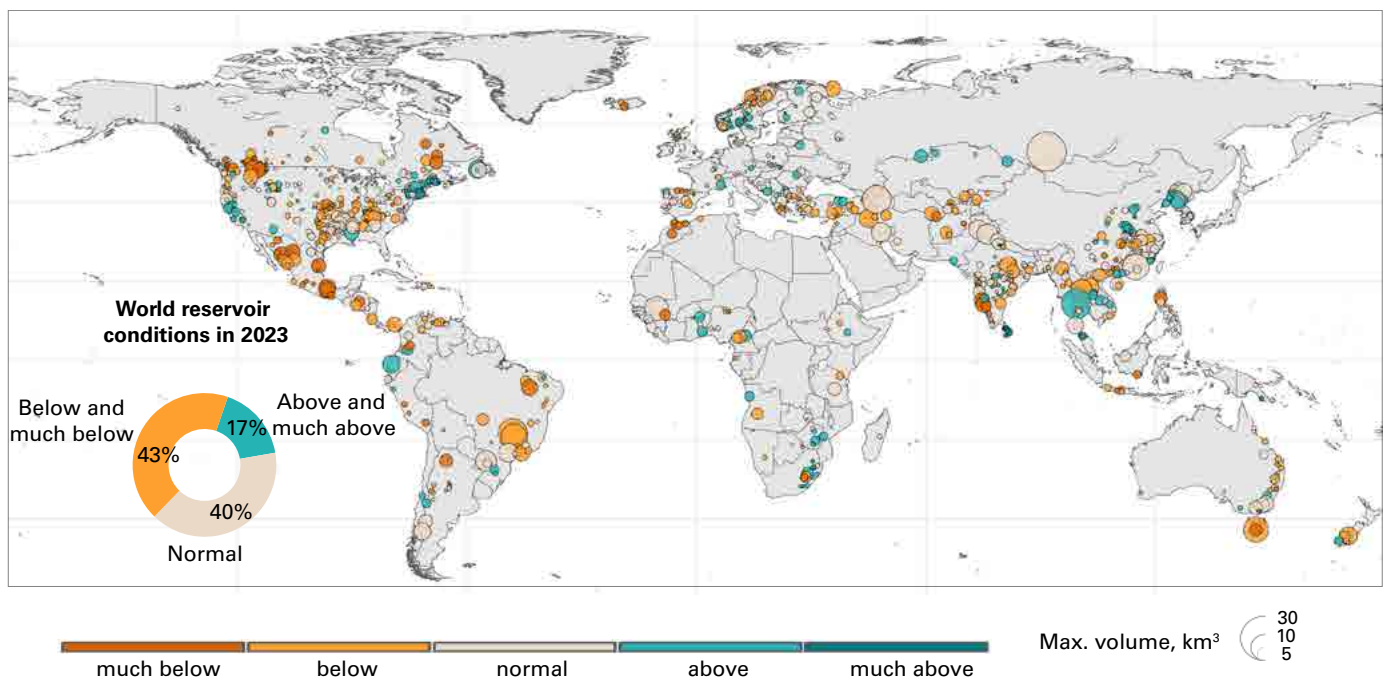


Figure 5. Mean annual inflow into selected reservoirs in 2023 as compared to the historical period 1991–2020. The size of the dots corresponds to the maximum storage volume of the reservoirs. The inset (bottom left) shows the percentages of reservoirs under the given conditions.

In contrast, South African reservoirs saw higher-than-usual inflows following wetter-than-usual discharge conditions. Northern Europe, particularly Sweden and southern Norway, also experienced increased reservoir inflows. However, in the far north of Norway, inflows were below normal.

RESERVOIR STORAGE

This section presents the results on basin-wide reservoir storage anomalies in 2023. The approach used involves merging several satellite-based datasets, as described in Biswas et al.³⁸ Monthly individual reservoir storage time series were calculated and then accumulated into monthly basin-wide reservoir storage time series for 237 basins (Figure 6).

Reservoir storage is influenced not only by climatic conditions and inflow into reservoirs but also by anthropogenic regulation of the storage. The effects of management can lead to results that differ compared to the inflow; for instance, inflow can be low, but water can be stored, resulting in increased volume and decreased discharge downstream of the reservoirs.

In Africa, the Orange, Zambezi, Congo, and Nile river basins exhibited much-above-normal reservoir storage levels. In Europe, the Danube and Rhine basins and the Iberian Peninsula experienced much-below-normal reservoir storage. In contrast, Eastern European catchments such as the Dniepr in Ukraine saw much-above-normal storage, as did the Volga, Enisey and Ob river basins.

In North America, the Nelson River and upper parts of the Mississippi River had much-above-normal basin-wide storage. However, catchments in the eastern and southern United States and Mexico experienced much-below- to below-normal reservoir storage. In South America, reservoirs in the Amazon and Paraná basins had much-above-normal storage levels. In Asia, the Ganges Basin in India and the Yangtze Basin in China saw above-normal reservoir storage. In Australia, the Murray–Darling Basin experienced much-above-normal reservoir storage levels.

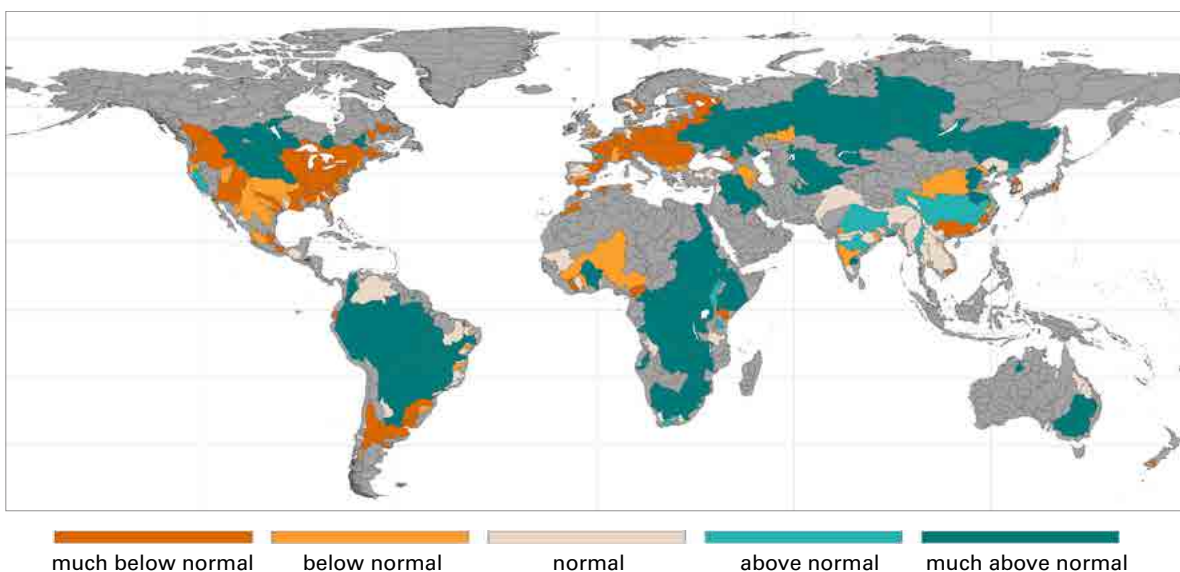


Figure 6. The annual mean of monthly basin-wide reservoir storage in 2023 with respect to the reference period (2000–2023)

Lakes

The water levels in 30 selected large lakes were obtained from the GloLakes product.³⁹ The GloLakes product estimates lake and reservoir storage data by combining measurements of water levels and water body extents from various satellites, with additional local topography information when needed.^{40,41} The data record starts in 1984 and is regularly updated as part of the [Global Water Monitor](#) and associated annual summary report. To determine the dynamics of lake and reservoir surface water extents, high-resolution optical remote sensing data from Landsat and Sentinel-2 satellites were used. The anomaly was calculated with respect to the 1991–2020 historical period, and the 2023 annual volume anomaly is presented in Figure 7.

In the Amazon, the volume of Lake Coari was below normal. Record-breaking heatwaves and reduced water levels caused the water temperature rise to 34 °C, leading to an algae bloom and causing the death of a substantial number of pink dolphins (*Inia geoffrensis*).^{42,43}

The volume of Lake Superior, the largest lake in North America, was above normal in 2023; this began in December 2022.⁴⁴ Despite the drought event that affected Central America, Lake Nicaragua saw above-normal water volumes in 2023. Similarly, Lake Balaton in Central Europe experienced much-above-normal volume levels, as did Lake Peipus in Estonia and Lake Mälaren in Sweden.

In Asia, the Small Aral Sea and Lake Aydar in Kazakhstan and Uzbekistan, as well as Eling Lake, Kaoyu Lake and Bositeng Lake in China, saw normal volumes in 2023. Hulun Lake and Lake Khsanka, which is shared by China and Russia, also experienced above-normal water volumes. Tonle Sap Lake in Cambodia, located in the Mekong river basin, exhibited above-normal water volumes as well.

Lake Turkana, the world’s largest desert lake, which is shared between Kenya and Ethiopia, had above-normal water volumes, following much-above-normal discharge conditions.

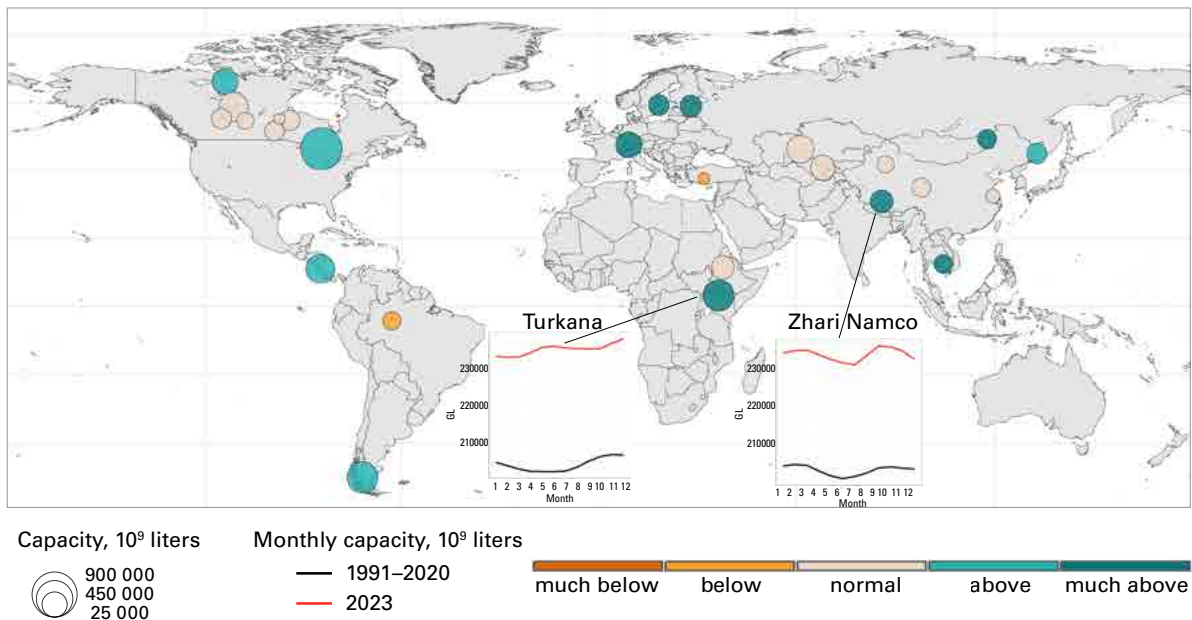


Figure 7. Volume of 30 large lakes in 2023 as ranked with respect to the historical period 1991–2020 based on the GloLakes product

Groundwater levels

This section provides an evaluation of groundwater levels in 2023 in comparison with historical records.⁴⁵ It relies on in situ groundwater level monitoring data made available by the national (subnational, in some cases) institutions in charge of groundwater monitoring. In total, groundwater level monitoring data were collected for over 160 000 wells in 40 countries. Data were collected over the period covering the last 20 years, from 2004 to 2023. Where it was not possible to collect the data over this entire period, for instance in countries where groundwater monitoring is less than 20 years old, data covering the last 10 years were used instead. This is the case for Brazil, Bulgaria, Costa Rica and Israel. Groundwater level monitoring data were first filtered to guarantee a certain level of data consistency and completeness. After filtering, data could be analysed for some 35 459 of the wells.⁴⁶ In total, the average groundwater level in 2023 was much below normal in 6 756 wells (19%), below normal in 4 087 wells (11%), normal in 14 030 wells (40%), above normal in 3 489 wells (10%) and much above normal in 7 097 wells (20%).

The results are shown on a world map and on a selection of regional maps (Figure 8a and 8b). The results show that the ranking is rarely uniform over a given area, because of the heterogeneous nature of aquifers and the importance of local variables influencing groundwater levels, such as a pumping well or the vicinity of a river. Nevertheless, regional patterns are observed, indicating that groundwater is also subject to regional influences.

The average groundwater level in 2023 was below normal or much below normal in a high proportion of wells over a large part of North America, in particular in the western and midwestern United States, and in central and northern Chile, western and southern Brazil, Southern Europe (Portugal, Spain, most of France), Central Europe (Hungary, Austria, Bavaria (Germany), the north of Poland), as well as in western and southern Australia.

Conversely, the average groundwater level in 2023 was above normal or much above normal in a high proportion of wells in New England (United States), the Maritime provinces of

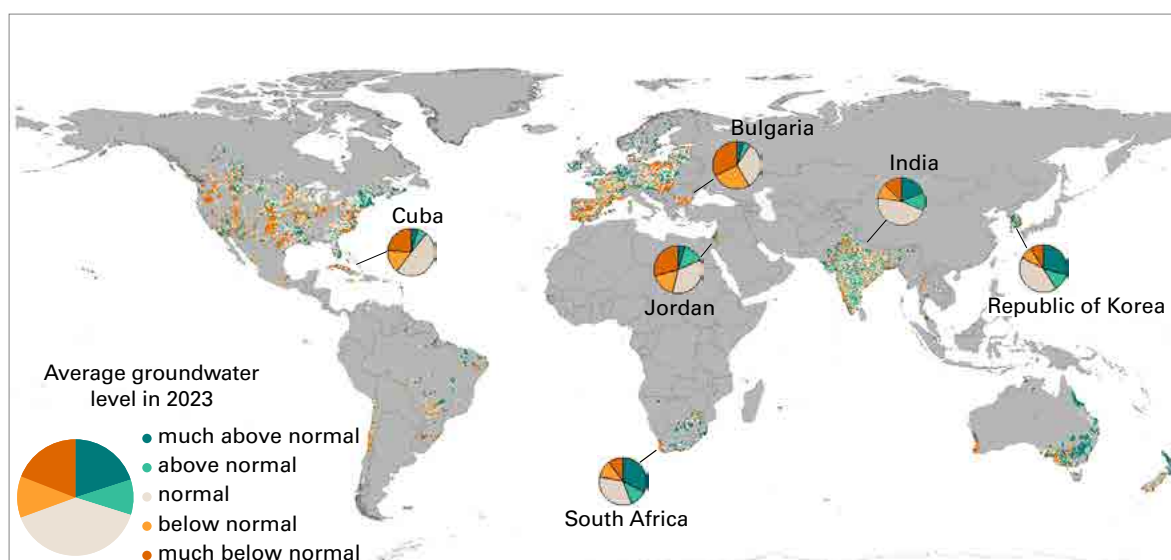


Figure 8a. Mean groundwater levels in 2023 as compared to the historical period of 2004–2023 (2014–2023 in the case of Brazil, Bulgaria, Costa Rica and Israel).

Note: There are 3 175 monitoring sites comprising two or more monitoring stations. The results of these stations have been slightly displaced in the map to keep them from overlapping.

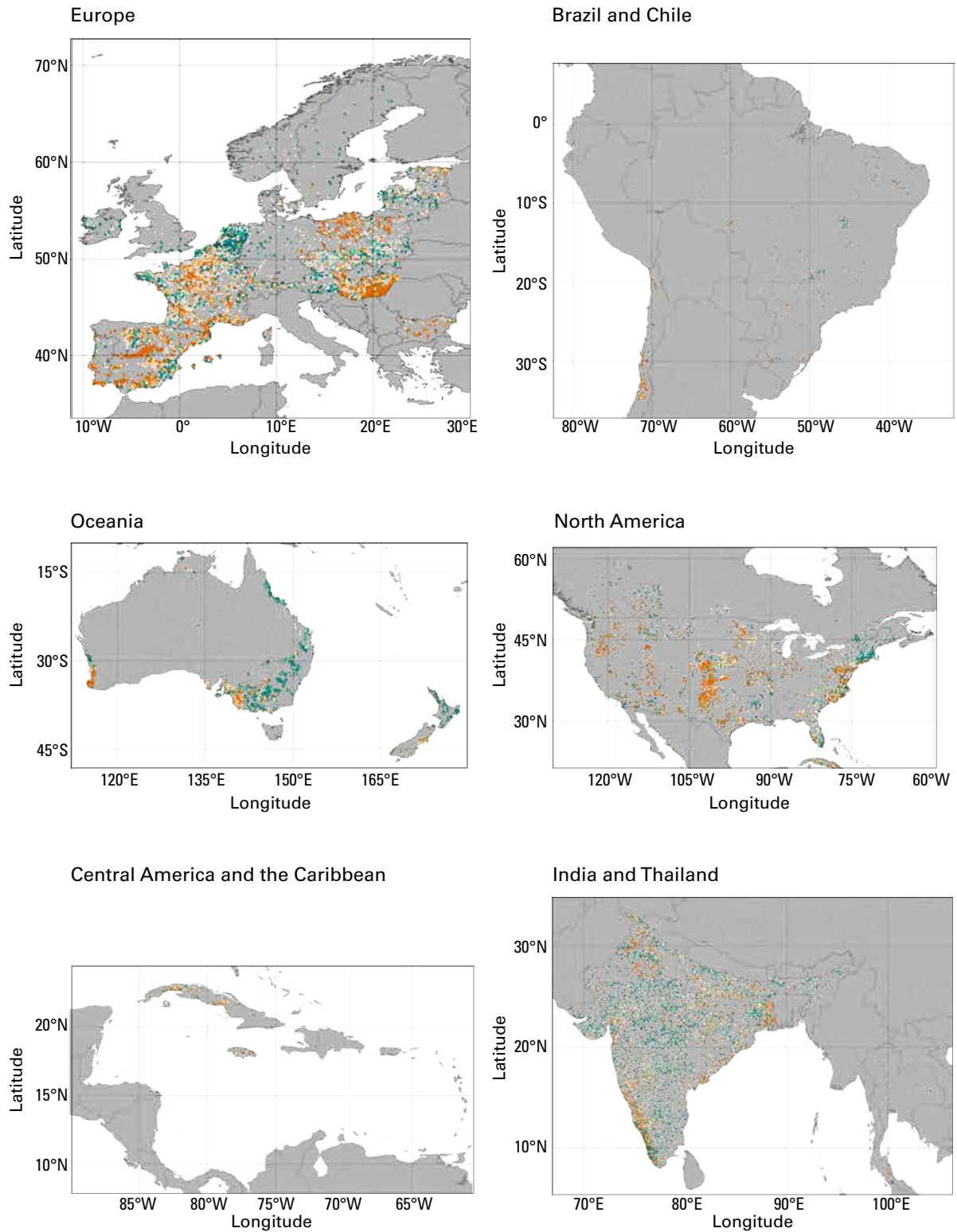


Figure 8b. Snapshots for selected countries showing mean groundwater levels in 2023 as compared to the historical period (as in Figure 8a)



Canada, along the Atlantic coast of north-eastern Brazil, Northern Europe (the British Isles and Scandinavia), Israel, Southern Africa, several parts of India, the Republic of Korea, eastern Australia, and the North Island of New Zealand.

It is not straightforward to identify the reasons behind these regional trends, because groundwater is under the influence of climatic variables and other anthropogenic variables, such as abstraction and land use. Some aquifers have a rapid response time between the change in the boundary conditions (such as a groundwater recharge) and the corresponding change in groundwater level,⁴⁷ however the response time in other aquifers can be several years or decades long. Nevertheless, some explanations can be put forward. In South Africa, the high proportion of wells where the average groundwater level in 2023 was above normal is consistent with the above-normal amount of rainfall received in 2023 and the years before,⁴⁸ while some of the wells with groundwater levels below normal can be linked to over-abstraction for irrigation. The impact of high precipitation in recent years on groundwater levels has also been observed in some parts of India,⁴⁹ in Ireland,⁵⁰ in Australia^{51,52} and in Israel, for example. High precipitation directly contributes to an increase in groundwater levels through the recharge of aquifers. In countries where groundwater abstraction is significant, such as Australia, high precipitation also tends to reduce groundwater abstraction, as more surface water is available and the soil moisture is higher, which indirectly contributes to an increase in groundwater levels. The high proportion of wells where the average groundwater level in 2023 was below normal in Chile and in Jordan cannot be explained by climatic factors, reflecting instead the long-term decline of groundwater levels due to over-abstraction.^{53,54} The results from India are mixed, however they rely predominantly on data collected in shallow dug wells (80% of total),⁵⁵ where groundwater levels reflect the impact of the climate. It would be necessary to distinguish the monitoring data collected in boreholes to assess the impact of over-abstraction due to groundwater irrigation, which is particularly significant in the north-west of the country.^{56,57,58} Finally, the high proportion of wells where the average groundwater level in 2023 was below normal could reflect a combination of climatic drought and over-abstraction. North America, for instance, was affected by the 2020–2023 North American drought, but is also subject to groundwater depletion, in particular in California and in the High Plains.⁵⁹ Europe has also been affected by droughts in recent years, but there are cases of groundwater over-abstraction, mostly in the southern part of the continent, for example in France, Hungary and Spain.⁶⁰

Despite the significant number of countries covered in this evaluation, the data availability is such that large parts of the world are missing from this analysis, in particular in Africa and in Asia. This does not mean, however, that there are no data. There are several countries where groundwater level monitoring data have been collected for less than 10 years (such as the Gambia, Rwanda and Somalia). It will be possible to include these countries in the evaluation within a few years, which is a promising prospect. There are also challenges in accessing the latest data. Data from Croatia and Qatar could not be used because most of the data from 2023 were not yet available for sharing.

Soil moisture

Surface soil moisture is one of the crucial variables for hydrological processes. It influences the exchange of water and energy fluxes at the land surface/atmosphere interface, impacts streamflow generation, is important for biogeochemical cycles and co-controls vegetation development. Understanding soil moisture patterns is essential for sustainable water resources management and for the assessment and understanding of food production.^{61,62}

OBSERVED SOIL MOISTURE FROM THE INTERNATIONAL SOIL MOISTURE NETWORK

For the 2023 assessment, ISMN⁶³ applied strict filtering, selecting about 160 stations globally, each with a minimum of 15 years of data and more than 50% data availability (monthly), to visualize soil moisture in three categories: below normal, normal and above normal. The report focuses on soil moisture at two depths: near-surface (up to 10 cm) and deeper (down to 0.5 m). The analysis includes data from up to 154 near-surface stations and 90 deeper stations. The soil moisture observations do not account for irrigation and may be influenced by human activities.

The data show variability in soil moisture across regions. In Europe, 47% of near-surface stations reported below-normal or normal conditions, while the United States exhibited 81% normal or above-normal conditions, although significant regional differences were noted (Figure 9). It is reported that July was a very diverse month in terms of soil water availability. While substantial parts of the United States were under dry conditions, simultaneously wet conditions were observed over other parts of the country (10% of the contiguous United States).⁶⁴ Note that the surface soil moisture is very dynamic compared with deeper soil layers where soil water is more persistent. A similar spatial clustering of in situ data can be observed in the data from the deeper stations (Figure 10). Within these clusters the majority

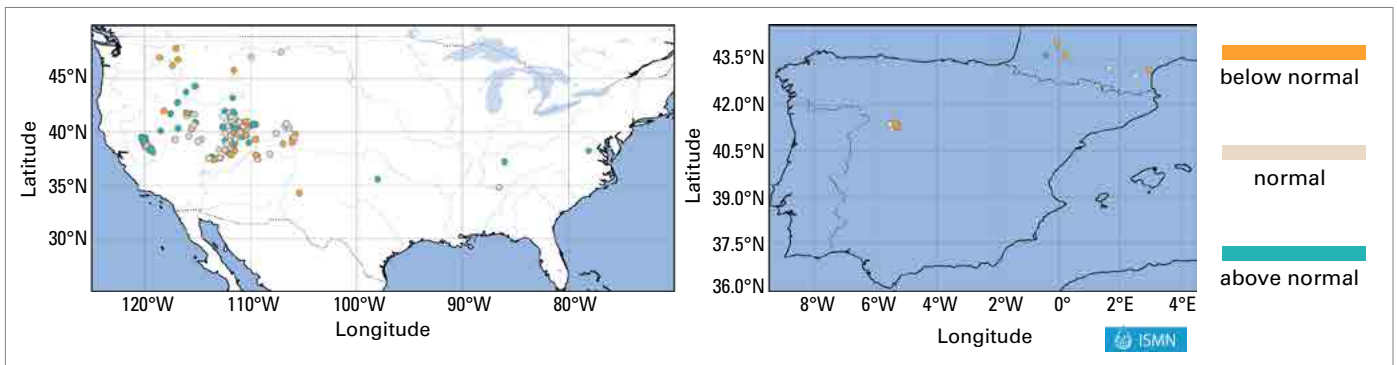


Figure 9. Soil moisture in July 2023 compared with all Julys 2008–2022 (15-year reference period) for the top layer of soil (down to 0.11 m). The left panel shows the situation in the contiguous United States, whereas south-west Europe is shown on the right. Due to limited data availability (data were available from 150 stations – 135 in the contiguous United States and 15 in Europe – all of which are displayed in the maps above), only limited data coverage is achieved by using in situ soil moisture data.

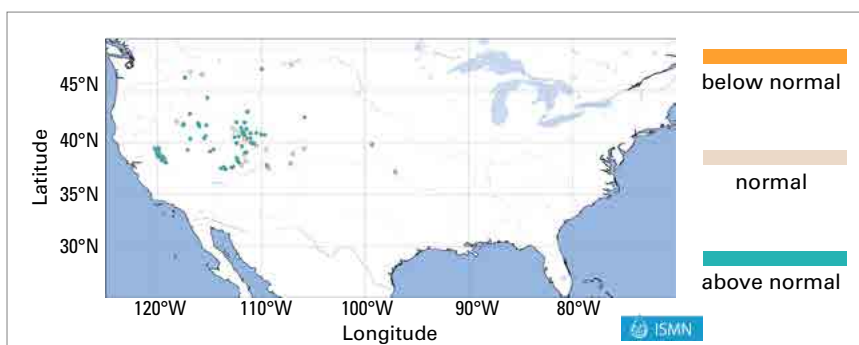


Figure 10. Soil moisture status down to 0.51 m depth in September 2023 in the contiguous United States. The reference data are the monthly averaged soil moisture of all Septembers 2008–2015. Due to limited data availability, data from only 88 stations located in the United States could be analysed.

of soil moisture observation points reported above-normal conditions. Such conditions were reported for the western United States, while other parts of the country endured drought conditions. These findings highlight the need for long-term, widespread data to assess soil moisture conditions accurately at regional and global scales.

MODELLED SOIL MOISTURE

The anomaly in surface soil moisture in 2023 has been obtained from three GHMSs (see [Table A1](#) in the Annex for model names) and ranked relative to the historical period 1991–2020 on a monthly basis to understand root zone soil moisture patterns (2 m depth). The anomaly calculation used was the same as for river discharge and reservoir inflow (as per [Box 1](#)). The results are presented in Figure 11.

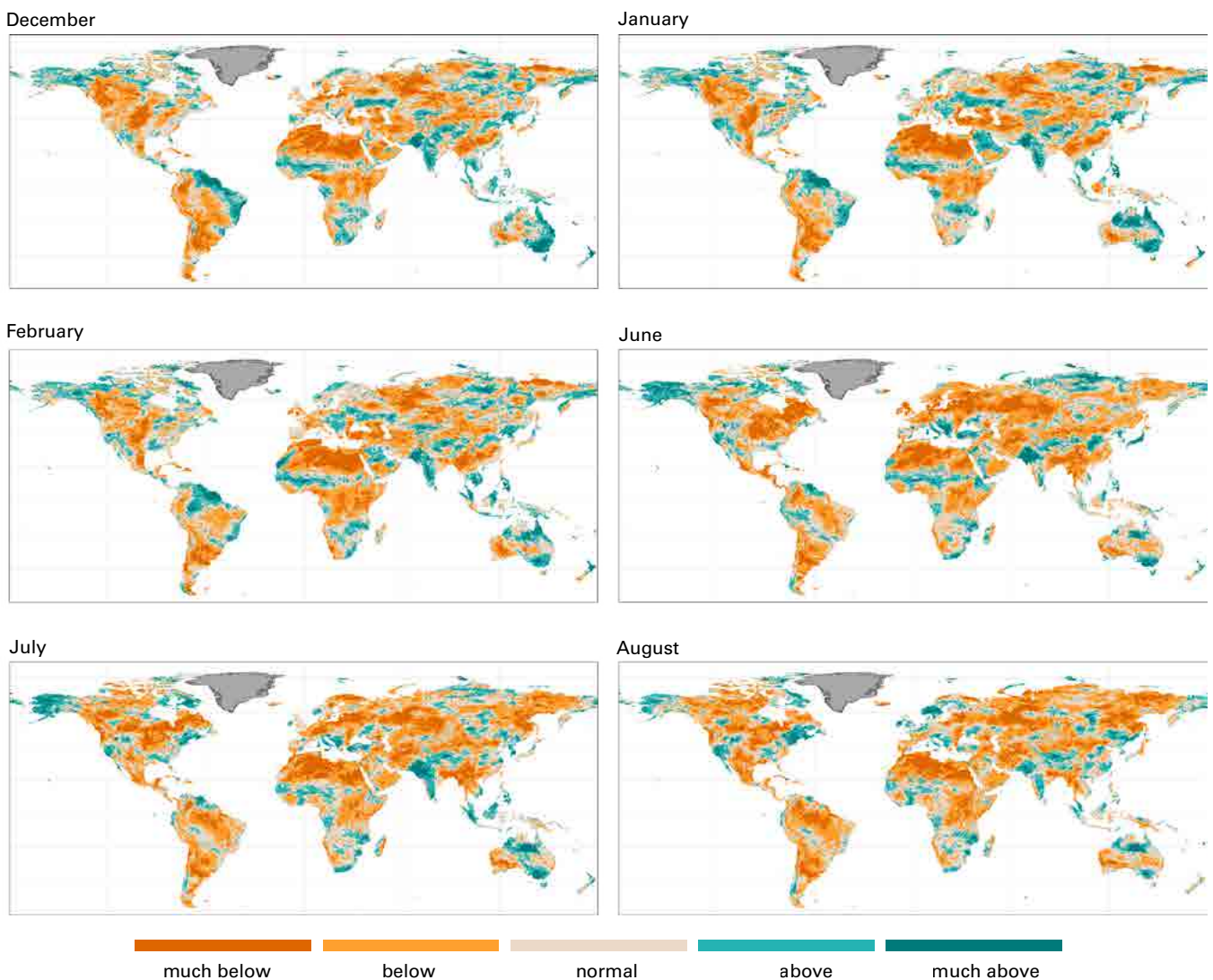


Figure 11. Soil moisture in 2023 (Dec. 2022–Feb. 2023 and Jun.–Aug. 2023) as ranked with respect to the historical period 1991–2020. Greenland is masked in accordance with the Global Land Ice Measurements from Space (GLIMS).



Soil moisture in 2023 was predominantly below normal and much below normal across large territories globally throughout the year. For example, almost the entire territories of North America, South America, North Africa and the Middle East experienced much-below-normal soil moisture levels, particularly during June, July and August. In fact, according to the United States Department of Agriculture (USDA), the proportion of the nation's topsoil classified as dry or very dry peaked at 58% in mid-September. The year 2023 ranks just behind 2022 in the recent historical record for dry soils.⁶⁵ Over the same period of June–August, almost the entire territories of Europe, the Russian Federation, Central Asia and China experienced below- to much-below-normal soil moisture conditions. The same was observed in sub-Saharan Africa, including the Horn of Africa, which was actually affected by flooding. Only in South Africa, where 2023 was much wetter than usual, were soil moisture conditions above normal.

Alaska, north-eastern Canada, India and the north-eastern Russian Federation had much-above-normal soil moisture conditions. Similar conditions were observed along the northern and south-eastern coasts of Australia, as well as on the North Island of New Zealand, which was affected by flooding.

Due to a mismatch in spatial representativeness and variation in the depth of the measurements between the modelled soil moisture data and the data from ISMN stations, the validation of modelled results was not possible. This highlights the importance of ensuring that observations are accessible and applied with good spatial coverage. Additionally, there was a variation in the scale of spatial representativeness between the modelled and observed data: the observed soil moisture is only representative for a few cm³ whereas the models represent a few km³.

Evapotranspiration

Actual evapotranspiration (AET), which is one of the key elements in the hydrological cycle, refers to the process by which water is evaporated, encompassing evaporation from the soil or vegetation surface (including interception evaporation) and transpiration from plants.⁶⁶ Elements influencing the rate of evapotranspiration include the level of solar radiation, atmospheric vapour pressure, humidity, air temperature, wind, soil moisture content and vegetation type and cover. This process is responsible for a large part of the water loss from the soil during a crop's growth cycle and is critical for understanding the state of water resources. The rates of AET are controlled by the amount of water that is available (which is dependent on the existing hydrological conditions in the basin) in addition to the meteorological forcing.

This chapter presents an anomaly of AET at the global scale for four seasons in 2023 with respect to the historical period 1991–2020, derived from five GHMSs (listed in the Annex, [Table A1](#)) and averaged over the river basins derived from the Hydrobasins level 4 delineation.⁶⁷

The seasons considered are: December–January–February (DJF) (includes December 2022), June–July–August (JJA), March–April–May (MAM) and September–October–November (SON). As presented in Figure 12, during the DJF and JJA months, AET rates were normal to below normal in sub-Saharan Africa, except for West Africa, the Niger and Lake Chad catchments, and the coastal basins in South Africa. In the Horn of Africa, the situation changed in the MAM and SON months, showing above-normal AET. In October, intense rainfall and associated flooding impacted the region. Territories in Libya, which were struck by Cyclone *Daniel* in September, exhibited much-above-normal AET over the SON period.

In India, the entire territory experienced much-above-normal AET during MAM, as did the Arabian Peninsula and parts of the Volga and Don catchments in Eastern Europe. In the Russian

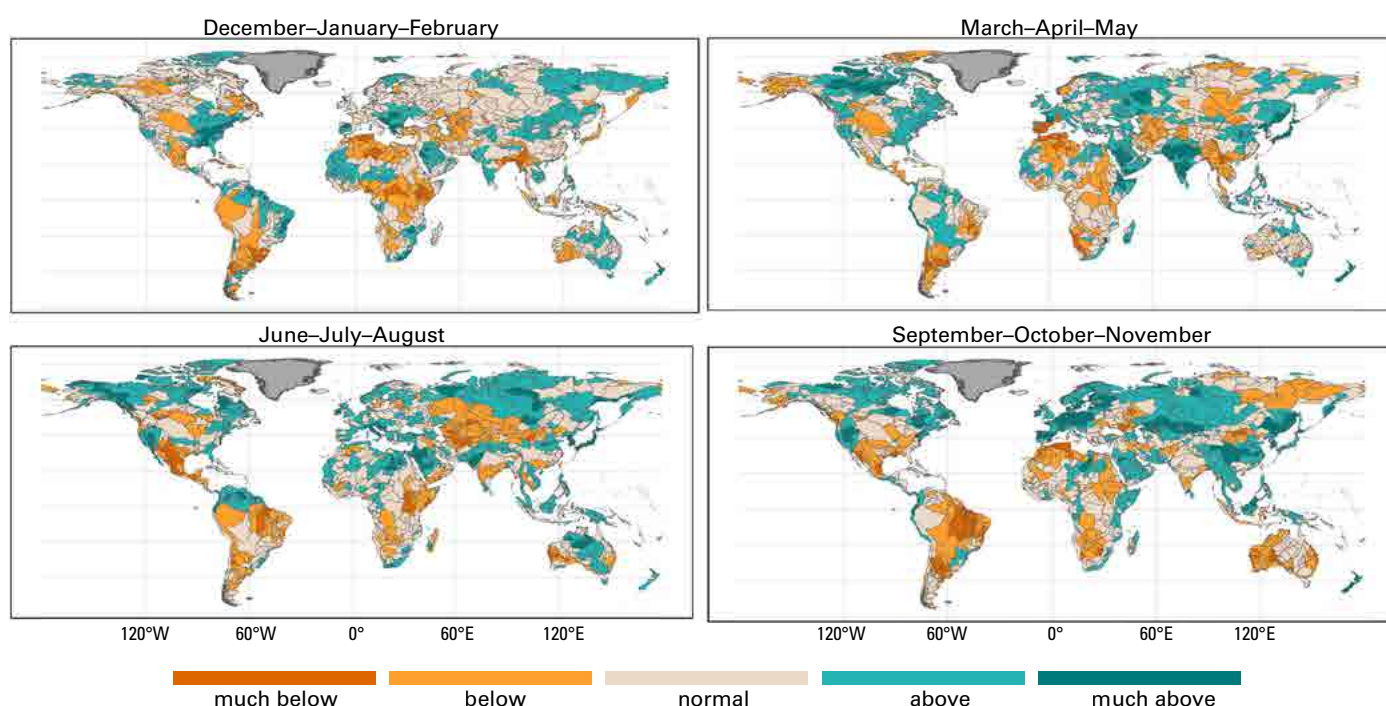


Figure 12. Seasonal actual evapotranspiration (AET) in 2023 as ranked with respect to the historical period 1991–2020 based on an ensemble of five GHMSs



Federation's far eastern catchments, such as the Ob and Enisey, AET was much above normal in both JJA and SON. Central Asian catchments, such as the Syr Darya, also saw much-above-normal AET during SON.

In Central and South America, which were severely impacted by heatwaves and drought in 2023, Brazil and Argentina experienced much-below-normal AET over large areas during SON. Mexico saw much-below-normal AET in DJF, JJA and SON. In the central part of the United States, AET was below normal or normal throughout the year, while northern catchments like the Mackenzie had above-normal AET in MAM, JJA and SON.

New Zealand had much above-normal AET throughout the entire year. Australian catchments were normal to below normal in AET during SON, mostly normal in MAM, and above normal in the northern territories during DJF and JJA.

In Europe, the Iberian Peninsula's catchments saw much-below-normal AET during MAM. Over SON, the entire territory of Central, Eastern and Northern Europe exhibited above- and much-above-normal AET.

Terrestrial water storage

Satellite gravimetry is a remote-sensing-based method (used by GRACE and GRACE-FO satellites)^{68,69} that is capable of observing all large-scale mass changes on and below the Earth's surface. This includes, in particular, those caused by water storage changes, including in surface water, soil moisture, groundwater, as well as snow and ice. Terrestrial water storage (TWS), defined as the sum of all these storage compartments, is expressed as an anomaly relative to its long-term mean in equivalent water heights in centimetres as an area-averaged height of the water column over the area being considered. This chapter provides results of the TWS anomaly in the year 2023 obtained from the GRACE/GRACE-FO-based product.

The section on [Terrestrial water storage](#) in the Annex provides more details on TWS and how TWS anomalies were calculated.

Figure 13 provides the TWS anomalies for 2023 in comparison to the 2002–2020 historical period, that is, the same reference period as for the *State of Global Water Resources 2022* (WMO-No. 1333). The TWS observations for 2023 reflect anomalies presented in previous chapters for other variables and further emphasize several critical hotspots for the year 2023. It should be noted that the integrative TWS signal shown here, also represents water storage variations in the unsaturated zone deeper than the soil moisture data shown in a previous chapter, besides groundwater.

In particular, large territories around the globe saw below- and much-below-normal TWS values in 2023: Canada, Mexico and the southern United States as well as large parts of Southern, Central and Eastern Europe. Also, Northern Europe saw some hotspots of much-below-normal TWS conditions in Sweden and Norway.

In Africa, the entire area of sub-Saharan Africa exhibited much-above-normal TWS in 2023, as did the Horn of Africa. These positive TWS anomalies reflect the strong overall and longer-term water storage increase in these areas after 2019 in particular, that is, a signal with longer persistence or memory effects, while below-average soil moisture conditions

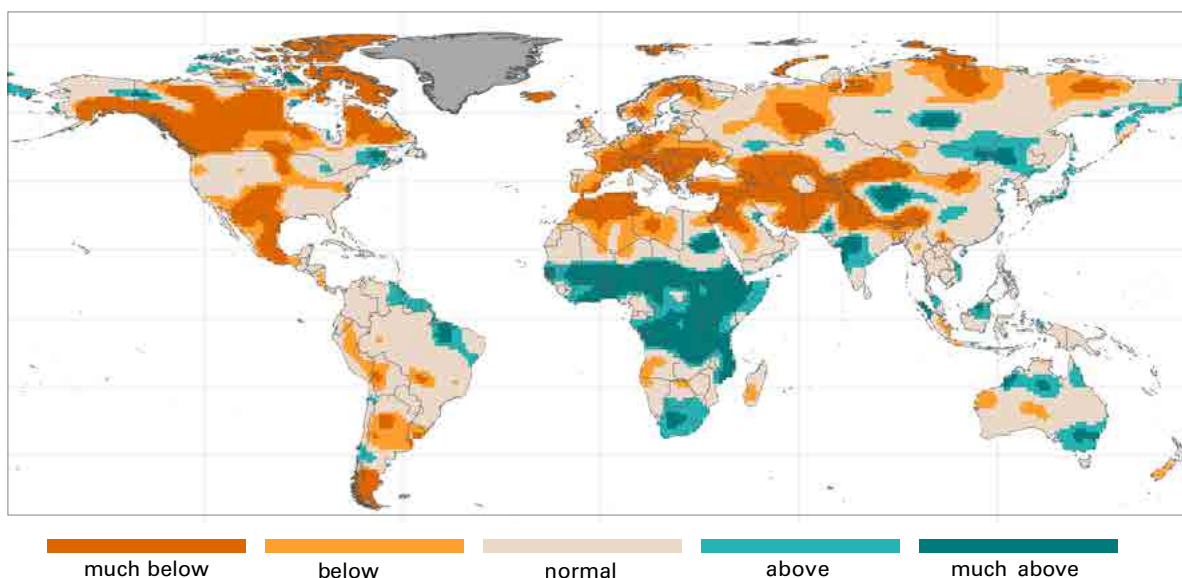


Figure 13. Terrestrial water storage in the year 2023 ranked with respect to the historical period 2002–2020, that is, the same reference period as for the *State of Global Water Resources 2022* (WMO-No. 1333). Note that Greenland and Antarctica are not included, as their ice mass balance trends are large and therefore hide the other TWS anomalies when plotted with the same colour range.

in parts of the region in 2023 (see [Soil moisture](#) chapter) represent the short-term near-surface dynamics. At the same time, TWS in Libya and Algeria remained much below normal in 2023. The entire territory of the Middle East, Central Asia and northern India saw much-below-normal TWS. On the other hand, in India, the upper Godavari river basin and basins in the central and western part of the country experienced much-above-normal TWS anomalies in 2023.

In South America, dry conditions, with below-normal TWS, were experienced in the La Plata region, with observations similar to those for soil moisture (see [Soil moisture](#) chapter). Much-below-normal TWS was also visible in South America along the Andes range, in particular in Patagonia, caused by ice-mass loss. In Australia, TWS was above normal to much above normal in the Murray–Darling catchment. The North Island of New Zealand saw normal TWS, while the South Island, on the contrary, saw much-below-normal TWS.

CASE STUDY ON THE WATER STORAGE SITUATION IN CENTRAL EUROPE DURING 2023

Figure 14 shows the simulated yearly anomaly for 2023 with regard to 2011–2022 for subsurface water storage (shallow groundwater from the land surface down to 60 m depth) and near-surface subsurface water storage (which includes the root zone, from 0 to 2 m depth). Note that contrary to TWS from satellite gravimetry discussed above, these water storage data do not represent storage anomalies in surface water bodies, snow cover and glaciers. Much-above-normal subsurface water storage is simulated in the Kingdom of the Netherlands and north-western Germany due to a positive precipitation anomaly, leading to floods at the end of the year in that region. Dry conditions prevailed in France, southern and eastern Germany, the Alps, northern Italy and around the Baltic Sea. This dry anomaly is a continuation from the 2022 drought and preceding drought years in the area. However, near-surface water

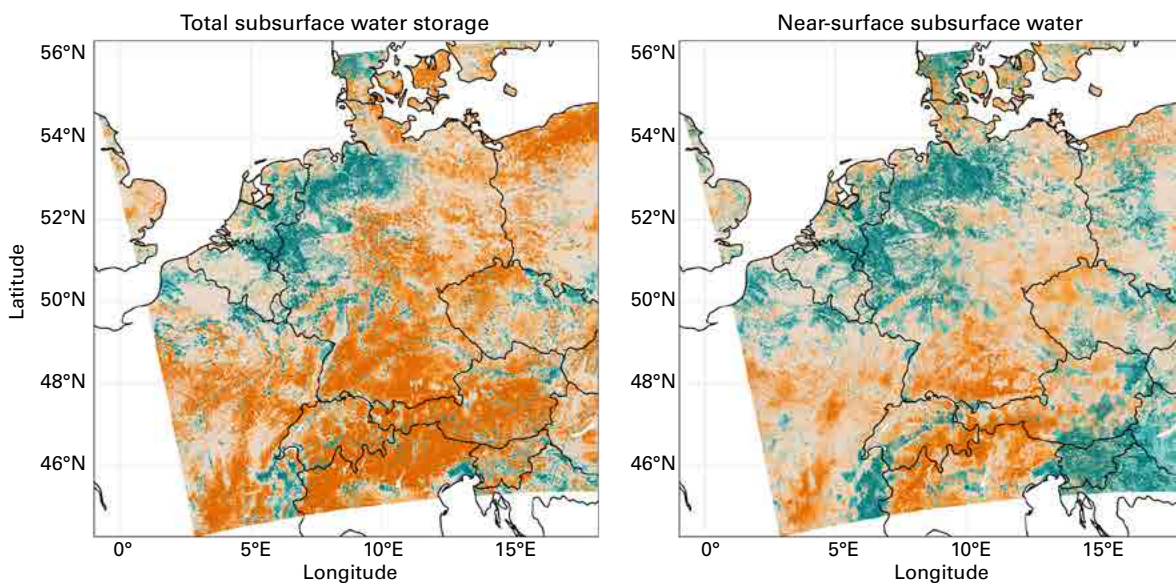


Figure 14. Total subsurface water storage (0–60 m) and near-surface subsurface water storage (0–2 m) in Central Europe in the year 2023 ranked with respect to the historical period (2011–2022)



storage modelling shows a weakening of negative anomalies in 2023, caused by above-normal rainfall during spring and autumn. This is indicative of memory effects and the persistence associated with such negative groundwater anomalies.⁷⁰

All data have been computed with the uncalibrated, physics-based model ParFlow/CLM at a resolution of 0.6 km.⁷¹ Modelling approaches like this allow for a spatially continuous analysis, eventually leading to a better planning and management of water resources. For example, this hydrological modelling approach is used in a quasi-operational forecasting system, which produces daily forecasts with a lead time of nine days (see the German Wasser-Monitor for plant available water, www.wasser-monitor.de) as well as an experimental Water Resources Bulletin (www.adapter-projekt.de/bulletin) providing seasonal forecasts four times per year of the total subsurface water storage over the upcoming seven months. However, the simulation results also show the need for in situ observations of various components of the water cycle (soil moisture content, groundwater level, river discharge, etc.), for example for validation, data assimilation and model-data fusion,⁷² which is only possible through dense hydrological monitoring networks and open data sharing.

Snow cover and glaciers

This chapter presents the state of snow cover and glaciers in 2023, focusing on snow water equivalent in March, peak snow mass over the northern hemisphere and glacier mass balance.

SNOW WATER EQUIVALENT

The March SWE in the northern hemisphere was obtained as an ensemble mean over the 1991–2023 period from four individual gridded products:

- (1) The European Space Agency Snow CCI SWE version 2 product derived through a combination of satellite passive microwave brightness temperatures and climate station snow depth observations;⁷³
- (2) The Modern-Era Retrospective Analysis for Research and Applications version 2 (MERRA-2) daily SWE fields;⁷⁴
- (3) SWE output from the ERA5-Land analysis;⁷⁵
- (4) The physical snowpack model Crocus⁷⁶ driven by ERA5 meteorological forcing.

March mean data from each product were regridded to a common $0.5^\circ \times 0.5^\circ$ regular grid and averaged together (Figure 15). This is the same suite of products currently used to produce annually updated SWE data for the Arctic Report Card⁷⁷ and the Bulletin of the American Meteorological Society (BAMS) State of the Climate Report.⁷⁸ March 2023 SWE values were converted to anomalies using the 1991–2020 reference period on a pixel-wise basis, as per Box 1.

In March, the SWE was much above normal in the northern catchments of the Lena and Khatanga Rivers in the far eastern Russian Federation. The basins of the Dnieper, Don, Danube, Ural, Yangtze and Amur all experienced below- to much-below-normal March SWE levels likely due to earlier onset of snowmelt compared to the reference period as a result of increasing temperatures. In North America, March SWE in the Nelson catchment was above normal, and in the Columbia catchment, it was much above normal. The SWE in the Mackenzie and parts of Yukon catchments was normal.

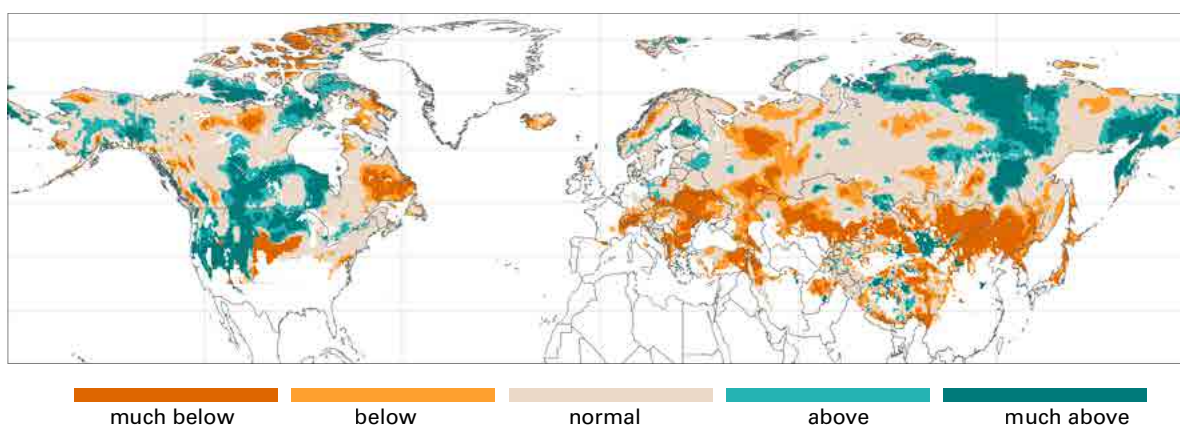


Figure 15. March 2023 snow water equivalent anomaly compared with the reference period (1991–2020). Results are based on four gridded products (see the [Snow water equivalent](#) section in the Annex for more details).



PEAK SNOW MASS IN NORTH AMERICAN BASINS

Daily frequency SWE output from the Crocus-ERA5 snow model⁷⁹ was aggregated over a given land region to produce daily snow mass time series. Peak snow mass values were then calculated for each water year, and the resulting series of values were used to calculate 2023 percentiles relative to the 1991–2020 reference period (Figure 16). In the majority of the North American basins the peak snow mass in 2023 was within the historical normal. Only in the Yukon, Nelson-Saskatchewan, Churchill and Colorado river basins and the Great Basin was the peak snow mass above or much above normal. Seasonal peak snow mass for 2023 was much above normal in North America and much below normal on the Eurasian continent.

GLACIERS

The present assessment of global glacier mass loss is based on a combination of glaciological field measurements (~500 glaciers or 1% of global glaciers) and geodetic satellite measurements (>200 000 glaciers or 96% of global glaciers) derived from the Fluctuations of Glaciers (FoG) database compiled by the World Glacier Monitoring Service.^{80,81} Winter and summer regional balances are calculated by downscaling the annual values using seasonal observations from FoG and the sine function analytical model proposed by Zemp and Welty (Figure 17).⁸²

GLACIER CONTRIBUTION TO SEASONAL RIVER RUNOFF

The annual mass balance of a glacier, defined as the difference between winter snow accumulation (mass gain) and summer melt (mass loss), reflects atmospheric conditions and serves as a key indicator of climate change. The global net loss of glacier mass contributes to sea level rise. Seasonal melting of ice and snow contributes to runoff. Therefore, glaciers

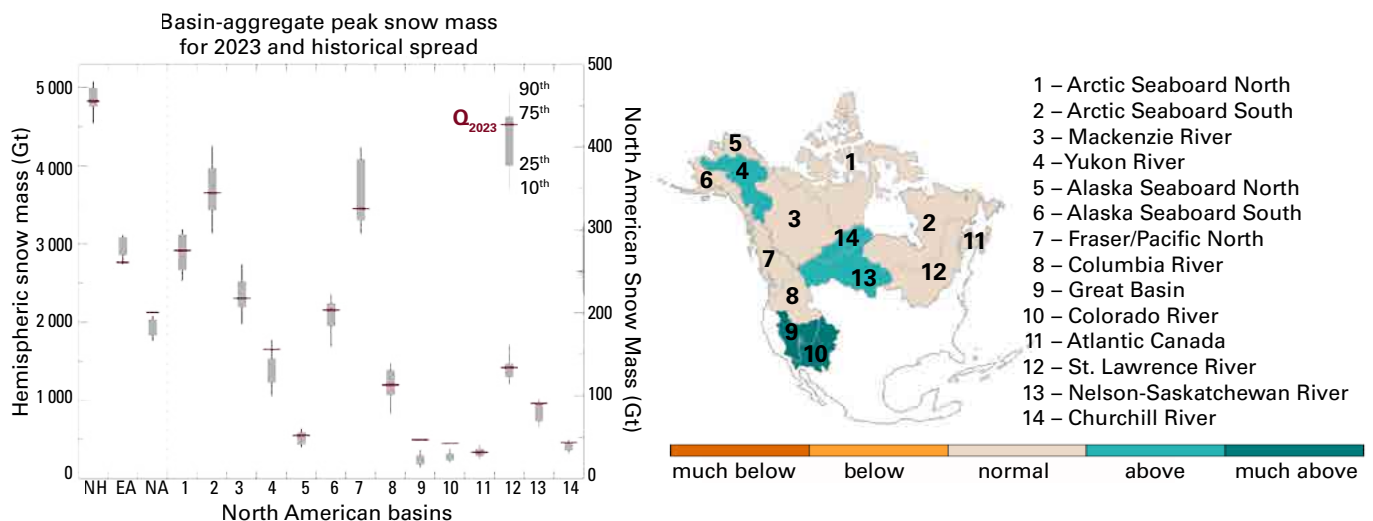


Figure 16. Box and whisker plot (left) showing seasonal peak snow mass for 2023 compared to historical spread (1991–2020) over various regions: entire northern hemisphere (NH), Eurasian continent (EA), North American continent (NA) and selected North American basins (numbered). Box and whiskers illustrate historical spread with percentile values as shown in legend. Values for 2023 shown by red lines. Map (right) illustrates category rankings for 2023 snow mass compared to reference period.

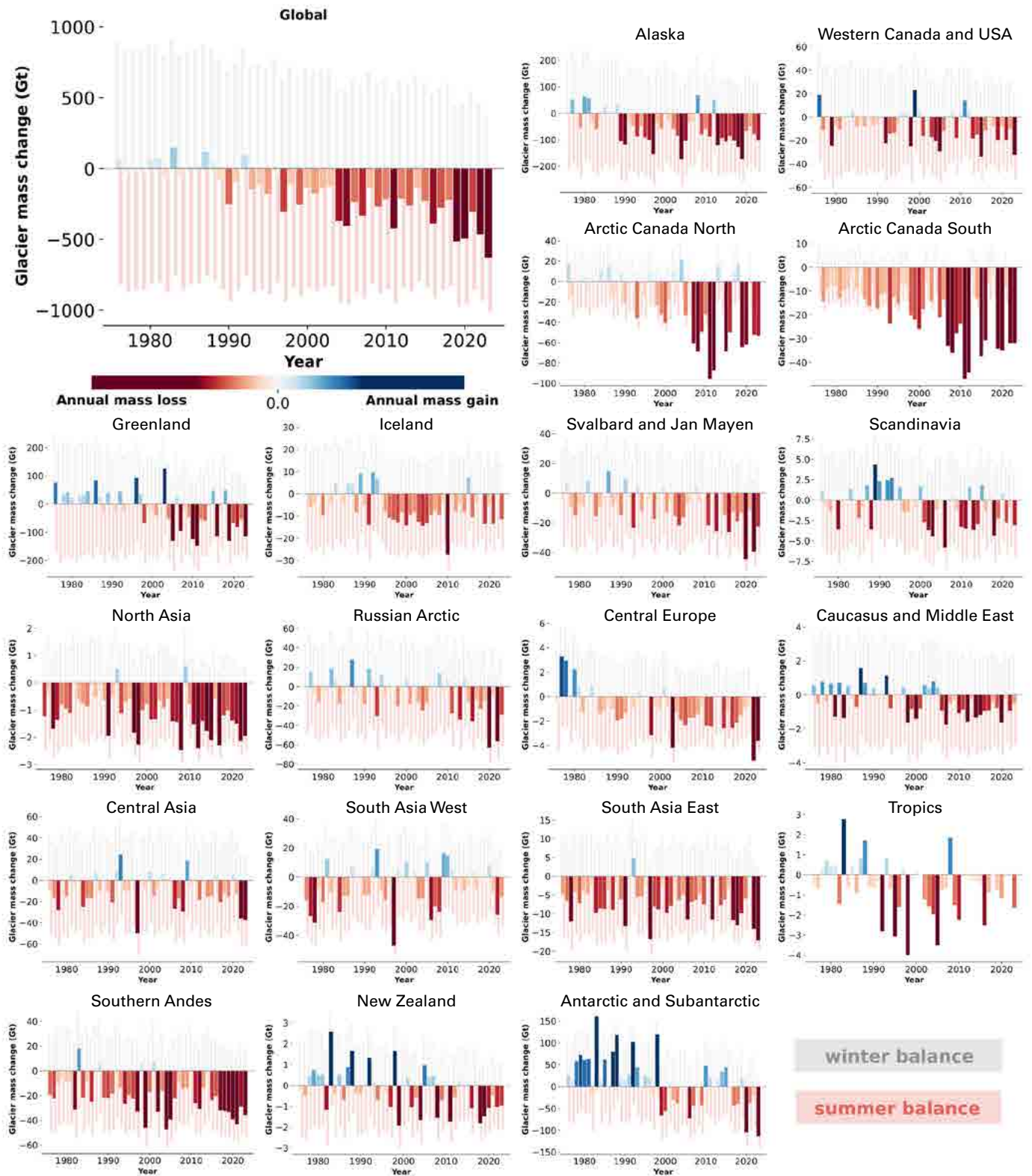


Figure 17. Annual and seasonal mass changes in gigatonnes (Gt) from 1976 to 2023 for the 19 GTN-G glacier regions. Annual net mass loss is represented in red and net mass gain in blue with white corresponding to balanced years. The colour scale is set to the regional annual net mass change range, with darker colours representing the most negative and positive years, respectively.⁸³



contribute to seasonal runoff even in years with balanced conditions or positive annual mass balance. This can be seen in Figure 17, where negative summer mass balance values (ice mass loss contributing to river flow) are measured even in years in which regions experienced a net positive annual mass balance (blue bars, for example the early 1990s in Scandinavia, or 1983 in most regions).

In many regions, precipitation and snowmelt primarily drive seasonal streamflow, but glaciers play a crucial role during specific months, especially in arid and semi-arid regions. Here, the delayed release of meltwater from glaciers helps sustain river flows during the driest months and periods of drought.^{84,85,86,87,88}

As glaciers respond to warming, their runoff initially increases, reaching a point of “peak water”,⁸⁹ after which it declines as glacier volumes shrink.⁹⁰ If temperatures continue to increase, the glacier will disappear, and with it, its hydrological contribution. This trend is expected globally, with significant reductions in glacier runoff by the century’s end, particularly in Central Asia and the Andes, where glaciers provide over 50% of basin runoff. Many regions with smaller glaciers have likely already passed peak water.⁹¹

THE YEAR 2023 IN CONTEXT

In 2023, glaciers lost more than 600 Gt of water, the largest mass loss registered in the last five decades. This is about 100 Gt more than in any other year on record since 1976, equivalent to 1.7 mm of contribution to global mean sea level rise. After 2022, 2023 is the second consecutive year in which all glaciated regions in the world reported ice loss.

Global estimates of annual glacier mass loss are good indicators of annual glacier contribution to global sea level rise. However, because winters and summers occur at different times of the calendar year in the two hemispheres, looking at global winter and summer estimates is not as good a proxy to understand the impact of annual glacier mass loss on the hydrological cycle. Regional winter and summer mass balances, however, can provide a better understanding of the evolution and impact of glacier contribution to runoff.

Glaciers in many regions were close to balanced or had slightly negative conditions during the 1970s and 1980s, with alternating years of positive and negative balances. Since the 1990s, ice loss has been increasing in almost all regions, and it accelerated considerably after 2000.⁹² This is mostly due to regions consistently presenting larger summer melt than winter accumulation after the 1990s (Figure 18).

In most regions dominated by small glaciers, peak water has already been reached, or it is expected to occur within the coming decades.⁹³ The slightly reduced summer balance trends observed in Central Europe, Scandinavia, the Caucasus and Middle East, Arctic Canada North, South Asia West and New Zealand over the last years might indicate that these regions have passed peak water conditions. In contrast, the Southern Andes (dominated by the Patagonian region) and Russian Arctic, as well as Svalbard and Jan Mayen, seem to present melt rates that are still increasing slightly (Figure 17).

In Central Asia, approximately 28 000 glaciers in the Tien Shan and Pamir mountains serve as vital sources of fresh water, providing essential meltwater for agricultural, domestic and industrial use in the densely populated lowlands. However, over the years, most glaciers in Central Asia have shown a negative trend in mass balance. Small glaciers, in particular, exhibit more intensive retreat, evidenced by a significant reduction in area and surface elevation.



Figure 18. Glaciers and their mass balances as measured by glaciological expeditions conducted in Central Asia in 2023

Source: Nikolay Kassatkin, Central Asian Regional Glaciological Centre under the auspices of UNESCO; Kabutov Khusrav, Center for Glacier Research of the National Academy of Sciences of Tajikistan; Abror Gafurov, GFZ; Gulomjon Umirzakov, National University of Uzbekistan; Ryskul Usabaliyev, CAIAG, Iulii Didovets, Potsdam Institute for Climate Impact Research, Green Central Asia programme



For instance, the Central Tuyuksu Glacier in Kazakhstan recorded a mass balance of -28.0 m or -0.42 m water equivalent per year from 1958 to 2022. In Uzbekistan during the 2022/2023 season the Barkrak Glacier experienced its highest melt since surveys began in 2016, with a change of -81 cm. Figure 18 presents the mass balance data for the Barkrak and Tuyuksu glaciers, alongside photos from other glaciers in the region obtained during expeditions in 2023, highlighting these changes.

Similarly, the glaciers of tropical areas (low latitudes) in northern South America (specifically in Colombia) are also natural indicators of the climate change trend. The glacier area in Colombia continues to decrease, despite the occurrence of the La Niña climate variability phenomenon in 2021 and 2022. At the beginning of 2022, it was 33.09 ± 0.63 km², which, compared to the area at the beginning of 2021 (34.20 ± 0.67 km²), shows a reduction of approximately 1.11 km² (3.2%) of the national glacier cover.⁹⁴

High-impact hydrological events

This chapter presents a non-exhaustive review of selected major extreme events that occurred in 2023 (Figure 19). The events were selected based on the number of deaths (>100) or overall impact on people affected/displaced, using data from several sources, including the EM-DAT database,⁹⁵ WMO *State of the Global Climate 2023* (WMO-No. 1347), direct communication of WMO Members to the WMO Secretariat through an online form and other public sources such as ReliefWeb.

FLOODING IN LIBYA

The extreme Mediterranean tropical cyclone *Daniel* reached north-eastern Libya on 10 and 11 September, leading to unprecedented rainfall. Al-Bayda station recorded an extraordinary 414 mm of rain within a 24-hour period, which caused severe flooding across the area. The most catastrophic effects were witnessed in Derna, where significant portions of the city centre were destroyed and swept into the sea due to floodwaters and the collapse of two dams.⁹⁶ The disaster was unprecedented, leading to at least 4 700 deaths, with more than 8 000 missing.⁹⁷ It affected nearly 22% of the nation's population.⁹⁸ The estimated cost for reconstruction and recovery from the devastating floods amounts to USD 1.8 billion, which represents 3.6% of Libya's gross domestic product (GDP) for 2022.⁹⁹ The housing sector was particularly hard hit, with over 18 500 homes either destroyed or damaged, accounting for 7% of all housing in the country.¹⁰⁰

FLOODING IN DEMOCRATIC REPUBLIC OF THE CONGO AND RWANDA

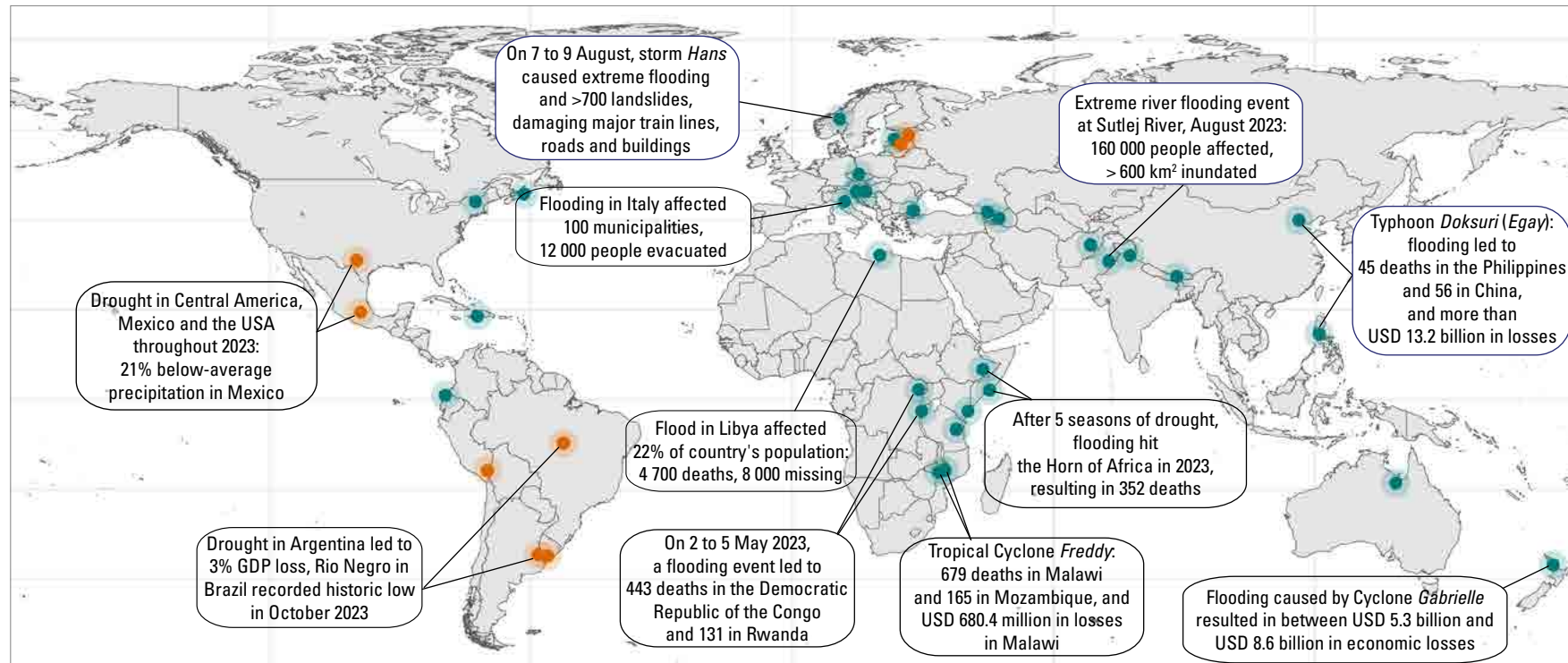
From 2 to 5 May 2023, a significant flooding event accompanied by landslides impacted the Lake Kivu area, situated on the border between Rwanda and the Democratic Republic of the Congo, in Central Africa. On 2 May, Mushubati in Rwanda recorded 182.6 mm of rainfall, setting a new national daily record.¹⁰¹ The event resulted in at least 574 casualties, with 443 in the Democratic Republic of the Congo and 131 in Rwanda.¹⁰²

FLOODING IN THE HORN OF AFRICA

Following five consecutive seasons of below-average rainfall, which led to one of the most severe droughts ever recorded in the region, the Horn of Africa experienced significant flooding in 2023, especially later in the year, due to heavy rains linked to El Niño and the positive Indian Ocean Dipole.¹⁰³ Starting in October, this persistent rainfall caused almost 4 million people to be displaced throughout Somalia, Kenya and Ethiopia.¹⁰⁴ In these devastating events, more than 350 persons lost their lives in Somalia, Kenya and Ethiopia.¹⁰⁵

FLOODING IN MOZAMBIQUE AND MALAWI

In March 2023, Malawi and Mozambique faced one of the most severe tropical cyclones on record, Tropical Cyclone *Freddy*, which originated in the Western Indian Ocean and tracked eastwards.¹⁰⁶ This storm brought unprecedented rainfall to southern Malawi. The most devastating effects of *Freddy* occurred during its final landfall, affecting both Mozambique and Malawi with exceptionally intense rainfall, reaching up to 672 mm in Mozambique.¹⁰⁷



Data sources: WMO Members, *State of the Global Climate 2023* (WMO-No. 1347), EM-DAT and others

● Drought ● Flood/Heavy rainfall

Figure 19. Selected notable high-impact hydrological events across the globe in 2023



Both countries were still reeling from storms in 2022.^{108,109} Malawi, in particular, was significantly affected by *Freddy*, with at least 679 lives lost,¹¹⁰ and Mozambique reported a further 165 fatalities.¹¹¹ The total cost of recovery and reconstruction is USD 680.4 million in Malawi.¹¹²

DROUGHT IN CENTRAL AMERICA AND THE SOUTHERN UNITED STATES

Throughout 2023, a severe drought spread from the southern United States across much of Mexico and Central America.¹¹³ Initially emerging in Honduras and Panama in April, the drought extended to most of eastern Central America by May and reached much of Mexico by June and July.¹¹⁴ By late August, areas in eastern Texas and Louisiana (United States) were experiencing exceptional drought conditions. Mexico recorded its driest year ever, with precipitation levels 21% below normal, impacting nearly all regions at various times throughout the year. However, late in the year, tropical cyclones brought significant rainfall that alleviated drought conditions in Baja California and some Pacific coastal areas.¹¹⁵ Also, in August 2023, the negative precipitation anomaly showed slight improvement in eastern Central America, specifically Honduras, Nicaragua and Guatemala, yet meteorological drought conditions continued to persist across the region.¹¹⁶ Heatwave and associated drought caused USD 14.5 billion losses in the United States.¹¹⁷

DROUGHT IN ARGENTINA, URUGUAY AND BRAZIL

From August 2022 to March 2023 in Argentina, rainfall was 20% to 50% below normal across much of the northern and central regions, marking the fourth consecutive year of significantly reduced precipitation.¹¹⁸ Uruguay faced critically low water storage levels, affecting water supply in Montevideo and other large centres.¹¹⁹ In Brazil, the Amazon saw below-normal rainfall, with eight states experiencing the lowest rainfall from July to September in over 40 years.¹²⁰ On 26 October the Rio Negro at Manaus saw the lowest level recorded since 1902, with water levels reaching 12.70 m.¹²¹ The Amazon region experienced a loss of storage between 2022 and 2023, resulting in the longest drought ever recorded in the basin.^{122,123} In the central and north-eastern regions of Brazil, the gain in groundwater storage can be associated with intense precipitation processes between 2022 and 2023,^{124,125} interrupting a long trend of storage loss.¹²⁶ In a complementary way, in the south-eastern portion of Brazil a loss of storage was observed in the monitoring wells with a probable origin in the typical pattern of precipitation induced by La Niña – a dipole of anomalies between the north-east and the south-west.¹²⁷ The drought led to a 3% GDP reduction in Argentina in 2023.¹²⁸

DROUGHT IN PERU

During January 2023, several rivers on the Lake Titicaca drainage (TLD) in Peru presented hydrological droughts characterized as extreme by the National Meteorological and Hydrological Service of Peru (SENAMHI). Thus, the river discharges of the TLD tributaries to Lake Titicaca in Peru (Ramis, Coata, Huanacán and Ilave) presented anomalies characterized by SENAMHI as “well below normal”; these droughts had been more extreme since the 1990s.¹²⁹ These rivers’ discharge anomalies in the TLD are associated with the precipitation deficits that occurred during the pre-rainy-season period (October–December 2022), when the TLD and the adjacent Andean–Amazon region experienced reductions of up to 60% in precipitation. Consequently, Lake Titicaca water levels decreased by 0.05 m from December to January. Such conditions had not been seen since the El Niño-related drought of 1982/1983. This new



historic drought was associated with southern moisture flux anomalies, which reduced the input of moisture-laden winds from the Amazon Basin to the TLD. Anomalies of this type in moisture transport had not been observed since at least the 1950s.¹³⁰

FLOODING ON THE NORTH ISLAND OF NEW ZEALAND

In early 2023, the east coast of New Zealand's North Island faced severe flooding during Cyclone *Gabrielle* on 13–14 February, which delivered over 500 mm of rainfall in a day in some areas, resulting in 15 deaths¹³¹ and economic losses estimated between USD 5.3 billion and 8.6 billion.^{132,133}

FLOODING IN CHINA AND THE PHILIPPINES

In July 2023 Typhoon *Doksuri (Egay)* caused substantial flooding in both the Philippines and China, with some of the most significant flooding occurring in the Beijing region from the remnants of the storm. A 24-hour total of 744.8 mm was observed at Wangjiayuan Reservoir, in the hills near Beijing. *Doksuri* led to 56 fatalities in China, and 45 in the Philippines.^{134,135} Officials in China have estimated an economic loss of more than USD 13.2 billion.¹³⁶

FLOODING IN ITALY

Two intense rainfall events in the first half of May (1–3 May, 16–18 May) led to extensive flooding in Italy.¹³⁷ The hydrological combination of the two intense weather events, which had similar amounts of rainfall (210 mm total precipitation in the first one, 240 mm in the second one),¹³⁸ amplified the impacts of the second one, resulting in the flooding of an area of 540 km² with approximately 350 million cubic metres of water.¹³⁹ This impacted 100 municipalities in the Emilia-Romagna region. Twenty three rivers overflowed, due mainly to diffuse levee breaches, and 13 others rose to alarming levels, resulting in thousands of landslides, which led to 15 persons losing their lives and 23 067 individuals being evacuated.¹⁴⁰ The majority of evacuees were in the Ravenna area (16 445), with 4 462 in the province of Forlì-Cesena and 2 160 in the Bologna area.¹⁴¹ The flood caused USD 8.6–9.75 billion in losses.^{142,143}

Early warning systems in Italy^{144,145}

STATE OF EMERGENCY AND ACTIONS TAKEN DURING THE EMILIA-ROMAGNA FLOODS, MAY 2023

The national early warning service (network of regional coordinated centres) issued red alerts on 16 May with 24 hours' notice and the description of the expected impacts, in particular, a forecast of floods close to the embankment levels and historical maximums in the Romagna basins and tributaries of the Reno River, and the possibility of numerous and extensive landslides. The precipitation observed in the first half of May was eight times the climatological monthly average.¹⁴⁶ Twenty three rivers had overflowed by 25 May 2023, and 13 had reached threatening water levels, resulting in thousands of landslides, 15 deaths, the evacuation of more than 23 000 people and the closure of almost 700 roads.^{147,148,149}

Role of the Early Warnings for All (EW4All) initiative:

The advance prediction of the event, with the issuing of the civil protection red alert, allowed the highest level of mobilization to be put in place, through the activation of the national Crisis Unit and the regional mobile columns,¹⁵⁰ with numerous evacuations, both preventive and during the event.

Synthesis

This 2023 edition of the State of Global Water Resources report continues to build on the increasing engagement from WMO Members, NMHSs and global hydrological modelling communities.

The 2023 report benefitted from a significant increase in observed data points. The number of in situ discharge measurement stations rose from 273 in 14 countries in the previous annual report to 713 stations (out of 1 595 stations that were available in total, many of which could not be used because of gaps in the time series) in 33 countries. There was also a substantial increase in groundwater data collection, with data from over 35 000 wells in 40 countries being used (out of more than 130 000 from which data were originally collected), compared to 8 246 wells in 10 countries in 2022. This increased availability of data has been crucial for assessing water resource conditions more extensively and validating the modelling tools used. The majority of data points for discharge were concentrated in Europe and North America, with 46% and 21% of the stations, respectively. Meanwhile, Africa, South America and Asia were still underrepresented, underscoring the need for increased and improved hydrological monitoring efforts and data sharing in underrepresented regions, particularly in the developing countries. Also, stations in Europe were located mainly in Scandinavia, which could influence the interpretation of the results, as the signal from Southern/Central Europe will be missing from any analysis based on in situ observation only. The contribution from the International Soil Moisture Network (ISMN) underscores the importance of in situ soil moisture data. These soil moisture measurements are foundational for validating satellite and modelled soil moisture products and are crucial for environmental assessments. However, challenges persist with in situ data (out of 3 000 stations in the ISMN network, only 160 could be used for this study due to data gaps), including their localized nature, lack of standardization across institutions and difficulties in maintaining data continuity when sensors are replaced. Despite these challenges, in situ data remain vital as the only direct measure of soil water availability. The 2023 report also highlighted the potential usage of Earth observation-based products to augment existing observation data by infilling gaps. In general, an urgent need remains for more support from WMO Members to build better monitoring networks and use innovative methods to improve data management and data sharing.

The 2023 report includes new chapters and variables, such as lake volumes, reservoir volumes and snow water equivalent, thus offering a more comprehensive picture of the global water cycle. This expanded scope contributes to a better understanding of the interconnectedness of different hydrological factors and their impact on water resource management. Substantial contributions from the global hydrological modelling community strengthened the analysis of variables such as evapotranspiration, soil moisture, snow and ice cover and terrestrial water storage (TWS). These contributions are particularly valuable for data-sparse regions and help reduce uncertainty in the findings, providing more reliable information for policymaking.

Validation of modelled results for 2023 showed agreement in over 73% of basins between observed and simulated anomalies, especially in Central and Northern Europe, New Zealand, Australia, the upper Paraná River in Brazil and Paraguay, the Ganges in India and the Irrawaddy River in Myanmar. However, discrepancies between modelled and observed anomalies were noted in South Africa, the upper Amazon basin, the Lule basin in Sweden, the Nelson and upper Mississippi basins in North America, and the Niger River in Africa. While models are able to provide a coherent and trustworthy picture of the discharge conditions in many catchments around the world, validation of the results plays a critical role in the assessment of the results. In general, a global systematic observing system for the global hydrological cycle is still lacking, due to lack of in situ measurements and/or data exchange. This report highlights the benefit of having both better monitoring and the implementation of the WMO Unified Data Policy for hydrological observations to ensure that Members are able to calibrate and run hydrological models which help in assessing the current status as well as make



forecasts, thus aiding water management. The principle of having a common method, used across the globe, for the indicator calculations and common variables also underpins the WMO HydroSOS initiative to unite hydrological monitoring and forecasting systems worldwide.

The year 2023 was marked by unprecedented heat, becoming the hottest year on record at 1.45 °C above pre-industrial levels. Europe, North America and China faced heatwaves, while Canada experienced its most extreme wildfire season ever, with over 18 million hectares affected. The transition from La Niña to El Niño conditions contributed to this extreme heat and varied weather impacts, including heavy rains, floods and droughts. Total precipitation in 2023 exceeded the long-term normal in several regions, including East and Central Asia, parts of North Asia, the western Indian summer monsoon area, and parts of Africa, Europe and North America. Significant rainfall deficits were observed in south-eastern South America, the Amazon basin, much of Central America, southern Canada, the western Mediterranean region, and parts of Africa and Asia.

The year 2023, compared to the historical period, was marked by mostly drier-than-normal to normal discharge conditions. Similar to 2022 and 2021, over 50% of global catchment areas showed river discharge deviations from near-normal conditions, predominantly lower than normal, with fewer basins exhibiting above- and much-above-normal conditions.

In the Americas, below- and much-below-normal conditions prevailed across large territories. Throughout most of North America, except for Alaska, 2023 was characterized by below- to much-below-normal discharge conditions. In fact, in the southern United States drought conditions had already been in place for more than three years. In 2023 Central America and South America also experienced below-normal to much-below-normal conditions across almost their entire territories. In 2023, every country in the Amazon basin saw record low levels of rainfall. As a result, reservoir inflows were lower than usual across North and South America, particularly in the Mackenzie River in North America, Mexico and the Paraná River in southern Brazil and Argentina. Groundwater levels in North America were also below normal, particularly in the western and central United States, as they were in central and northern Chile, and in western and southern Brazil, likely due to prolonged drought conditions. Also, soil moisture was below normal across North and South America during June–August. As reported by the United States National Oceanic and Atmospheric Administration (NOAA),¹⁵¹ 2023 ranks just behind 2022 in the recent historical record for dry soils in the United States. Following reduced water availability, the AET values were much below normal in Central America, Brazil and Argentina in September–November, and over the entire year in Mexico. Much-below-normal TWS values reflected significant water storage deficits in this region; for example, the La Plata region saw below-normal TWS, consistent with dry soil moisture conditions. North America’s Nelson and Columbia catchments saw above- and much-above-normal March SWE, respectively. Also, the peak snow mass in the southern Colorado basin and Great Basin was much above normal. Glaciers in the southern Andes (dominated by the Patagonian region) presented slightly increasing melt rates.

Discharge conditions in Europe saw varying patterns. Northern Europe, including the United Kingdom and Ireland, experienced above-normal river discharge, and groundwater levels were also above-normal. Reservoir inflows in Northern Europe, particularly Sweden, were higher than usual, reflecting the discharge patterns. Only the far north of Norway saw below-normal inflows. Central and Western Europe exhibited normal annual discharge conditions; however, northern Italy was hit by a devastating flood. Much-above-normal subsurface water storage was observed in the Netherlands and north-western Germany due to positive precipitation anomalies, leading to year-end floods in those regions. Meanwhile, dry conditions persisted in France, southern and eastern Germany, the Alps, northern Italy and the Baltic Sea area, continuing the drought trends from previous years, although near-surface water storage



showed some improvement in 2023 due to above-normal spring and autumn rainfall. The TWS was below normal and much below normal across Southern, Central and Eastern Europe, with some hotspots in Sweden and Norway.

The Iberian Peninsula faced much-below-normal AET during spring, while Central, Eastern and Northern Europe exhibited above- and much-above-normal AET over the autumn months. Groundwater levels were below normal in Southern Europe, including Portugal, Spain and most of France, as well as Central Europe. Soil moisture conditions were predominantly below normal, particularly during June, July and August. March snow mass for 2023 was much below normal in the Eurasian continent, the basins of the Dnieper, Don, Danube, Ural, Amur and Yangtze all experienced below- to much-below-normal March SWE levels. Groundwater levels in Southern Europe, including Portugal, Spain and most of France, as well as in Central Europe, were below normal. Glaciers of Europe and the Caucasus showed slightly reduced summer balance trends in 2023 as well as previous years.

Africa was hit by severe floods in 2023. Libya, Mozambique, Malawi, the Democratic Republic of the Congo, Rwanda and the Horn of Africa (which had suffered from five consecutive low rainy seasons) all faced severe flooding, likely triggered by El Niño conditions. The floods led in total to more than 12 600 casualties, with over 11 000 victims in Libya alone. The east coast of Africa, including the Limpopo and Zambezi river basins, experienced above- and much-above-normal river discharge. Reservoirs in South Africa saw above-normal inflows following above-normal discharge conditions. Soil moisture levels across sub-Saharan Africa were generally below normal, except in South Africa, which experienced above-normal soil moisture conditions. Evapotranspiration (AET) rates in sub-Saharan Africa during the December–February and June–August months were normal to below normal, except for West Africa and the coastal basins in South Africa. The Horn of Africa showed above-normal AET during the March–May and September–November months, with intense rainfall and associated flooding experienced in October. Groundwater levels across much of North Africa, including Libya, were below normal, reflecting long-term declines likely due to over-abstraction rather than climatic factors. Sub-Saharan Africa and the Horn of Africa both experienced much-above-normal TWS in 2023, reflecting a significant and persistent increase in water storage since 2019, highlighting long-term positive trends in these regions.

In Asia significant flooding occurred in the Philippines and China due to Typhoon *Doksuri*. The east coast of the North Island of New Zealand faced severe flooding during Cyclone *Gabrielle*. Major river basins such as the Ganges, Brahmaputra and Mekong experienced below-normal conditions throughout most of the year. The northern and eastern coasts of Australia saw above-normal discharge conditions, while the Murray–Darling basin experienced predominantly normal conditions; the reservoirs there had above-normal inflows. The Murray–Darling Basin also experienced above- to much-above-normal TWS, while New Zealand saw mixed conditions, with the North Island having normal TWS and the South Island experiencing much-below-normal TWS. Soil moisture levels were predominantly below normal in Central Asia and China during the summer months. However, India saw much-above-normal soil moisture conditions, indicating regional variability. Evapotranspiration (AET) rates were high across several regions. India experienced much-above-normal AET during the March–May period, and catchments in the far eastern Russian Federation, such as the Ob and Enisey, also saw much-above-normal AET during June–August and September–November. Central Asian catchments like that of the Syr Darya experienced above-normal AET during September–November. Groundwater levels in several parts of India were above normal due to increased rainfall. However, over-abstraction impacted groundwater levels in the north of India, with most data reflecting climatic conditions. The eastern basins of the Danube and Dnieper saw above-normal discharge conditions. In 2023, SWE levels varied, with northern catchments



of the Lena and Khatanga Rivers in the far-eastern Russian Federation experiencing much-above-normal SWE in March. However, most catchments below 50°N latitude had below- to much-below-normal March SWE, indicating an earlier onset of snowmelt due to rising temperatures. The slightly reduced summer glacier balance trends observed over western South Asia and New Zealand over the last few years might indicate that these regions have passed peak water conditions, while the Russian Arctic and Svalbard still seem to present slightly increasing melt rates. In Central Asia, most glaciers have shown a negative trend in mass balance. Small glaciers, in particular, exhibit more intensive retreat, evidenced by a significant reduction in area and surface elevation, as is the case for the Central Tuyuksu Glacier in Kazakhstan and Barkrak Glacier in Uzbekistan.

Endnotes

- ¹ United Nations (UN). *Summary of Proceedings by the President of the General Assembly: United Nations Conference on the Midterm Comprehensive Review of the Implementation of the Objectives of the International Decade for Action “Water for Sustainable Development”, 2018–2028*; UN, 2023. <https://www.un.org/pga/77/wp-content/uploads/sites/105/2023/05/PGA77-Summary-for-Water-Conference-2023.pdf>.
- ² The findings presented in this chapter largely follow the information presented in WMO’s *State of the Global Climate 2023* (WMO-No. 1347).
- ³ Lindsey, R. *Climate Change: Atmospheric Carbon Dioxide* webpage. National Oceanic and Atmospheric Administration (NOAA) Climate.gov. <https://www.climate.gov/news-features/understanding-climate/climate-change-atmospheric-carbon-dioxide>.
- ⁴ World Meteorological Organization (WMO). *WMO Global Annual to Decadal Climate Update: 2024–2028*; WMO: Geneva, 2024.
- ⁵ <https://www.worldweatherattribution.org/climate-change-made-the-deadly-heatwaves-that-hit-millions-of-highly-vulnerable-people-across-asia-more-frequent-and-extreme/>
- ⁶ World Meteorological Organization (WMO). *State of the Global Climate 2023* (WMO No. 1347). Geneva, 2024.
- ⁷ <https://www.worldweatherattribution.org/climate-change-fuelled-extreme-weather-in-2023-expect-more-records-in-2024/>
- ⁸ WMO Members have different criteria to declare ENSO modes, and those that look at ocean parameters first may have declared El Niño earlier.
- ⁹ See [Table A1](#) in the Annex for a list of GHMSs contributing to each variable.
- ¹⁰ Global Runoff Data Centre (GRDC). WMO *Basins and Sub-Basins*; 3rd rev. ext. ed., Federal Institute of Hydrology (BfG): Koblenz, Germany, 2023.
- ¹¹ Elmi, O.; Tourian, M. J.; Saemian, P. et al. Remote Sensing-Based Extension of GRDC Discharge Time Series - A Monthly Product with Uncertainty Estimates. *Scientific Data* **2024**, 11 (1), 240. <https://doi.org/10.1038/s41597-024-03078-6>.
- ¹² Biswas, N. K.; Hossain, F.; Bonnema, M. et al. Towards a Global Reservoir Assessment Tool for Predicting Hydrologic Impacts and Operating Patterns of Existing and Planned Reservoirs. *Environmental Modelling & Software* **2021**, 140, 105043. <https://doi.org/10.1016/j.envsoft.2021.105043>.
- ¹³ Hou, J.; van Dijk, A. I. J. M.; Beck, H. E. et al. Remotely Sensed Reservoir Water Storage Dynamics (1984–2015) and the Influence of Climate Variability and Management at a Global Scale. *Hydrology and Earth System Sciences* **2022**, 26 (14), 3785–3803. <https://doi.org/10.5194/hess-26-3785-2022>.
- ¹⁴ Hou, J.; Van Dijk, A. I. J. M.; Renzullo, L. J. et al. GloLakes: Water Storage Dynamics for 27 000 Lakes Globally from 1984 to Present Derived from Satellite Altimetry and Optical Imaging. *Earth System Science Data* **2024**, 16 (1), 201–218. <https://doi.org/10.5194/essd-16-201-2024>.
- ¹⁵ Landerer, F. W.; Flechtner, F. M.; Save, H. et al. Extending the Global Mass Change Data Record: GRACE Follow-On Instrument and Science Data Performance. *Geophysical Research Letters* **2020**, 47 (12), e2020GL088306. <https://doi.org/10.1029/2020GL088306>.
- ¹⁶ Belleflamme, A.; Goergen, K.; Wagner, N. et al. Hydrological Forecasting at Impact Scale: The Integrated ParFlow Hydrological Model at 0.6 Km for Climate Resilient Water Resource Management over Germany. *Frontiers in Water* **2023**, 5. <https://doi.org/10.3389/frwa.2023.1183642>.
- ¹⁷ Mudryk, L. R.; Elias Chereque, A.; Derksen, C. et al. *NOAA Arctic Report Card 2023: Terrestrial Snow Cover*; NOAA Technical Report OAR ARC; 23-03; National Oceanic and Atmospheric Administration (NOAA): 2023. <https://repository.library.noaa.gov/view/noaa/56613>.
- ¹⁸ Mudryk, L. R.; Elias Chereque, A.; Derksen, C. et al. Terrestrial Snow Cover [in “State of the Climate in 2023”]. *Bulletin of the American Meteorological Society* **2024**, 105 (8), S307–S310. <https://doi.org/10.1175/BAMS-D-24-0101.1>.
- ¹⁹ EM-DAT, CRED/UCLouvain, Brussels, Belgium. <http://www.emdat.be>.
- ²⁰ In this report, the term “anomaly” is used to describe the status of water resources in each basin in comparison to the long-term historical near-normal conditions for that basin.
- ²¹ Historical periods differ from variable to variable, as well as spatially for observed discharge data; refer to [Table A2](#) in the Annex.



- ²² Note that throughout the text the term “normal” refers to near-normal conditions for each variable.
- ²³ World Meteorological Organization (WMO) Hydrological Coordination Panel. *Statement on the Term Hydrological Normal*. https://wmoomm.sharepoint.com/b:s/wmocpdb/Eet3ljBnhyZloWU5xIATC7UBAF0GsATvEuhf8SE_Xzes0Q.
- ²⁴ Lehner, B.; Verdin, K.; Jarvis, A. New Global Hydrography Derived from Spaceborne Elevation Data. *Eos, Transactions American Geophysical Union* **2008**, *89* (10), 93–94. <https://doi.org/10.1029/2008EO100001>.
- ²⁵ More data will likely be available and accessible for all regions in the future, but quality assured data were not available in time to be considered in this report.
- ²⁶ More than 50% of models agreed on the trend for 97% of the area.
- ²⁷ Note that there was a change in basin delineation adopted in 2022, and the number of models was different from year to year.
- ²⁸ National Oceanic and Atmospheric Administration (NOAA) National Centers for Environmental Information (NCEI). *Annual 2023 Drought Report*; NCEI: 2024. <https://www.ncei.noaa.gov/access/monitoring/monthly-report/drought/202313>.
- ²⁹ Espinoza, J.-C.; Jimenez, J. C.; Marengo, J. A. et al. The New Record of Drought and Warmth in the Amazon in 2023 Related to Regional and Global Climatic Features. *Scientific Reports* **2024**, *14* (1), 8107. <https://doi.org/10.1038/s41598-024-58782-5>.
- ³⁰ Espinoza, J.-C.; Jimenez, J. C.; Marengo, J. A. et al. The New Record of Drought and Warmth in the Amazon in 2023 Related to Regional and Global Climatic Features. *Scientific Reports* **2024**, *14* (1), 8107. <https://doi.org/10.1038/s41598-024-58782-5>.
- ³¹ World Health Organization (WHO). *SITUATION REPORT: 01 November–31 December 2023. Greater Horn of Africa Food Insecurity and Health Grade 3 Emergency*; WHO: Geneva, 2024. <https://www.who.int/publications/m/item/situation-report-greater-horn-of-africa-food-insecurity-and-health-grade-3-emergency-01-november-31-december-2023>.
- ³² Biswas, N. K.; Hossain, F.; Bonnema, M. et al. Towards a Global Reservoir Assessment Tool for Predicting Hydrologic Impacts and Operating Patterns of Existing and Planned Reservoirs. *Environmental Modelling & Software* **2021**, *140*, 105043. <https://doi.org/10.1016/j.envsoft.2021.105043>.
- ³³ van Verseveld, W. J.; Weerts, A. H.; Visser, M. et al. Wflow_sbm v0.6.1, a Spatially Distributed Hydrologic Model: from Global Data to Local Applications. *Geoscientific Model Development Discussions* **2022** [preprint]. <https://doi.org/10.5194/gmd-2022-182>.
- ³⁴ Hanazaki, R.; Yamazaki, D.; Yoshimura, K. Development of a Reservoir Flood Control Scheme for Global Flood Models. *Journal of Advances in Modeling Earth Systems* **2022**, *14* (3), e2021MS002944. <https://doi.org/10.1029/2021MS002944>.
- ³⁵ Yamazaki, D.; Kanae, S.; Kim, H. et al. A Physically Based Description of Floodplain Inundation Dynamics in a Global River Routing Model. *Water Resources Research* **2011**, *47* (4). <https://doi.org/10.1029/2010WR009726>.
- ³⁶ Arheimer, B.; Pimentel, R.; Isberg, K. et al. Global Catchment Modelling Using World-Wide HYPE (WWH), Open Data, and Stepwise Parameter Estimation. *Hydrology and Earth System Sciences* **2020**, *24* (2), 535–559. <https://doi.org/10.5194/hess-24-535-2020>.
- ³⁷ Lehner, B.; Reidy Liermann, C.; Revenga, C. et al. *Global Reservoir and Dam Database, Version 1 (GRanDv1): Dams, Revision 01*; NASA Socioeconomic Data and Applications Center (SEDAC), 2011. <https://doi.org/10.7927/H4N877QK>.
- ³⁸ Biswas, N. K.; Hossain, F.; Bonnema, M. et al. Towards a Global Reservoir Assessment Tool for Predicting Hydrologic Impacts and Operating Patterns of Existing and Planned Reservoirs. *Environmental Modelling & Software* **2021**, *140*, 105043. <https://doi.org/10.1016/j.envsoft.2021.105043>.
- ³⁹ Dataset includes lake volume data for any lakes or reservoirs with an area exceeding 500 km², if they are accurately measured by remote sensing (not all large lakes are included).
- ⁴⁰ Hou, J.; van Dijk, A. I. J. M.; Beck, H. E. et al. Remotely Sensed Reservoir Water Storage Dynamics (1984–2015) and the Influence of Climate Variability and Management at a Global Scale. *Hydrology and Earth System Sciences* **2022**, *26* (14), 3785–3803. <https://doi.org/10.5194/hess-26-3785-2022>.
- ⁴¹ Hou, J.; Van Dijk, A. I. J. M.; Renzullo, L. J. et al. GloLakes: Water Storage Dynamics for 27 000 Lakes Globally from 1984 to Present Derived from Satellite Altimetry and Optical Imaging. *Earth System Science Data* **2024**, *16* (1), 201–218. <https://doi.org/10.5194/essd-16-201-2024>.
- ⁴² Marmontel, M.; Fleischmann, A.; Val, A. et al. Safeguard Amazon’s Aquatic Fauna against Climate Change. *Nature* **2024**, *625* (7995), 450–450. <https://doi.org/10.1038/d41586-024-00114-8>.



- ⁴³ Santos de Lima, L.; Magalhães de Oliveira, H. F.; Fleischmann, A. S. et al. Extreme Drought Is Again Isolating People in Amazonia. *Nature* **2023**, 622 (7984), 697–697. <https://doi.org/10.1038/d41586-023-03311-z>.
- ⁴⁴ Environment and Climate Change Canada (ECCC). Great Lakes – St. Lawrence River Water Levels. *LEVELNews* **2023**, 31 (1). https://publications.gc.ca/collections/collection_2023/eccc/En162-1-31-1-eng.pdf.
- ⁴⁵ This reporting methodology has been peer-reviewed by several experts from national departments and research institutions. It builds upon the pilot study included in the previous edition. The data filtering and the spatial aggregation steps have been improved in particular. A complete description of the methodology can be found in the methodology report (<https://github.com/UNIGRAC/Global-Reporting-Groundwater-Levels>).
- ⁴⁶ The number of wells discarded during the data filtration step varies across countries.
- ⁴⁷ Chávez García Silva, R.; Reinecke, R.; Copty, N. K. et al. Multi-Decadal Groundwater Observations Reveal Surprisingly Stable Levels in Southwestern Europe. *Communications Earth & Environment* **2024**, 5 (1), 1–10. <https://doi.org/10.1038/s43247-024-01554-w>.
- ⁴⁸ Department of Water and Sanitation (DWS). *National State of Water Report 2023*; Integrated Water Resource Studies Report Number WII/IWRS/NSoW 2023; DWS: Pretoria, South Africa, 2024. https://www.dws.gov.za/Projects/National%20State%20of%20Water%20Report/Documents/National%20State%20of%20Water%20Report%202023_FinalVer3.0.pdf.
- ⁴⁹ Bhatnagar, I.; Dhanya, C. T.; Chahar, B. R. Do Groundwater Systems Experience a ‘Silent’ Stress? A Paradox of Rising Groundwater Levels and Stressed Aquifers. *Groundwater for Sustainable Development* **2024**, 25, 101111. <https://doi.org/10.1016/j.gsd.2024.101111>.
- ⁵⁰ Environmental Protection Agency (EPA). *Hydrology Bulletin on Rainfall, River Flows, Lake Levels, Groundwater Levels and Spring Outflows* **2023**, 40. <https://www.epa.ie/publications/monitoring--assessment/freshwater--marine/hydrology-bulletin/hydrology-bulletin/EPA-Hydrology-Bulletin-August-2023.pdf>.
- ⁵¹ Bureau of Meteorology (BOM). Australian Groundwater Insight webpage. <http://www.bom.gov.au/water/groundwater/insight/#/gwlevel/summary>.
- ⁵² Bureau of Meteorology (BOM). *Annual Climate Statement 2023: Groundwater Continues to Recover in the East while Declining in the Victoria–South Australia Border Region and South-west Western Australia* webpage. <http://www.bom.gov.au/climate/current/annual/aus/#tabs=Water&waterSection=Groundwater>.
- ⁵³ Taucare, M.; Viguier, B.; Figueroa, R. et al. The Alarming State of Central Chile’s Groundwater Resources: A Paradigmatic Case of a Lasting Overexploitation. *Science of The Total Environment* **2024**, 906, 167723. <https://doi.org/10.1016/j.scitotenv.2023.167723>.
- ⁵⁴ Brückner, F.; Bahls, R.; Alqadi, M. et al. Causes and Consequences of Long-Term Groundwater Overabstraction in Jordan. *Hydrogeology Journal* **2021**, 29 (8), 2789–2802. <https://doi.org/10.1007/s10040-021-02404-1>.
- ⁵⁵ In total, 63% of the monitoring network of India consists of shallow dug wells (see Central Ground Water Board (CGWB). *Groundwater Year Book India 2022–2023*. CGWB, 2023).
- ⁵⁶ Dangar, S.; Asoka, A.; Mishra, V. Causes and Implications of Groundwater Depletion in India: A Review. *Journal of Hydrology* **2021**, 596, 126103. <https://doi.org/10.1016/j.jhydrol.2021.126103>.
- ⁵⁷ Central Ground Water Board (CGWB). *Groundwater Year Book India 2022–2023*. CGWB, 2023.
- ⁵⁸ Central Ground Water Board (CGWB). *National Compilation on Dynamic Ground Water Resources of India, 2023*. CGWB, 2023.
- ⁵⁹ Mieno, T.; Foster, T.; Kakimoto, S. et al. Aquifer Depletion Exacerbates Agricultural Drought Losses in the US High Plains. *Nature Water* **2024**, 2 (1), 41–51. <https://doi.org/10.1038/s44221-023-00173-7>.
- ⁶⁰ European Environment Agency (EEA). *Europe’s Groundwater – a Key Resource under Pressure*; EEA, 2022. <https://www.eea.europa.eu/publications/europes-groundwater>.
- ⁶¹ European Environment Agency (EEA). *Soil Moisture Deficit*; EEA, 2021. <https://www.eea.europa.eu/ims/soil-moisture-deficit>.
- ⁶² Global Climate Observing System (GCOS). *Soil Moisture: Essential Climate Variable (ECV) Factsheet* webpage. <https://gcos.wmo.int/en/essential-climate-variables/soil-moisture>.
- ⁶³ ISMN hosts the largest global collection of freely available soil moisture observations, harmonizing and quality-controlling data from around the world. The network primarily consists of research institutions, leading to relatively short observation periods, averaging 10 years across approximately 3 000 sites.



- ⁶⁴ Due to the clustering of available observation points the map in Figure 9 could not reproduce this observation.
- ⁶⁵ National Oceanic and Atmospheric Administration (NOAA) National Centers for Environmental Information (NCEI). *Annual 2023 Drought Report*; NCEI: 2024. <https://www.ncei.noaa.gov/access/monitoring/monthly-report/drought/202313>.
- ⁶⁶ Here we refer to actual evapotranspiration as AET or evapotranspiration throughout the text. Actual ET should not be mixed with potential ET. AET measures the amount of water that is actually evapotranspired and is limited by the amount of water that is available, while PET is the maximum amount of water that would be evapotranspired if enough water were available.
- ⁶⁷ Lehner, B.; Verdin, K.; Jarvis, A. New Global Hydrography Derived from Spaceborne Elevation Data. *Eos, Transactions American Geophysical Union* **2008**, *89*(10), 93–94. <https://doi.org/10.1029/2008EO100001>.
- ⁶⁸ Tapley, B. D.; Watkins, M. M.; Flechtner, F. et al. Contributions of GRACE to Understanding Climate Change. *Nature Climate Change* **2019**, *9*(5), 358–369. <https://doi.org/10.1038/s41558-019-0456-2>.
- ⁶⁹ Landerer, F. W.; Flechtner, F. M.; Save, H. et al. Extending the Global Mass Change Data Record: GRACE Follow-On Instrument and Science Data Performance. *Geophysical Research Letters* **2020**, *47*(12), e2020GL088306. <https://doi.org/10.1029/2020GL088306>.
- ⁷⁰ Hartick, C.; Furusho-Percot, C.; Goergen, K. et al. An Interannual Probabilistic Assessment of Subsurface Water Storage Over Europe Using a Fully Coupled Terrestrial Model. *Water Resources Research* **2021**, *57*(1), e2020WR027828. <https://doi.org/10.1029/2020WR027828>.
- ⁷¹ Belleflamme, A.; Goergen, K.; Wagner, N. et al. Hydrological Forecasting at Impact Scale: The Integrated ParFlow Hydrological Model at 0.6 Km for Climate Resilient Water Resource Management over Germany. *Frontiers in Water* **2023**, *5*. <https://doi.org/10.3389/frwa.2023.1183642>.
- ⁷² Naz, B. S.; Kollet, S.; Franssen, H.-J. H. et al. A 3 km Spatially and Temporally Consistent European Daily Soil Moisture Reanalysis from 2000 to 2015. *Scientific Data* **2020**, *7*(1), 111. <https://doi.org/10.1038/s41597-020-0450-6>.
- ⁷³ Luojus, K.; Moisander, M.; Pulliainen, J. et al. *ESA Snow Climate Change Initiative (Snow_cci): Snow Water Equivalent (SWE) Level 3C Daily Global Climate Research Data Package (CRDP) (1979–2020), version 2.0*; NERC EDS Centre for Environmental Data Analysis, 2022. <https://doi.org/10.5285/4647cc9ad3c044439d6c643208d3c494>.
- ⁷⁴ National Aeronautics and Space Administration (NASA) Global Modeling and Assimilation Office (GMAO). *MERRA-2 tavg1_2d_ind_nx: 2d,1-Hourly, Time-Averaged, Single-Level, Assimilation, Land Surface Diagnostics V5.12.4*; GMAO, 2015. <https://doi.org/10.5067/RKPH78K8C1Y1T>.
- ⁷⁵ Muñoz Sabater, J. *ERA5-Land Hourly Data from 1950 to Present*. Copernicus Climate Change Service (C3S) Climate Data Store (CDS); 2019 <https://doi.org/10.24381/cds.e2161bac>.
- ⁷⁶ Decharme, B.; Barbu, A. Crocus-ERA5 Daily Snow Product over the Northern Hemisphere at 0.25° Resolution; Version 2023; *Zenodo* **2024**. <https://doi.org/10.5281/zenodo.10943718>.
- ⁷⁷ Mudryk, L. R.; Elias Chereque, A.; Derksen, C. et al. *NOAA Arctic Report Card 2023: Terrestrial Snow Cover*; NOAA Technical Report OAR ARC; 23-03; National Oceanic and Atmospheric Administration (NOAA): 2023. <https://repository.library.noaa.gov/view/noaa/56613>.
- ⁷⁸ Mudryk, L. R.; Elias Chereque, A.; Derksen, C. et al. Terrestrial Snow Cover [in “State of the Climate in 2023”]. *Bulletin of the American Meteorological Society* **2024**, *105*(8), S307–S310. <https://doi.org/10.1175/BAMS-D-24-0101.1>.
- ⁷⁹ Decharme, B.; Barbu, A. Crocus-ERA5 Daily Snow Product over the Northern Hemisphere at 0.25° Resolution; Version 2023; *Zenodo* **2024**. <https://doi.org/10.5281/zenodo.10943718>.
- ⁸⁰ World Glacier Monitoring Service (WGMS). *Global Glacier Change Bulletin No. 5 (2020–2021)*. Zemp, M.; Gärtner-Roer, I.; Nussbaumer, S. U. et al., Eds.; WGMS: Zurich, Switzerland, 2023, 134 pp. [publication based on database version: doi:10.5904/wgms-fog-2023-09]. https://wgms.ch/downloads/WGMS_GGCB_05.pdf.
- ⁸¹ Dussailant, I.; Bannwart, J.; Paul, F. et al. *Glacier Mass Change Gridded Data from 1976 to Present Derived from the Fluctuations of Glaciers Database*; Copernicus Climate Change Service Climate Data Store, 2023. <https://doi.org/10.24381/CDS.BA597449>.
- ⁸² Zemp, M.; Welty, E. Temporal Downscaling of Glaciological Mass Balance Using Seasonal Observations. *Journal of Glaciology* **2023**, 1–6. <https://doi.org/10.1017/jog.2023.66>.
- ⁸³ A hydrological year’s winter and summer seasons are not the same for the northern hemisphere (NH), southern hemisphere (SH) and tropical (low-latitude) regions. A hydrological year cycle starts at the beginning of winter, finishes at the end of summer and is given the name of the year at the end of the cycle. For the NH, we assume winter to be Oct.–Mar. and summer



to be Apr.–Sep.; for the SH, we assume winter to be Apr.–Sep. and summer to be Oct.–Mar., and we assume no seasonality for the low-latitude season and have only plotted the annual values for this region.

- ⁸⁴ Huss, M.; Hock, R. Global-Scale Hydrological Response to Future Glacier Mass Loss. *Nature Climate Change* **2018**, *8* (2), 135–140. <https://doi.org/10.1038/s41558-017-0049-x>.
- ⁸⁵ Kaser, G.; Großhauser, M.; Marzeion, B. Contribution Potential of Glaciers to Water Availability in Different Climate Regimes. *Proceedings of the National Academy of Sciences* **2010**, *107* (47), 20223–20227. <https://doi.org/10.1073/pnas.1008162107>.
- ⁸⁶ Radić, V.; Hock, R. Glaciers in the Earth’s Hydrological Cycle: Assessments of Glacier Mass and Runoff Changes on Global and Regional Scales. *Surveys in Geophysics* **2014**, *35* (3), 813–837. <https://doi.org/10.1007/s10712-013-9262-y>.
- ⁸⁷ Pritchard, H. D. Asia’s Shrinking Glaciers Protect Large Populations from Drought Stress. *Nature* **2019**, *569* (7758), 649–654. <https://doi.org/10.1038/s41586-019-1240-1>.
- ⁸⁸ Dussailant, I.; Berthier, E.; Brun, F. et al. Two Decades of Glacier Mass Loss along the Andes. *Nature Geoscience* **2019**, *12* (10), 802–808. <https://doi.org/10.1038/s41561-019-0432-5>.
- ⁸⁹ “Peak water” refers to the point at which the annual runoff from glaciers reaches its maximum level. After this peak, the runoff begins to decline as the glaciers continue to lose mass, (see Huss, M.; Hock, R. Global-Scale Hydrological Response to Future Glacier Mass Loss. *Nature Climate Change* **2018**, *8* (2), 135–140. <https://doi.org/10.1038/s41558-017-0049-x>).
- ⁹⁰ Huss, M.; Hock, R. Global-Scale Hydrological Response to Future Glacier Mass Loss. *Nature Climate Change* **2018**, *8* (2), 135–140. <https://doi.org/10.1038/s41558-017-0049-x>.
- ⁹¹ Huss, M.; Hock, R. Global-Scale Hydrological Response to Future Glacier Mass Loss. *Nature Climate Change* **2018**, *8* (2), 135–140. <https://doi.org/10.1038/s41558-017-0049-x>.
- ⁹² Hugonnet, R.; McNabb, R.; Berthier, E. et al. Accelerated Global Glacier Mass Loss in the Early Twenty-First Century. *Nature* **2021**, *592* (7856), 726–731. <https://doi.org/10.1038/s41586-021-03436-z>.
- ⁹³ Huss, M.; Hock, R. Global-Scale Hydrological Response to Future Glacier Mass Loss. *Nature Climate Change* **2018**, *8* (2), 135–140. <https://doi.org/10.1038/s41558-017-0049-x>.
- ⁹⁴ Instituto de Hidrología, Meteorología y Estudios Ambientales (Ideam). *Informe del estado de los glaciares colombianos 2022*. Ideam: Bogotá, 2023.
- ⁹⁵ EM-DAT, CRED/UCLouvain, Brussels, Belgium. <http://www.emdat.be>.
- ⁹⁶ World Meteorological Organization (WMO). *Significant Weather & Climate Events*; WMO: Geneva, 2024.
- ⁹⁷ World Meteorological Organization (WMO). *Significant Weather & Climate Events*; WMO: Geneva, 2024.
- ⁹⁸ World Meteorological Organization (WMO). *Significant Weather & Climate Events*; WMO: Geneva, 2024.
- ⁹⁹ World Meteorological Organization (WMO). *Significant Weather & Climate Events*; WMO: Geneva, 2024.
- ¹⁰⁰ World Meteorological Organization (WMO). *Significant Weather & Climate Events*; WMO: Geneva, 2024.
- ¹⁰¹ World Meteorological Organization (WMO). *Significant Weather & Climate Events*; WMO: Geneva, 2024.
- ¹⁰² EM-DAT, CRED/UCLouvain, Brussels, Belgium. <http://www.emdat.be>.
- ¹⁰³ World Meteorological Organization (WMO). *Significant Weather & Climate Events*; WMO: Geneva, 2024.
- ¹⁰⁴ World Health Organization (WHO). *SITUATION REPORT: 01 November–31 December 2023. Greater Horn of Africa Food Insecurity and Health Grade 3 Emergency*; WHO: Geneva, 2024. <https://www.who.int/publications/m/item/situation-report-greater-horn-of-africa-food-insecurity-and-health---grade-3-emergency---01-november---31-december-2023>.
- ¹⁰⁵ World Health Organization (WHO). *SITUATION REPORT: 01 November–31 December 2023. Greater Horn of Africa Food Insecurity and Health Grade 3 Emergency*; WHO: Geneva, 2024. <https://www.who.int/publications/m/item/situation-report-greater-horn-of-africa-food-insecurity-and-health---grade-3-emergency---01-november---31-december-2023>.
- ¹⁰⁶ Government of Malawi. *Malawi 2023 Tropical Cyclone Freddy Post-Disaster Needs Assessment*; Government of Malawi, Lilongwe. <https://www.preventionweb.net/media/87994/download?startDownload=20240926>.
- ¹⁰⁷ World Meteorological Organization (WMO). *Significant Weather & Climate Events*; WMO: Geneva, 2024.
- ¹⁰⁸ <https://floodlist.com/africa/malawi-flood-storms-december-2022>



- ¹⁰⁹ <https://reliefweb.int/report/mozambique/mozambique-operational-annual-report-2022>
- ¹¹⁰ Government of Malawi. *Malawi 2023 Tropical Cyclone Freddy Post-Disaster Needs Assessment*; Government of Malawi, Lilongwe. <https://www.preventionweb.net/media/87994/download?startDownload=20240926>.
- ¹¹¹ <https://reliefweb.int/report/mozambique/unhcr-mozambique-cyclone-freddy-flash-update-3-24-march-2023>
- ¹¹² Government of Malawi. *Malawi 2023 Tropical Cyclone Freddy Post-Disaster Needs Assessment*; Government of Malawi, Lilongwe. <https://www.preventionweb.net/media/87994/download?startDownload=20240926>.
- ¹¹³ World Meteorological Organization (WMO). *State of the Global Climate 2023* (WMO No. 1347). Geneva, 2024.
- ¹¹⁴ Toreti, A.; Bavera, D.; Acosta, N. J. et al. *Drought in central America and Mexico – August 2023*; JRC135033. Publications Office of the European Union: Luxembourg, 2023. <https://doi.org/10.2760/00589>.
- ¹¹⁵ World Meteorological Organization (WMO). *State of the Global Climate 2023* (WMO No. 1347). Geneva, 2024.
- ¹¹⁶ Toreti, A.; Bavera, D.; Acosta, N. J. et al. *Drought in central America and Mexico – August 2023*; JRC135033. Publications Office of the European Union: Luxembourg, 2023. <https://doi.org/10.2760/00589>.
- ¹¹⁷ Smith, A. 2023: A Historic Year of U.S. *Billion-dollar Weather and Climate Disasters*. National Oceanic and Atmospheric Administration (NOAA) Climate.gov; 2024. <https://www.climate.gov/news-features/blogs/beyond-data/2023-historic-year-us-billion-dollar-weather-and-climate-disasters>.
- ¹¹⁸ World Meteorological Organization (WMO). *State of the Global Climate 2023* (WMO No. 1347). Geneva, 2024.
- ¹¹⁹ World Meteorological Organization (WMO). *State of the Global Climate 2023* (WMO No. 1347). Geneva, 2024.
- ¹²⁰ World Meteorological Organization (WMO). *State of the Global Climate 2023* (WMO No. 1347). Geneva, 2024.
- ¹²¹ Espinoza, J.-C.; Jimenez, J. C.; Marengo, J. A. et al. The New Record of Drought and Warmth in the Amazon in 2023 Related to Regional and Global Climatic Features. *Scientific Reports* **2024**, *14* (1), 8107. <https://doi.org/10.1038/s41598-024-58782-5>.
- ¹²² Espinoza, J.-C.; Jimenez, J. C.; Marengo, J. A. et al. The New Record of Drought and Warmth in the Amazon in 2023 Related to Regional and Global Climatic Features. *Scientific Reports* **2024**, *14* (1), 8107. <https://doi.org/10.1038/s41598-024-58782-5>.
- ¹²³ Li, B.; Rodell, M. Terrestrial Water Storage in 2023. *Nature Reviews Earth & Environment* **2024**, *5* (4), 247–249. <https://doi.org/10.1038/s43017-024-00545-x>.
- ¹²⁴ Vasconcelos Junior, F. das C.; Zachariah, M.; Silva, T. L. do V. et al. An Attribution Study of Very Intense Rainfall Events in Eastern Northeast Brazil. *Weather and Climate Extremes* **2024**, *45*, 100699. <https://doi.org/10.1016/j.wace.2024.100699>.
- ¹²⁵ Lyra, M.; Herdies, D.; Gomes, H. et al. *Extreme Precipitation Events in the Northeast Brazil during the Winters of 2022 and 2023*; EGU24-12954; Copernicus Meetings, 2024. <https://doi.org/10.5194/egusphere-egu24-12954>.
- ¹²⁶ Renna Camacho, C.; Getirana, A.; Rotunno Filho, O. C. et al. Large-Scale Groundwater Monitoring in Brazil Assisted with Satellite-Based Artificial Intelligence Techniques. *Water Resources Research* **2023**, *59* (9), e2022WR033588. <https://doi.org/10.1029/2022WR033588>.
- ¹²⁷ Li, B.; Rodell, M. Terrestrial Water Storage in 2023. *Nature Reviews Earth & Environment* **2024**, *5* (4), 247–249. <https://doi.org/10.1038/s43017-024-00545-x>.
- ¹²⁸ <https://reliefweb.int/report/argentina/drought-south-america-april-2023-gdo-analytical-report>
- ¹²⁹ Servicio Nacional de Meteorología e Hidrología del Perú (SENAMHI). Condiciones hidrológicas en la región hidrográfica del Titicaca (Perú): Déficit de caudales – Período Setiembre 2022 a Enero 2023; SENAMHI: Lima, 2023. <https://www.senamhi.gob.pe/load/file/02662SENA-7.pdf>.
- ¹³⁰ Gutierrez-Villarreal, R. A.; Espinoza, J.-C.; Lavado-Casimiro, W. et al. The 2022-23 Drought in the South American Altiplano: ENSO Effects on Moisture Flux in the Western Amazon during the Pre-Wet Season. *Weather and Climate Extremes* **2024**, *45*, 100710. <https://doi.org/10.1016/j.wace.2024.100710>.
- ¹³¹ World Meteorological Organization (WMO). *State of the Global Climate 2023* (WMO No. 1347). Geneva, 2024.
- ¹³² World Meteorological Organization (WMO). *State of the Global Climate 2023* (WMO No. 1347). Geneva, 2024.
- ¹³³ The Treasury New Zealand. *Impacts from the North Island Weather Events*; The Treasury, 2023. <https://www.treasury.govt.nz/sites/default/files/2023-04/impacts-from-the-north-island-weather-events.pdf>.



- ¹³⁴ World Meteorological Organization (WMO). *State of the Global Climate 2023* (WMO No. 1347). Geneva, 2024.
- ¹³⁵ EM-DAT, CRED/UCLouvain, Brussels, Belgium. <http://www.emdat.be>.
- ¹³⁶ <https://disasterphilanthropy.org/disasters/2023-china-floods/>
- ¹³⁷ World Meteorological Organization (WMO). *State of the Global Climate 2023* (WMO No. 1347). Geneva, 2024.
- ¹³⁸ https://civil-protection-humanitarian-aid.ec.europa.eu/news-stories/news/floods-eu-mobilises-emergency-equipment-assist-italian-authorities-2023-05-22_en
- ¹³⁹ <https://reliefweb.int/report/italy/italy-flood-2023-dref-operation-mdrit004>
- ¹⁴⁰ <https://reliefweb.int/report/italy/italy-flood-2023-dref-operation-mdrit004>
- ¹⁴¹ <https://reliefweb.int/report/italy/italy-flood-2023-dref-operation-mdrit004>
- ¹⁴² Direct communication from WMO Member.
- ¹⁴³ EM-DAT, CRED/UCLouvain, Brussels, Belgium. <http://www.emdat.be>.
- ¹⁴⁴ <https://reliefweb.int/report/italy/italy-flood-2023-dref-operation-mdrit004>
- ¹⁴⁵ Valente, M.; Zanellati, M.; Facci, G. et al. Health System Response to the 2023 Floods in Emilia-Romagna, Italy: A Field Report. *Prehospital and Disaster Medicine* **2023**, *38* (6), 813–817. <https://doi.org/10.1017/S1049023X23006404>.
- ¹⁴⁶ <https://www.cimafoundation.org/en/news/the-italian-floods-of-may-2023-a-scientific-analysis/>
- ¹⁴⁷ <https://reliefweb.int/report/italy/italy-flood-2023-dref-operation-mdrit004>
- ¹⁴⁸ Valente, M.; Zanellati, M.; Facci, G. et al. Health System Response to the 2023 Floods in Emilia-Romagna, Italy: A Field Report. *Prehospital and Disaster Medicine* **2023**, *38* (6), 813–817. <https://doi.org/10.1017/S1049023X23006404>.
- ¹⁴⁹ <https://www.regione.emilia-romagna.it/alluvione/aggiornamenti/2023/maggio/piene-e-allagamenti-gli-ultimi-aggiornamenti>
- ¹⁵⁰ Regional mobile columns are organized units of emergency personnel, vehicles and equipment that can be rapidly deployed to different regions in response to a crisis or disaster. These units are typically designed to be mobile and flexible, allowing them to be quickly sent to areas where they are most needed.
- ¹⁵¹ National Oceanic and Atmospheric Administration (NOAA) National Centers for Environmental Information (NCEI). *Annual 2023 Drought Report*; NCEI: 2024. <https://www.ncei.noaa.gov/access/monitoring/monthly-report/drought/202313>.

Annex. Technical annex

METHODS

This Annex provides high-level information on the main methodological steps applied to portray the state of global water resources in the year 2023.

For the *State of Global Water Resources 2023* report, the resolution of primary hydrological basins was increased, resulting in 986 basins spanning the globe. The basin map was based on Hydrosheds level 4 data.¹ The original dataset contained about 1 300 basins. However, due to global hydrological modelling system (GHMS) resolution, basins with a drainage area of less than 10 000 km² were filtered out together with some regions (such as Greenland), leaving 986 basins (Figure A1).

DATA SOURCES

Several sources of information on water resources were used to produce this report (refer also to the overview provided in [Table A1](#) of this Annex), in particular, the following:

- Observed river discharge data were obtained from the National Meteorological and Hydrological Services (NMHSs), the Global Runoff Data Centre (GRDC)² and enhanced streamflow observations using Earth system-based products.³
- Simulated river discharge data were obtained from 10 GHMSs. For more information on the models used, please refer to the [Global hydrological modelling systems](#) section of this Annex.
- Inflow into selected reservoirs globally was obtained from Wflow_sbm,⁴ CaMa-Flood⁵ and World-Wide HYPE model (WWH).⁶
- Reservoir volume anomalies were obtained from the United States National Aeronautics and Space Administration (NASA), following the methodology described by Biswas et al.⁷
- Lake volume data were provided by the Global Water Monitor.^{8,9}

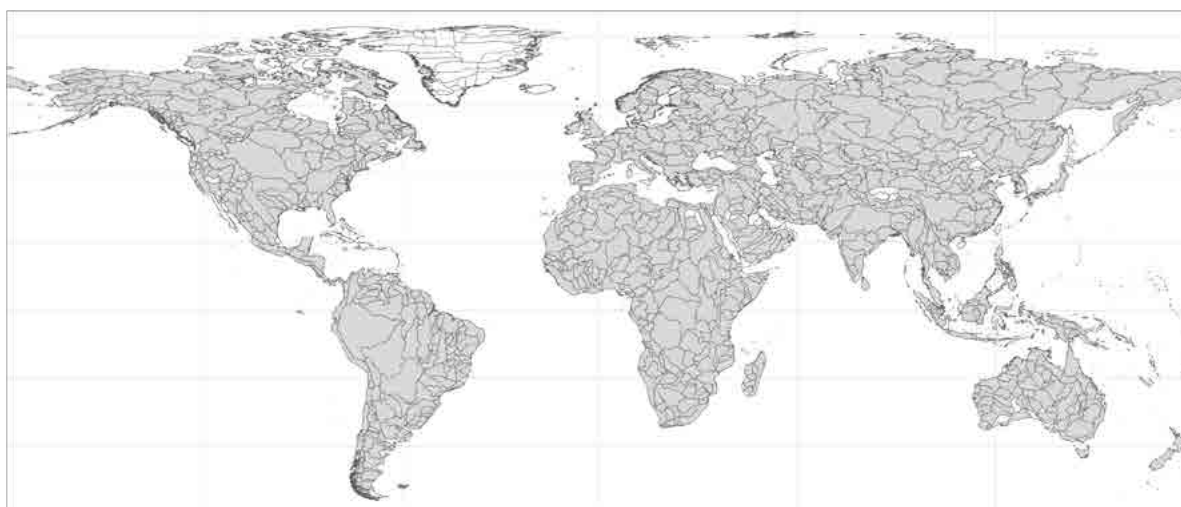


Figure A1. Global coverage of selected hydrological basins



Table A1. Data sources per chapter

<i>Institution</i>	<i>Product name</i>	<i>Key reference</i>	<i>River discharge</i>	<i>Reservoirs</i>	<i>Lakes</i>	<i>Ground-water levels</i>	<i>Soil moisture</i>	<i>Evapotranspiration</i>	<i>Terrestrial water storage</i>	<i>Snow cover and glaciers</i>	<i>Extreme events</i>
Observed datasets											
Members											
Global Runoff Database Centre (GRDC), Germany		GRDC, 2023 ¹⁰									
International Groundwater Resources Assessment Centre (IGRAC), Netherlands											
International Soil Moisture Network (ISMN), Germany											
World Glacier Monitoring Service (WGMS), Germany											
Central-Asian Institute for Applied Geosciences (CAIAG)											
National University of Uzbekistan											
Center for Glacier Research of the National Academy of Sciences of Tajikistan											



<i>Institution</i>	<i>Product name</i>	<i>Key reference</i>	<i>River discharge</i>	<i>Reservoirs</i>	<i>Lakes</i>	<i>Ground-water levels</i>	<i>Soil moisture</i>	<i>Evapotranspiration</i>	<i>Terrestrial water storage</i>	<i>Snow cover and glaciers</i>	<i>Extreme events</i>
Models and Earth observation datasets											
Goethe University Frankfurt, Germany	WaterGAP 2.2e	Müller Schmied et al., 2021; ¹¹ Müller Schmied et al., 2023 ¹²									
Institute of Atmospheric Physics, Chinese Academy of Sciences	CSSPv2 Conjective Surface-Subsurface Process version 2 (CSSPv2)	Yuan et al., 2018 ¹³									
Helmholtz Centre for Environmental Research – UFZ, Germany	mesoscale Hydrologic Model (mHM)	Samaniego et al., 2010; ¹⁴ Kumar et al., 2013; ¹⁵ Samaniego et al. 2019 ¹⁶									
Swedish Meteorological and Hydrological Institute (SMHI), Sweden	World-Wide HYPE (WWH) version 1.3.9	Arheimer et al., 2020 ¹⁷									
DHI, Denmark	DHI-GHM	Murray et al., 2023 ¹⁸									
University of Tokyo, Japan	CaMa-Flood with Dam	Hanazaki et al., 2022; ¹⁹ Yamazaki et al., 2011 ²⁰									
University of Tokyo/Japan Aerospace Exploration Agency, Japan	Today’s Earth – Global (TEJRA55)	Yoshimura et al., 2008; ²¹ Ma et al., 2021 ²²									



<i>Institution</i>	<i>Product name</i>	<i>Key reference</i>	<i>River discharge</i>	<i>Reservoirs</i>	<i>Lakes</i>	<i>Ground-water levels</i>	<i>Soil moisture</i>	<i>Evapotranspiration</i>	<i>Terrestrial water storage</i>	<i>Snow cover and glaciers</i>	<i>Extreme events</i>
Models and Earth observation datasets											
European Commission Joint Research Centre (JRC)	Global Flood Awareness System (GloFAS)	Alfieri et al., 2013; ²³ Grimaldi et al., 2022 ²⁴									
Deltares, Netherlands	Wflow_sbm	Verseveld et al., 2022; ²⁵ Imhoff et al., 2021; ²⁶ Eilander et al., 2021 ²⁷									
Brigham Young University, USA	GEOGLOWS	Hales et al., 2022 ²⁸									
Research Centre Jülich, Germany	ParFlow/CLM	Belleflamme et al., 2023 ²⁹									
Environment and Climate Change Canada	Crocus ERA5	Mudryk et al., 2023; ³⁰ Mudryk et al., 2024 ³¹									
NASA, USA	-	Biswas et al., 2021 ³²									
Australian National University, Australia	Global Water Monitor	Hou et al., 2022; ³³ Hou et al., 2024 ³⁴									
GFZ Research Centre for Geosciences, Germany	GRACE	Landerer et al., 2020 ³⁵									
University of Stuttgart Germany	Remote Sensing-based Extension of GRDC (RSEG)	Elmi et al., 2024 ³⁶									



- Groundwater data were provided by the International Groundwater Resources Assessment Centre (IGRAC) for 40 selected countries.
- The global terrestrial water storage (TWS) anomaly was obtained from the GRACE project³⁷ globally and locally for Central Europe from the Water Resources Bulletin, based on the physics-based model ParFlow/CLM.³⁸
- Glacier data were obtained from WMO Member States and Territories, the World Glacier Monitoring Service (WGMS), Central-Asian Institute for Applied Geosciences (CAIAG), German Research Centre for Geosciences (GFZ), National University of Uzbekistan, Center for Glacier Research of the National Academy of Sciences of Tajikistan and external experts.
- Snow-water equivalent data were obtained from Environment and Climate Change Canada^{39,40} and from two GHMSs: Today's Earth – Global (TEJRA55)^{41,42} and mesoscale Hydrologic Model (mHM).
- Qualitative and quantitative information on high-impact events was obtained from open data sources, such as the EM-DAT database (CRED, 2023),⁴³ ReliefWeb, WMO State of the Climate reports and others.

VARIABLE RANKING (ANOMALY CALCULATION)

To provide a coherent picture across different datasets obtained, a consistent method of variable ranking was applied to the variables listed in the previous section: river discharge, inflow into reservoirs, groundwater level, soil moisture, evapotranspiration and TWS.

Averages over historical periods for modelled and observed datasets were calculated for each year. The resulting array was ranked. The yearly average of a selected variable for the year 2023 was then compared to this ranked array and classified according to the following rule:

much below normal:	$Q_{2023} \leq 10\text{th percentile}$
below normal:	$10\text{th} < Q_{2023} < 25\text{th percentile}$
normal:	$25\text{th} \leq Q_{2023} \leq 75\text{th percentile}$
above normal:	$75\text{th} < Q_{2023} < 90\text{th percentile}$
much above normal:	$Q_{2023} \geq 90\text{th percentile}$

Depending on the variable in question, the historical period varied, constrained by the data availability. Refer to [Table A2](#) for selected historical periods and to dataset-specific chapters of the main report for more details.

For the modelled data, where several data sources (ensembles of models) have been used (specifically, for data from GHMSs on inflow into and discharge from reservoirs), the averaging of the variable ranking results was done at the basin level. For each model in the ensemble, the above-specified rankings were assigned an integer (“much below normal” = 1, “below normal” = 2, “normal” = 3, “above normal” = 4, “much above normal” = 5), and then an average



was calculated across the outputs of the ensemble of models for each of the basins. The resulting number was rounded, and the average discharge ranking was derived for each basin, according to the thresholds listed above.

Table A2. Historical periods of selected datasets

<i>Dataset</i>	<i>Selected historical period</i>	<i>Length of historical period</i>
Simulated river discharge from GHMSs	1991–2020	30 years
Observed river discharge from GRDC and NMHSs	<2001–2020	Varying between 20 to 30 years
Inflow into reservoirs	1991–2020	30 years
Reservoir storage	2000–2023	24 years
Lake level	1991–2020	30 years
Groundwater level	2004–2023	20 years ^a
Evapotranspiration	1991–2020	30 years
Soil moisture modelled	1991–2020	30 years
Soil moisture observed	2008–2022	15 years
Snow water equivalent	1991–2020	30 years
Terrestrial water storage (TWS)	2002–2020	19 years

^a 10 years for Brazil, Bulgaria, Costa Rica and Israel

GLOBAL HYDROLOGICAL MODELLING SYSTEMS

The 2023 report predominantly uses outcomes from the GHMSs sourced from the modelling community. Despite improved availability, observed discharge data were still not sufficient to ensure a consistent global overview, requiring the need for an alternative source for discharge data. The simulated discharge produced by multiple GHMSs was analysed using the subbasin map obtained after processing the level 4 Hydrosheds dataset (Figure A1).

In total, 10 GHMSs were used in the modelling exercise:

- World-Wide HYPE v1.3.9⁴⁴
- WaterGAP 2.2e⁴⁵
- CSSPv2 Conjunctive Surface-Subsurface Process (CSSPv2)⁴⁶



- mesoscale Hydrologic Model (mHM)^{47,48,49}
- DHI-GHM⁵⁰
- CaMa-Flood with Dam^{51,52}
- Today's Earth – Global (TEJRA55)^{53,54}
- Global Flood Awareness System (GloFAS)^{55,56}
- Wflow_sbm^{57,58,59}
- GEOGLOWS⁶⁰

The global hydrological modelling community was requested to provide historical simulations for the chosen 986 basins for the years 1991–2020 and the target year of 2023, using meteorological input data of their choice. Before submitting the outputs, the modelling teams were required to complete a modelling dictionary, offering necessary technical details about the model and input data sources. An ensemble of models was employed to address potential uncertainties in the simulations, and the 2023 discharge ranking was conducted initially for the simulated discharge from each model for each basin, then averaged across all models for each basin (refer to the [Variable ranking](#) section for more details).

[Table A3](#) shows a technical breakdown of the various GHMSs, and the [Validation of modelled results](#) section summarizes the models' spatial coverage and provides a graphical representation of trends simulated by each model for each basin. Due to time restrictions, it was not feasible to homogenize input data sources for model setup across all modelling groups. Regarding climate forcing, all GHMSs used ERA5 reanalysis data,⁶¹ except for the WWH and TEJRA55 models, which were driven by the HydroGFD⁶² and JRA-55⁶³ datasets, respectively.

RIVER DISCHARGE

OBSERVED DATA AND VALIDATION OF MODELLED RESULTS

General availability of discharge data from GRDC and NMHSs for the year 2023

Observed discharge data were obtained from GRDC⁶⁴ and received from the NMHSs. Two selection criteria were adjusted to increase the potential volume of observed data: the historical period was permitted to span a minimum of 20 years, instead of 30 as for the modelled data, and datasets not yet subjected to quality checks were included. NMHSs could also supply calculated anomalies in case of data sensitivity.

In total, observed data from 713 stations for the year 2023 were collected from the GRDC database and NMHSs. Two subsets were derived from the total pool for further detailed analysis. The first subset, consisting of 713 stations with a maximum of 20 days of missing data in 2023, was selected for evaluating the 2023 discharge anomaly. The second subset, comprising 131 stations, was identified for validating the GHMSs' results. These stations were selected from the 713 stations based on their proximity to the chosen HydroBASIN outlet, ensuring a closer match between the observed and modelled data.



Table A3. Characteristics of global hydrological modelling systems used in the report

<i>Model name</i>	<i>Institution</i>	<i>Spatial coverage</i>	<i>Spatial model resolution</i>	<i>Climate data product used</i>
WaterGAP 2.2e	Goethe University Frankfurt	Global	0.5° × 0.5°	GSWP3-ERA5
Conjunctive Surface–Subsurface Process version 2 (CSSPv2)	Institute of Atmospheric Physics, Chinese Academy of Sciences	Global	0.25°	ERA5, with precipitation replaced by MSWEPv2
mesoscale Hydrologic Model (mHM)	Helmholtz Centre for Environmental Research – UFZ	Two setups available: (1) global and (2) individually delineated and calibrated GRDC basins	Last version was based on the 0.25° resolution	ERA5
World-Wide HYPE (WWH) version 1.3.9	Swedish Meteorological and Hydrological Institute (SMHI)	All continents except Antarctica	On average 1 000 km ²	HydroGFD
DHI-GHM	DHI	The model covers land surface of the globe between 80°N and 60°S	0.1° × 0.1°	ERA5
CaMa-Flood with Dam	University of Tokyo	90N°–60°S, 180°W–180°E (without Greenland)	0.25° lat./lon. deg.	ERA5-land runoff
Today’s Earth – Global (TEJRA55)	University of Tokyo/Japan Aerospace Exploration Agency	90N°–60°S, 180°W–180°E (without Greenland)	0.25° lat./lon. deg.	JRA-55
Global Flood Awareness System (GloFAS)	European Commission Joint Research Centre (JRC)	Global except for Antarctica (90°N–60°S, 180°W–180°E)	0.05° (~5 km, gridded)	ERA5
GEOGLOWS	Brigham Young University	Global	Irregular grid, ~150 km ²	ERA5
Wflow_sbm	Deltares	Global	30 arcsec (0.0083° ~ 1 km)	ERA5

Figure A2 presents the location of the 713 gauges for which data were received from the GRDC database and NMHSs for discharge anomaly analysis for the year 2023 and the 131 gauges selected for validation of modelling results, including the respective Hydrobasins where those were located. Note that the ranking of the streamflow for 2023 estimated from the ensemble of GHMSs might differ from the results obtained from the observed streamflow data at a finer spatial scale. Therefore, WMO emphasizes the importance of the availability of local in situ data for producing accurate global products such as the assessments presented in this report.

Figure A3 presents the locations of the 828 gauge stations for which data were obtained from the Remote Sensing-based Extension of GRDC (RSEG) dataset, which combines gauge discharge and remote sensing observations.⁶⁵ This product extends the GRDC time series using a stochastic nonparametric mapping algorithm derived from remote sensing data.

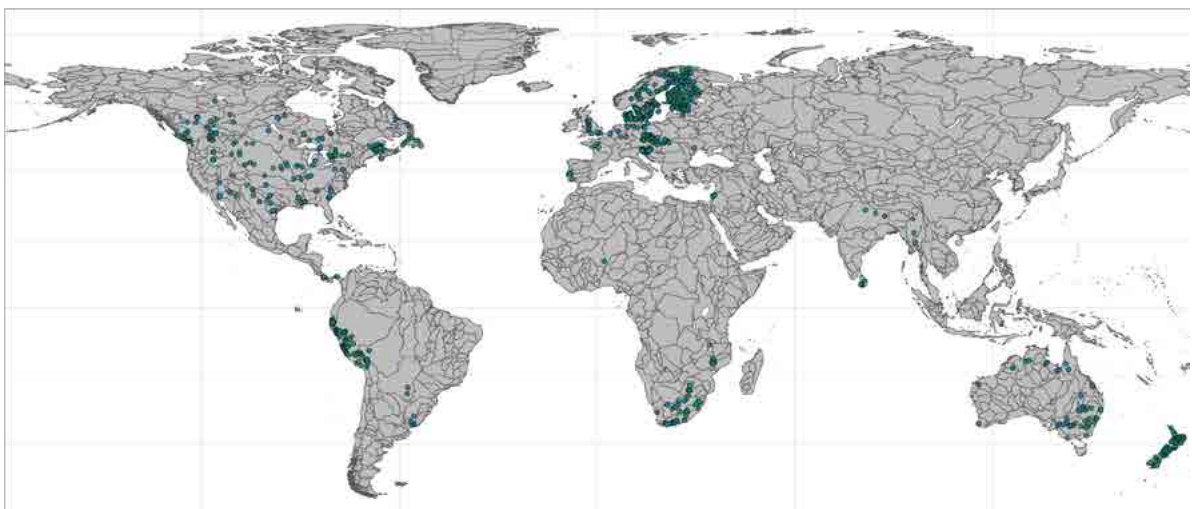


Figure A2. Location of gauges in the GRDC database and for which data were received from NMHSs (green points), and those selected for validation, along with the respective Hydrobasins in which those gauges were located (blue points)

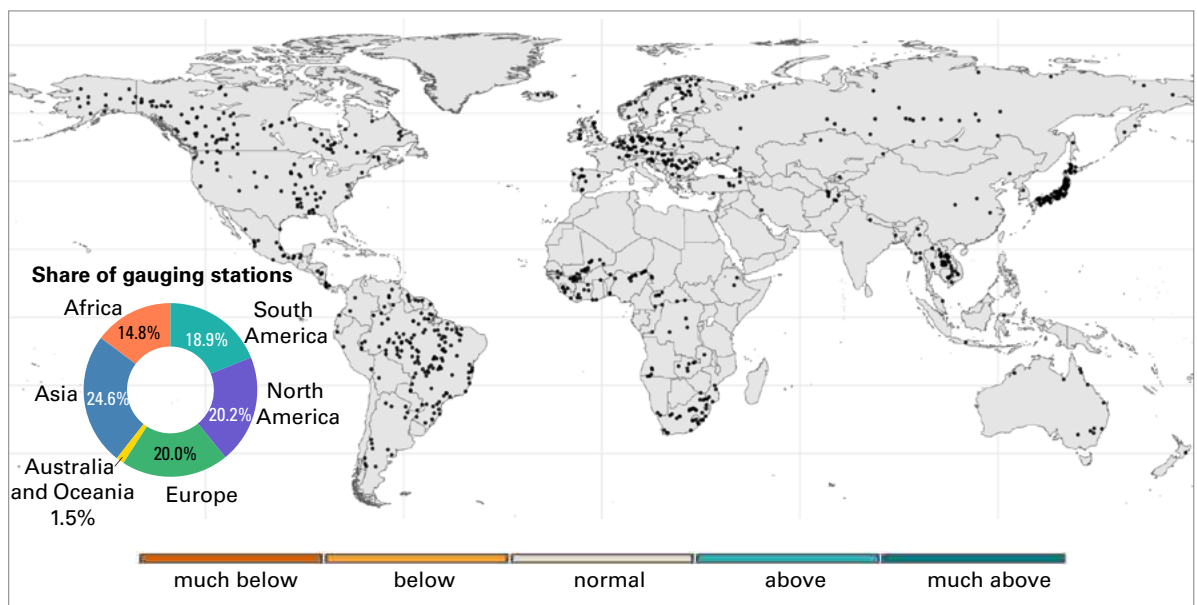


Figure A3. Location of gauges for which data were obtained from the Remote Sensing-based Extension of GRDC (RSEG)

VALIDATION OF MODELLED RESULTS

The discharge ranking obtained from the GHMS simulations was validated with discharge ranking obtained from the available observed data. Annual averages of flow observations from 2023 were ranked against the hydrological normals (obtained from at least 20 years of flow observations) at each WMO basin (where observed flow data were available). The discharge rankings from simulated and observed data for the year 2023 were classified by the sign of change with respect to the long-term normal (that is, “below”, “above” or “normal”) and then compared to each other. Note that in large basins where some of the downstream units (according to the WMO basin classification) import a considerable amount of water resources from the upstream catchments, comparisons/validations done between results from modelled data and observations for only one gauge per WMO basin might lead to inaccurate results. Therefore, using observations from intermediary gauges or redefining of the catchment areas must be considered in the future to minimize uncertainties in the results.

Figure A4 shows model agreement on the state of the annual river discharge with respect to the mean (above, below, normal (that is, no change)) among GHMSs used in the simulation task for each basin. The results show that more than 50% of GHMSs agree on the sign of trends for 97% of the area globally. Moreover, the agreement for Australia and South America is higher, lying between 75% and 100%.

Figure A5 presents observed discharge anomaly for the year 2023 for selected basins. Figure A6 shows the validation of trend simulations for the 2023 discharge. Areas where simulated and observed trends disagree on the direction of change are indicated by hashing.

The validation of modelled results showed agreement between observed and simulated anomalies for the year 2023 in New Zealand, the eastern and northern part of Australia, Myanmar, northern India, the United Kingdom, Norway, Finland, Latvia, Estonia, Austria, Slovakia, Hungary, the eastern part of Ukraine, the western part of Canada, the eastern and southern part of the United States and Paraguay. Modelled trends disagree with observations

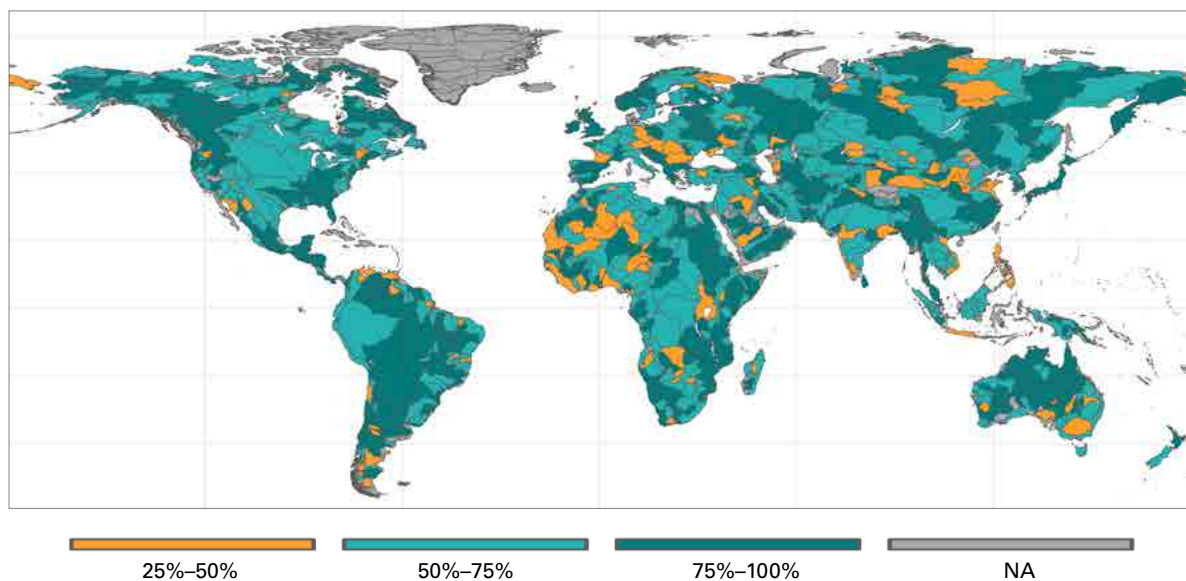


Figure A4. Share of GHMSs that agree on the sign of changes in the annual river discharge with respect to the mean (above, below, normal) for each basin

in the southern part of Europe (for example, Greece and Albania), Sweden, Southern Africa, the upper Amazon and the central part of the United States. In general, GHMS simulations align with observations in 69% of the basins with available observational data.

In some areas (for example, Great Britain and Ireland), there was a mismatch between the resolution of the models (catchments above 10 000 km² were selected for the analysis) and the observed

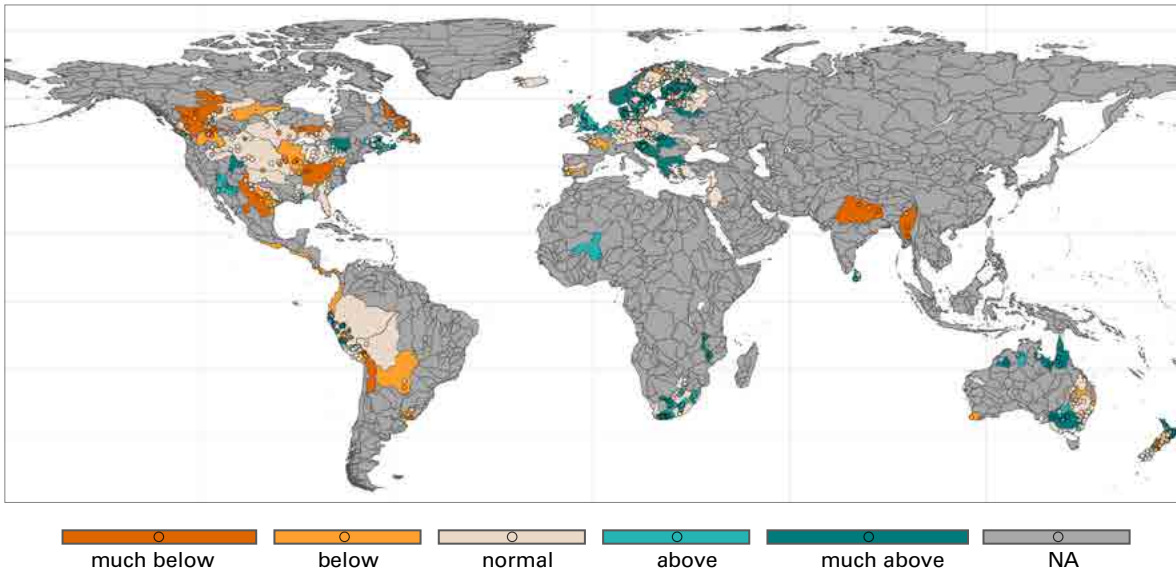


Figure A5. River discharge in 2023 as ranked with respect to the historical period 1991–2020. The results presented here were derived from the observed discharge data, which were obtained from NMHSs and the GRDC database. Dots represent the location of received observed gauges. Grey areas indicate missing discharge data.

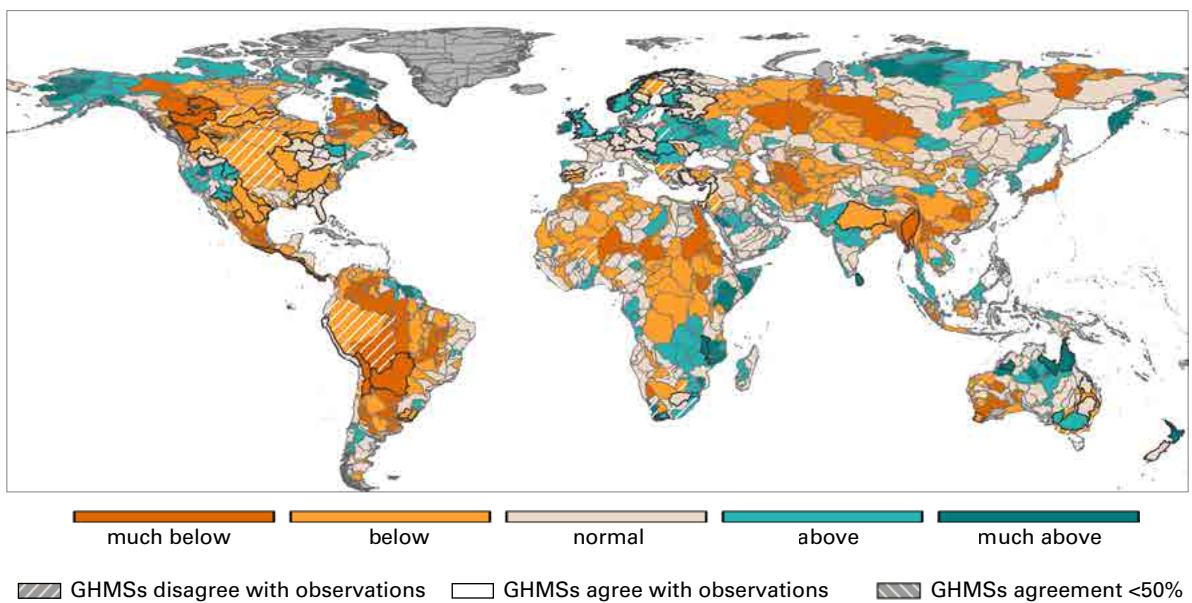


Figure A6. Validation of trends simulations for the 2023 discharge. Areas where simulated and observed trends agree on the direction of change is indicated by a bold outline. Areas where GHMSs disagree with each other are marked with left slanting hashing, and areas where GHMSs disagree with observations are marked with right slanting hashing.

datasets. The provision of a “national outflow” data series for the United Kingdom allowed for a simple validation of these model results, though this case underlines the importance of scale in small nations, and the need for better spatial representation of relevant catchments.

Figure A7 presents discharge ranking results obtained for each of the basins from 10 GHMSs. The results for the Wflow_sbm model are presented only for Europe.

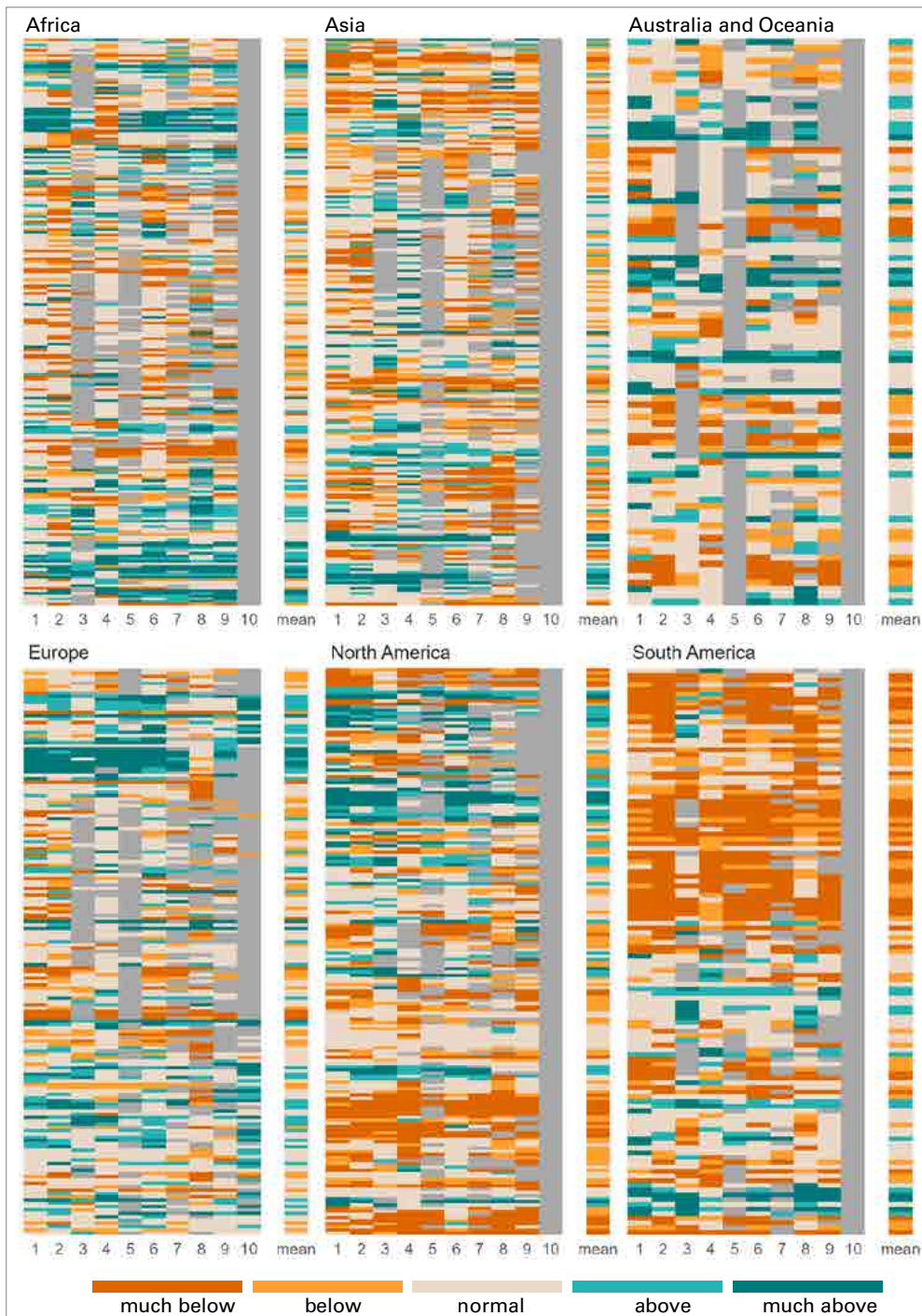


Figure A7. Simulated discharge rankings for the year 2023 for each basin by each of the GHMSs grouped by region.
 Note: 1 – DHI-GHM, 2 – GloFAS, 3 – TEJRA55, 4 – WWH, 5 – mHM, 6 – WaterGAP 2.2e, 7 – CaMa-Flood, 8 – CSSPv2, 9 – GEOGLOWS, 10 – Wflow_sbm. Grey area indicates no data values for a specific basin.



RESERVOIRS

INFLOW INTO SELECTED RESERVOIRS

The modelled results for the inflow into 926 reservoirs globally were obtained from three main sources: Wflow_sbm,⁶⁶ CaMa-Flood with dam^{67,68} and WWH.⁶⁹ The reservoirs were selected based on overlap between those three sources and identified by their GRanD id.⁷⁰ Daily inflow into selected GRanD reservoirs has been computed for the period 1991–2023.

Wflow_sbm:⁷¹ Daily inflow and daily reservoir volumes were calculated for the period 1991–2023 for the selected GRanD reservoirs.

CaMa Flood with Dam: The CaMa-Flood model⁷² along with the Dam operational scheme by Hanazaki et al.⁷³ was used to conduct global simulations. The model can simulate river flows encompassing 2 169 global dams and reservoirs with a drainage area of at least 1 000 km². The information for each reservoir, such as the dam's name, coordinates, storage capacity and drainage area, in the model is based on information from GRanD.⁷⁴ The model configuration, done by Hanazaki et al.,⁷⁵ enables global simulations at a spatial resolution of 0.25° using MERIT Hydro⁷⁶ as a baseline topography. The same model configuration settings, utilizing ERA5-Land reanalysis data⁷⁷ from 1991 to 2023 for runoff forcing, have been used for the current global simulations. The temporal resolution of the model is one hour. However, keeping in view the reporting requirements, the outputs have been prepared at 24-hour intervals.

Calibration of the model with the Dam operational scheme is unavailable. However, Hanazaki et al.⁷⁸ conducted model validation based on simulations spanning 2001 to 2019. Validation for the model is accessible for the daily streamflow discharge of 687 gauges (located downstream of dams) from GRDC and other institutions worldwide. The accuracy of discharge hydrographs compared to observations was evaluated by calculating Nash–Sutcliffe efficiency (NSE)⁷⁹ and peak discharge error (PDE).⁸⁰ In addition to the 687 global gauges, validation is also available for inflow, outflow and storage at the Seminole and Trinity reservoirs using insitu observation data.

World-Wide HYPE v1.3.9: Daily inflow into GRanD reservoirs and daily reservoir volume have been delivered for the period 1991–2023. The World-Wide HYPE model was calibrated in a stepwise manner using 2 475 discharge gauges and evaluated against an additional 2 863 independent discharge gauges.⁸¹ The model includes around 13 000 lakes and 2 500 reservoirs. These are described in a general fashion based on information from the GRanD database. Except for a handful of places, the operating routines of the reservoirs have not yet been calibrated in WWH.

RESERVOIR STORAGE

Anomalies in basin-wide reservoir storage were calculated in line with the methodology described by Biswas et al.⁸² A total of 50 068 reservoirs were selected worldwide from different dam datasets,^{83,84,85,86} all of which were within the 233 selected basins around the world. For each of the selected reservoirs, the area-elevation curve was generated using the SRTM elevation dataset following the methodology described in the Global Reservoir Assessment Tool.⁸⁷ From the area-elevation curve, the accumulated storage for each elevation band was

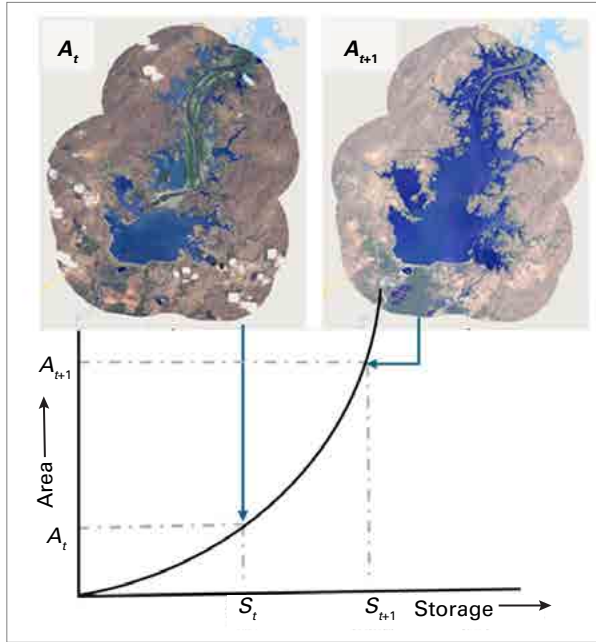


Figure A8. Surface water extent at timestamp 1 and $t-1$, and the area-elevation-storage curve used for calculation of monthly storage

calculated using Equation 1 to form a complete area-elevation-storage curve for individual reservoirs. Secondly, water extent area time series for each of the reservoirs were extracted using the application programming interface (API) and the GWW (Global Water Watch)⁸⁸ time-series data.

$$S_{i+1} = \frac{A_i + A_{i+1}}{2} \cdot (h_{i+1} - h_i) + S_i \text{ for } i=0 \text{ to } n-1 \quad (1)$$

where S is storage, A is area and h indicates elevation.

The water extent area time series were prepared using data from multiple satellites (Landsat series, Sentinel 2). The surface water extent time series data were then converted into monthly median time series spanning from 2000 to 2023. From the surface water extent area time series of the individual reservoir, monthly storage was calculated using the area-elevation-storage curve (shown in Figure A8). Finally, monthly individual reservoir storage time series were accumulated into monthly basin-wide reservoir storage time series for 237 basins.

The annual mean of monthly basin-wide reservoir storage for the reference period (2000–2023) of modelled data was calculated for each year and then ranked according to the rule described in the [Anomaly calculation](#) section.

LAKES

Lake and reservoir storage data in the GloLakes product are estimated by combining satellite measurements of water levels and water body extents from various satellites, along with local topography information where necessary.^{89,90} The data record extends from 1984 onwards. The dynamics of lake and reservoir surface water extents were estimated using high-resolution optical remote sensing data from Landsat and Sentinel-2. Water level fluctuations were measured with ICESat-2 laser altimetry, supplemented by radar altimetry data from Topex/Poseidon, Jason-1, -2, -3, and Sentinel-3 and -6 instruments.



For lakes with a surface extent between 0.1 km² and 500 km², the absolute water storage dynamics from 1984 to 2020 were estimated using a geostatistical model based on available water area and surrounding slope measurements. The historical absolute water storage estimates were extended to near-real-time monitoring using the volume–height relationship when radar or lidar altimetry data were available after 2020.

For lakes with a surface extent larger than 500 km², the height and area at capacity were estimated by determining the maximum observed surface water height and extent, respectively, and calculating the lake storage volume. If satellite-derived water height and extent were not available simultaneously, the lake storage volume estimates were extended using volume–height or volume–extent relationships based on the available observed height or extent.

GROUNDWATER

The methodology used to report on groundwater levels was developed and consolidated in 2023. It is described in a methodology report published in February 2024, which is available in [IGRAC’s GitHub repository](#). This document provides complementary information on the collection and the selection of the data and on the mapping of the results.

Groundwater level monitoring data were collected from 40 countries. The data were downloaded from the websites of the institutions in charge of groundwater monitoring, where available. Otherwise, the data were requested. Table A4 indicates how the data were collected for each country.

Table A4. Groundwater data sources per country

#	Country		Data source	Link
1	Australia		Downloaded	http://www.bom.gov.au/water/groundwater/explorer/map.shtml
2	Austria		Downloaded	https://ehyd.gv.at/
3	Belgium	Brussels	Requested	Environment and Energy Administration of the Brussels-Capital Region
		Wallonia	Downloaded	https://piezometrie.wallonie.be/home.html
		Flanders	Downloaded	https://www.dov.vlaanderen.be/portaal/
4	Brazil		Requested	Geological Survey of Brazil (SGB)
5	Bulgaria		Requested	Ministry of Environment and Water – The Executive Environment Agency (ExEA)
6	Canada		Requested	Natural Resources Canada (NRCan/RNCan)
7	Chile		Requested	General Directorate of Water (DGA)
8	Costa Rica		Requested	Ministry of Environment and Energy – Department of Water Development
9	Cuba		Requested	National Institute of Hydraulic Resources (INRH)
10	Czech Republic		Requested	Czech Hydrometeorological Institute
11	Denmark		Downloaded	https://data.geus.dk/JupiterWWW/



12	El Salvador	Requested	Ministry of Environment
13	Estonia	Requested	Geological Survey of Estonia
14	France	Downloaded	https://ades.eaufrance.fr/Spip?p=
15	Germany ^a	Downloaded	https://gruvo.bgr.de/website/fss
16	Hungary	Requested	Hungarian Hydrological Forecasting Service
17	India	Requested	India Water Resources Information System (WRIS)
18	Ireland	Downloaded	https://www.epa.ie/
19	Israel	Requested	Hydrological Service
20	Jamaica	Requested	Water Resources Authority
21	Jordan	Requested	Ministry of Water and Irrigation
22	Republic of Korea	Requested	Korea Water Resources Corporation (K-WATER)
23	Latvia	Downloaded	https://videscentrs.lvgmc.lv/noverojumu-arhivs/pazemes/
24	Lithuania	Downloaded	https://www.lgt.lt/epaslaugos/elpaslauga.xhtml
25	Luxembourg	Requested	Water Management Administration
26	Mexico	Requested	National Water Commission (CONAGUA)
27	Namibia	Requested	Ministry of Agriculture, Water and Forestry – Department of Water Affairs and Forestry – Division Water Environment
28	Netherlands	Downloaded	https://www.broloket.nl/ondergrondgegevens
29	New Zealand	Requested	GNS Science
30	Norway	Downloaded	https://www.nve.no/english/
31	Poland	Downloaded	https://www.pgi.gov.pl/psh/materialy-informacyjne-psh/
32	Portugal	Downloaded	https://snirh.apambiente.pt/
33	Slovakia	Requested	Slovak Hydrometeorological Institute
34	South Africa	Requested	Department of Water and Sanitation (DWS)
35	Spain	Requested	Ministry for the Ecological Transition and the Demographic Challenge (MITECO)
36	Sweden	Downloaded	https://www.sgu.se/grundvatten/grundvattennivaer/matstationer/
37	Switzerland	Requested	Swiss Federal Office for the Environment (FOEN)
38	Thailand	Requested	Department of Groundwater Resources (DGR)
39	UK	Requested	British Geological Survey (BGS)
40	USA	Downloaded	https://cida.usgs.gov/ngwmn/index.jsp

^a The website identifies reference monitoring stations in the country and provides the links to the states' websites where the data can be downloaded.

The data selection procedure works with a threshold, to specify the minimum number of years for which at least one data point is available. The threshold was set by default to 80%, which means that the time series that are selected have data for at least 16 years out of 20. However, in the case of Namibia the threshold was lowered to 60% to accommodate for the data gaps over the period 2017–2021.

Several boreholes are located at the same site to monitor different aquifers at various depths. To provide a clear representation of overlapping boreholes, a geographical information system (GIS) tool called “displacement tool” was used. This tool slightly offsets overlapping points, positioning them next to each other, as shown in Figure A9. In the first example in the figure, three different boreholes are at the same location; the average groundwater level in 2023 is “normal” in two of them and “above normal” in the third one. In the second example, two boreholes are at the same location; the average groundwater level in 2023 is “below normal” in both of them.

See further details at the [IGRAC website](#).



Figure A9. Representation of overlapping boreholes

SOIL MOISTURE

The anomaly in surface soil moisture in 2023 was obtained from three GHMSs (see [Table A1](#) for model names) and ranked relative to the historical period 1991–2020 ([Figure 9](#)) on a monthly basis to understand root zone soil moisture patterns (2 m depth).

EVAPOTRANSPIRATION

The actual evapotranspiration at the global scale for four seasons in 2023 with respect to the historical period 1991–2020 was derived from five GHMSs (listed in [Table A1](#)) and averaged over the river basins derived from the Hydrobasins level 4 delineation.⁹¹

SNOW WATER EQUIVALENT

The daily SWE output was obtained from the Crocus-ERA5 snow model⁹² and aggregated over a given land region to produce daily snow mass time series. Peak snow mass values were then calculated for each water year, and the resulting series of values were used to calculate 2023 percentiles relative to the 1991–2020 reference period.

Ensemble-mean, March-mean SWE fields over the 1991–2023 period were calculated using data from four individual gridded products:

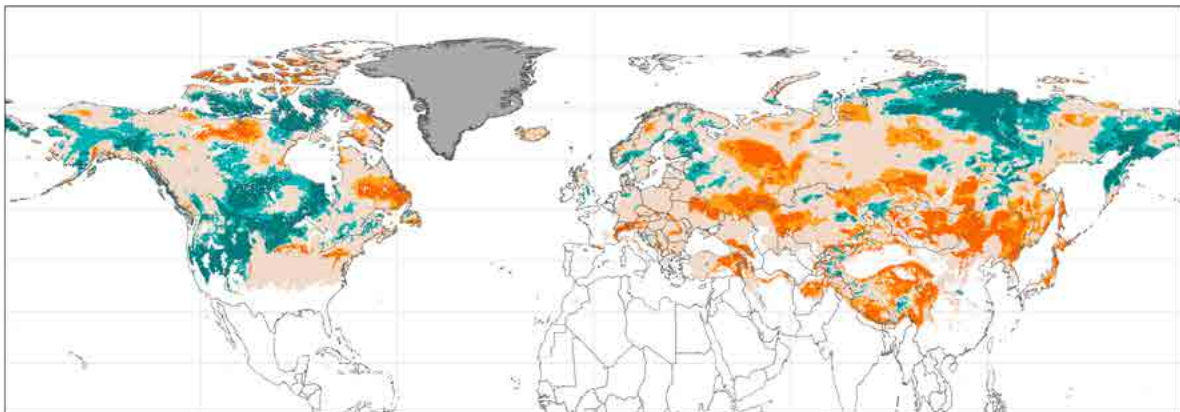
- (1) The European Space Agency Snow CCI SWE version 2 product derived through a combination of satellite passive microwave brightness temperatures and climate station snow depth observations;⁹³

- (2) The Modern-Era Retrospective Analysis for Research and Applications version 2 (MERRA-2, GMAO 2015) daily SWE fields;
- (3) SWE output from the ERA5-Land analysis;⁹⁴
- (4) The physical snowpack model Crocus⁹⁵ driven by ERA5 meteorological forcing.

March-mean fields from each product were regridded to a common 0.5° × 0.5° regular grid and averaged together. This is the same suite of products used to produce annually updated SWE data for the Arctic Report Card⁹⁶ and the Bulletin of the American Meteorological Society (BAMS) State of the Climate Report.⁹⁷ March 2023 SWE values were converted to percentiles using the 1991–2020 reference period on a pixel-wise basis.

In addition, the March SWE in the Northern Hemisphere was obtained for 2023 and compared to the 1991–2020 reference period based on two GHMSs: mHM and TEJRA55. Results are presented in Figure A10.

mHM



TEJRA55

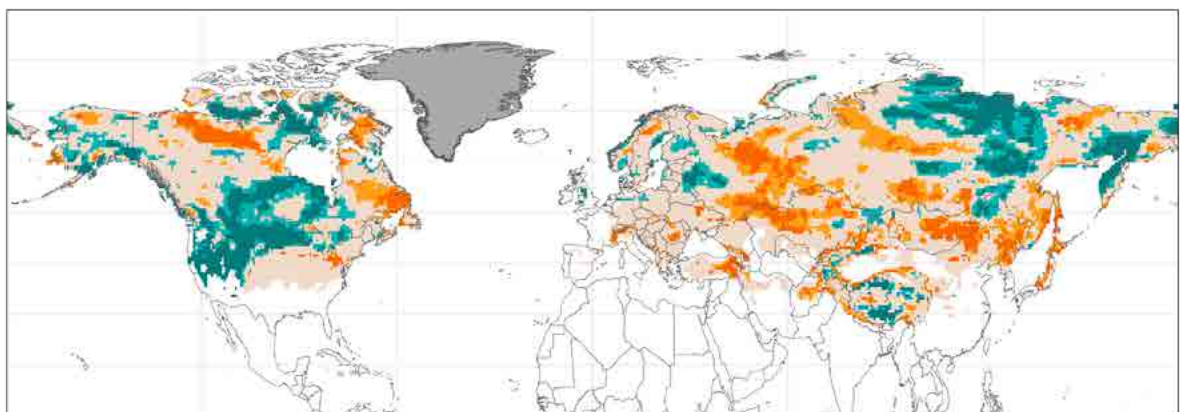


Figure A10. March 2023 snow water equivalent anomaly compared to the reference period (1991–2020)



TERRESTRIAL WATER STORAGE

GLOBAL

Satellite gravimetry is the only remote-sensing-based method capable of observing the whole water column, including surface water, soil moisture, groundwater, and snow and ice. This report presents an analysis of the TWS anomaly between the years 2002 and 2023, observed with the Gravity Recovery and Climate Experiment (GRACE) mission (2002–2017) and its successor GRACE-Follow-On (Grace-FO) (since 2018).^{98,99} The GRACE data provide the TWS anomaly compared to the baseline of 2004–2009, and then Equation 2 is used to adjust the TWS anomaly compared to the baseline of 2002–2020.

The TWS anomaly in equivalent water heights in centimetres was calculated according to Equation 2:

$$TWS_{\text{anomaly}} = TWS_t - \bar{X} \quad (2)$$

where TWS_t (cm) is the TWS value of the month t of the current year, and \bar{X} is the long-term average TWS (cm), as calculated for 2002–2020. Equivalent water height is the theoretical mean height of the water column over the whole area being considered.

TWS for the year 2023 was ranked in a manner similar to that used for discharge. However, the time series of TWS data were too short (19 years) to perform ranking on the yearly values, therefore an index for each month was computed and then aggregated to the yearly mean values.

CASE-STUDY ON TERRESTRIAL WATER STORAGE

In the case study on the hydrological situation in central Europe, the main variable of interest is the anomaly in subsurface water storage.

Subsurface water storage was calculated based on prognostic output from the ParFlow integrated hydrologic model and prescribed ParFlow soil hydraulic properties as provided through the external parameter fields for each model layer and grid element as in Equation 3:

$$S_{i,j,k} = sat_{i,j,k} \cdot \Phi_{i,j,k} \cdot dz_k \quad (3)$$

Where S (L) is the water storage per model layer k , $sat_{i,j,k}$ (–) is the simulated relative saturation, $\Phi_{i,j,k}$ (–) is the porosity for a grid element with indices i,j,k in the lateral and vertical direction, and dz_k (L) is the vertical extent of each model layer; layers have a laterally constant thickness.

The total subsurface water storage can be obtained by adding S along the vertical axis overall model layers; in the data used here, this is 15 layers with a variable thickness, with a vertical model extent from –60 m to 0 m. The near-surface root zone water storage is provided for the uppermost 9 layers from –2 m to 0 m depth.

Endnotes

- ¹ Lehner, B.; Verdin, K.; Jarvis, A. New Global Hydrography Derived from Spaceborne Elevation Data. *Eos, Transactions American Geophysical Union* **2008**, *89*(10), 93–94. <https://doi.org/10.1029/2008EO100001>.
- ² Global Runoff Data Centre (GRDC). *WMO Basins and Sub-Basins*; 3rd rev. ext. ed., Federal Institute of Hydrology (BfG): Koblenz, Germany, 2023.
- ³ Elmi, O.; Tourian, M. J.; Saemian, P. et al. Remote Sensing-Based Extension of GRDC Discharge Time Series – A Monthly Product with Uncertainty Estimates. *Scientific Data* **2024**, *11*(1), 240. <https://doi.org/10.1038/s41597-024-03078-6>.
- ⁴ van Verseveld, W. J.; Weerts, A. H.; Visser, M. et al. Wflow_sbm v0.6.1, a Spatially Distributed Hydrologic Model: from Global Data to Local Applications. *Geoscientific Model Development Discussions* **2022** [preprint]. <https://doi.org/10.5194/gmd-2022-182>.
- ⁵ Yamazaki, D.; Kanae, S.; Kim, H. et al. A Physically Based Description of Floodplain Inundation Dynamics in a Global River Routing Model. *Water Resources Research* **2011**, *47*(4). <https://doi.org/10.1029/2010WR009726>.
- ⁶ Arheimer, B.; Pimentel, R.; Isberg, K. et al. Global Catchment Modelling Using World-Wide HYPE (WWH), Open Data, and Stepwise Parameter Estimation. *Hydrology and Earth System Sciences* **2020**, *24*(2), 535–559. <https://doi.org/10.5194/hess-24-535-2020>.
- ⁷ Biswas, N. K.; Hossain, F.; Bonnema, M. et al. Towards a Global Reservoir Assessment Tool for Predicting Hydrologic Impacts and Operating Patterns of Existing and Planned Reservoirs. *Environmental Modelling & Software* **2021**, *140*, 105043. <https://doi.org/10.1016/j.envsoft.2021.105043>.
- ⁸ Hou, J.; van Dijk, A. I. J. M.; Beck, H. E. et al. Remotely Sensed Reservoir Water Storage Dynamics (1984–2015) and the Influence of Climate Variability and Management at a Global Scale. *Hydrology and Earth System Sciences* **2022**, *26*(14), 3785–3803. <https://doi.org/10.5194/hess-26-3785-2022>.
- ⁹ Hou, J.; Van Dijk, A. I. J. M.; Renzullo, L. J. et al. GloLakes: Water Storage Dynamics for 27 000 Lakes Globally from 1984 to Present Derived from Satellite Altimetry and Optical Imaging. *Earth System Science Data* **2024**, *16*(1), 201–218. <https://doi.org/10.5194/essd-16-201-2024>.
- ¹⁰ Global Runoff Data Centre (GRDC). *WMO Basins and Sub-Basins*; 3rd rev. ext. ed., Federal Institute of Hydrology (BfG): Koblenz, Germany, 2023.
- ¹¹ Müller Schmied, H.; Cáceres, D.; Eisner, S. et al. The Global Water Resources and Use Model WaterGAP v2.2d: Model Description and Evaluation. *Geoscientific Model Development* **2021**, *14*(2), 1037–1079. <https://doi.org/10.5194/gmd-14-1037-2021>.
- ¹² Müller Schmied, H.; Trautmann, T.; Ackermann, S. et al. The Global Water Resources and Use Model WaterGAP v2.2e: Description and Evaluation of Modifications and New Features. *Geoscientific Model Development Discussions* **2023** [preprint]. <https://doi.org/10.5194/gmd-2023-213>.
- ¹³ Yuan, X.; Ji, P.; Wang, L. et al. High-Resolution Land Surface Modeling of Hydrological Changes Over the Sanjiangyuan Region in the Eastern Tibetan Plateau: 1. Model Development and Evaluation. *Journal of Advances in Modeling Earth Systems* **2018**, *10*(11), 2806–2828. <https://doi.org/10.1029/2018MS001412>.
- ¹⁴ Samaniego, L.; Kumar, R.; Attinger, S. Multiscale Parameter Regionalization of a Grid-Based Hydrologic Model at the Mesoscale. *Water Resources Research* **2010**, *46*(5). <https://doi.org/10.1029/2008WR007327>.
- ¹⁵ Kumar, R.; Samaniego, L.; Attinger, S. Implications of Distributed Hydrologic Model Parameterization on Water Fluxes at Multiple Scales and Locations. *Water Resources Research* **2013**, *49*(1), 360–379. <https://doi.org/10.1029/2012WR012195>.
- ¹⁶ Samaniego, L.; Kaluza, M.; Kumar, R. et al. *Mesoscale Hydrologic Model*; Zenodo, 2019. <https://doi.org/10.5281/zenodo.3239055>.
- ¹⁷ Arheimer, B.; Pimentel, R.; Isberg, K. et al. Global Catchment Modelling Using World-Wide HYPE (WWH), Open Data, and Stepwise Parameter Estimation. *Hydrology and Earth System Sciences* **2020**, *24*(2), 535–559. <https://doi.org/10.5194/hess-24-535-2020>.
- ¹⁸ Murray, A. M.; Jørgensen, G. H.; Godiksen, P. N. et al. DHI-GHM: Real-Time and Forecasted Hydrology for the Entire Planet. *Journal of Hydrology* **2023**, *620*, 129431. <https://doi.org/10.1016/j.jhydrol.2023.129431>.
- ¹⁹ Hanazaki, R.; Yamazaki, D.; Yoshimura, K. Development of a Reservoir Flood Control Scheme for Global Flood Models. *Journal of Advances in Modeling Earth Systems* **2022**, *14*(3), e2021MS002944. <https://doi.org/10.1029/2021MS002944>.
- ²⁰ Yamazaki, D.; Kanae, S.; Kim, H. et al. A Physically Based Description of Floodplain Inundation Dynamics in a Global River Routing Model. *Water Resources Research* **2011**, *47*(4). <https://doi.org/10.1029/2010WR009726>.



- ²¹ Yoshimura, K.; Sakimura, T.; Oki, T. et al. Toward Flood Risk Prediction: A Statistical Approach Using a 29-Year River Discharge Simulation over Japan. *Hydrological Research Letters* **2008**, *2*, 22–26. <https://doi.org/10.3178/hrl.2.22>.
- ²² Ma, W.; Ishitsuka, Y.; Takeshima, A. et al. Applicability of a Nationwide Flood Forecasting System for Typhoon Hagibis 2019. *Scientific Reports* **2021**, *11* (1), 10213. <https://doi.org/10.1038/s41598-021-89522-8>.
- ²³ Alfieri, L.; Burek, P.; Dutra, E. et al. GloFAS – Global Ensemble Streamflow Forecasting and Flood Early Warning. *Hydrology and Earth System Sciences* **2013**, *17* (3), 1161–1175. <https://doi.org/10.5194/hess-17-1161-2013>.
- ²⁴ Grimaldi, S.; Salamon, P.; Disperati, J. et al. *GloFAS v4.0 Hydrological Reanalysis*. European Commission, Joint Research Centre (JRC), 2022 [Dataset]. <http://data.europa.eu/89h/f96b7a19-0133-4105-a879-0536991ca9c5>.
- ²⁵ van Verseveld, W. J.; Weerts, A. H.; Visser, M. et al. Wflow_sbm v0.6.1, a Spatially Distributed Hydrologic Model: from Global Data to Local Applications. *Geoscientific Model Development Discussions* **2022** [preprint]. <https://doi.org/10.5194/gmd-2022-182>.
- ²⁶ Imhoff, R.; Brauer, C.; van Heeringen, K.-J. et al. A Climatological Benchmark for Operational Radar Rainfall Bias Reduction. *Hydrology and Earth System Sciences* **2021**, *25* (7), 4061–4080. <https://doi.org/10.5194/hess-25-4061-2021>.
- ²⁷ Eilander, D.; van Verseveld, W.; Yamazaki, D. et al. A Hydrography Upscaling Method for Scale-Invariant Parametrization of Distributed Hydrological Models. *Hydrology and Earth System Sciences* **2021**, *25* (9), 5287–5313. <https://doi.org/10.5194/hess-25-5287-2021>.
- ²⁸ Hales, R. C.; Nelson, E. J.; Souffront, M. et al. Advancing Global Hydrologic Modeling with the GEOGloWS ECMWF Streamflow Service. *Journal of Flood Risk Management* **2022**, e12859. <https://doi.org/10.1111/jfr3.12859>.
- ²⁹ Belleflamme, A.; Goergen, K.; Wagner, N. et al. Hydrological Forecasting at Impact Scale: The Integrated ParFlow Hydrological Model at 0.6 Km for Climate Resilient Water Resource Management over Germany. *Frontiers in Water* **2023**, *5*. <https://doi.org/10.3389/frwa.2023.1183642>.
- ³⁰ Mudryk, L. R.; Elias Chereque, A.; Derksen, C. et al. *NOAA Arctic Report Card 2023: Terrestrial Snow Cover*; NOAA Technical Report OAR ARC; 23-03; National Oceanic and Atmospheric Administration (NOAA): 2023. <https://repository.library.noaa.gov/view/noaa/56613>.
- ³¹ Mudryk, L. R.; Elias Chereque, A.; Derksen, C. et al. Terrestrial Snow Cover [in “State of the Climate in 2023”]. *Bulletin of the American Meteorological Society* **2024**, *105* (8), S307–S310. <https://doi.org/10.1175/BAMS-D-24-0101.1>.
- ³² Biswas, N. K.; Hossain, F.; Bonnema, M. et al. Towards a Global Reservoir Assessment Tool for Predicting Hydrologic Impacts and Operating Patterns of Existing and Planned Reservoirs. *Environmental Modelling & Software* **2021**, *140*, 105043. <https://doi.org/10.1016/j.envsoft.2021.105043>.
- ³³ Hou, J.; van Dijk, A. I. J. M.; Beck, H. E. et al. Remotely Sensed Reservoir Water Storage Dynamics (1984–2015) and the Influence of Climate Variability and Management at a Global Scale. *Hydrology and Earth System Sciences* **2022**, *26* (14), 3785–3803. <https://doi.org/10.5194/hess-26-3785-2022>.
- ³⁴ Hou, J.; Van Dijk, A. I. J. M.; Renzullo, L. J. et al. GloLakes: Water Storage Dynamics for 27 000 Lakes Globally from 1984 to Present Derived from Satellite Altimetry and Optical Imaging. *Earth System Science Data* **2024**, *16* (1), 201–218. <https://doi.org/10.5194/essd-16-201-2024>.
- ³⁵ Landerer, F. W.; Flechtner, F. M.; Save, H. et al. Extending the Global Mass Change Data Record: GRACE Follow-On Instrument and Science Data Performance. *Geophysical Research Letters* **2020**, *47* (12), e2020GL088306. <https://doi.org/10.1029/2020GL088306>.
- ³⁶ Elmi, O.; Tourian, M. J.; Saemian, P. et al. Remote Sensing-Based Extension of GRDC Discharge Time Series – A Monthly Product with Uncertainty Estimates. *Scientific Data* **2024**, *11* (1), 240. <https://doi.org/10.1038/s41597-024-03078-6>.
- ³⁷ Boergens, E.; Güntner, A.; Dobslaw, H. et al. Quantifying the Central European Droughts in 2018 and 2019 With GRACE Follow-On. *Geophysical Research Letters* **2020**, *47* (14), e2020GL087285. <https://doi.org/10.1029/2020GL087285>.
- ³⁸ Belleflamme, A.; Goergen, K.; Wagner, N. et al. Hydrological Forecasting at Impact Scale: The Integrated ParFlow Hydrological Model at 0.6 Km for Climate Resilient Water Resource Management over Germany. *Frontiers in Water* **2023**, *5*. <https://doi.org/10.3389/frwa.2023.1183642>.
- ³⁹ Mudryk, L. R.; Elias Chereque, A.; Derksen, C. et al. *NOAA Arctic Report Card 2023: Terrestrial Snow Cover*; NOAA Technical Report OAR ARC; 23-03; National Oceanic and Atmospheric Administration (NOAA): 2023. <https://repository.library.noaa.gov/view/noaa/56613>.



- ⁴⁰ Mudryk, L. R.; Elias Chereque, A.; Derksen, C. et al. Terrestrial Snow Cover [in “State of the Climate in 2023”]. *Bulletin of the American Meteorological Society* **2024**, *105* (8), S307–S310. <https://doi.org/10.1175/BAMS-D-24-0101.1>.
- ⁴¹ Ma, W.; Ishitsuka, Y.; Takeshima, A. et al. Applicability of a Nationwide Flood Forecasting System for Typhoon Hagibis 2019. *Scientific Reports* **2021**, *11* (1), 10213. <https://doi.org/10.1038/s41598-021-89522-8>.
- ⁴² Yoshimura, K.; Sakimura, T.; Oki, T. et al. Toward Flood Risk Prediction: A Statistical Approach Using a 29-Year River Discharge Simulation over Japan. *Hydrological Research Letters* **2008**, *2*, 22–26. <https://doi.org/10.3178/hrl.2.22>.
- ⁴³ EM-DAT, CRED/UCLouvain, Brussels, Belgium. <http://www.emdat.be>.
- ⁴⁴ Arheimer, B.; Pimentel, R.; Isberg, K. et al. Global Catchment Modelling Using World-Wide HYPE (WWH), Open Data, and Stepwise Parameter Estimation. *Hydrology and Earth System Sciences* **2020**, *24* (2), 535–559. <https://doi.org/10.5194/hess-24-535-2020>.
- ⁴⁵ Müller Schmied, H.; Trautmann, T.; Ackermann, S. et al. The Global Water Resources and Use Model WaterGAP v2.2e: Description and Evaluation of Modifications and New Features. *Geoscientific Model Development Discussions* **2023** [preprint]. <https://doi.org/10.5194/gmd-2023-213>.
- ⁴⁶ Yuan, X.; Ji, P.; Wang, L. et al. High-Resolution Land Surface Modeling of Hydrological Changes Over the Sanjiangyuan Region in the Eastern Tibetan Plateau: 1. Model Development and Evaluation. *Journal of Advances in Modeling Earth Systems* **2018**, *10* (11), 2806–2828. <https://doi.org/10.1029/2018MS001412>.
- ⁴⁷ Samaniego, L.; Kumar, R.; Attinger, S. Multiscale Parameter Regionalization of a Grid-Based Hydrologic Model at the Mesoscale. *Water Resources Research* **2010**, *46* (5). <https://doi.org/10.1029/2008WR007327>.
- ⁴⁸ Kumar, R.; Samaniego, L.; Attinger, S. Implications of Distributed Hydrologic Model Parameterization on Water Fluxes at Multiple Scales and Locations. *Water Resources Research* **2013**, *49* (1), 360–379. <https://doi.org/10.1029/2012WR012195>.
- ⁴⁹ Samaniego, L.; Kaluza, M.; Kumar, R. et al. *Mesoscale Hydrologic Model*; Zenodo, 2019. <https://doi.org/10.5281/zenodo.3239055>.
- ⁵⁰ Murray, A. M.; Jørgensen, G. H.; Godiksen, P. N. et al. DHI-GHM: Real-Time and Forecasted Hydrology for the Entire Planet. *Journal of Hydrology* **2023**, *620*, 129431. <https://doi.org/10.1016/j.jhydrol.2023.129431>.
- ⁵¹ Hanazaki, R.; Yamazaki, D.; Yoshimura, K. Development of a Reservoir Flood Control Scheme for Global Flood Models. *Journal of Advances in Modeling Earth Systems* **2022**, *14* (3), e2021MS002944. <https://doi.org/10.1029/2021MS002944>.
- ⁵² Yamazaki, D.; Kanae, S.; Kim, H. et al. A Physically Based Description of Floodplain Inundation Dynamics in a Global River Routing Model. *Water Resources Research* **2011**, *47* (4). <https://doi.org/10.1029/2010WR009726>.
- ⁵³ Ma, W.; Ishitsuka, Y.; Takeshima, A. et al. Applicability of a Nationwide Flood Forecasting System for Typhoon Hagibis 2019. *Scientific Reports* **2021**, *11* (1), 10213. <https://doi.org/10.1038/s41598-021-89522-8>.
- ⁵⁴ Yoshimura, K.; Sakimura, T.; Oki, T. et al. Toward Flood Risk Prediction: A Statistical Approach Using a 29-Year River Discharge Simulation over Japan. *Hydrological Research Letters* **2008**, *2*, 22–26. <https://doi.org/10.3178/hrl.2.22>.
- ⁵⁵ Alfieri, L.; Burek, P.; Dutra, E. et al. GloFAS – Global Ensemble Streamflow Forecasting and Flood Early Warning. *Hydrology and Earth System Sciences* **2013**, *17* (3), 1161–1175. <https://doi.org/10.5194/hess-17-1161-2013>.
- ⁵⁶ Grimaldi, S.; Salamon, P.; Disperati, J. et al. *GloFAS v4.0 Hydrological Reanalysis*. European Commission, Joint Research Centre (JRC), 2022 [Dataset]. <http://data.europa.eu/89h/f96b7a19-0133-4105-a879-0536991ca9c5>.
- ⁵⁷ van Verseveld, W. J.; Weerts, A. H.; Visser, M. et al. Wflow_sbm v0.6.1, a Spatially Distributed Hydrologic Model: from Global Data to Local Applications. *Geoscientific Model Development Discussions* **2022** [preprint]. <https://doi.org/10.5194/gmd-2022-182>.
- ⁵⁸ Imhoff, R.; Brauer, C.; van Heeringen, K.-J. et al. A Climatological Benchmark for Operational Radar Rainfall Bias Reduction. *Hydrology and Earth System Sciences* **2021**, *25* (7), 4061–4080. <https://doi.org/10.5194/hess-25-4061-2021>.
- ⁵⁹ Eilander, D.; van Verseveld, W.; Yamazaki, D. et al. A Hydrography Upscaling Method for Scale-Invariant Parametrization of Distributed Hydrological Models. *Hydrology and Earth System Sciences* **2021**, *25* (9), 5287–5313. <https://doi.org/10.5194/hess-25-5287-2021>.
- ⁶⁰ Hales, R. C.; Nelson, E. J.; Souffront, M. et al. Advancing Global Hydrologic Modeling with the GEOGloWS ECMWF Streamflow Service. *Journal of Flood Risk Management* **2022**, e12859. <https://doi.org/10.1111/jfr3.12859>.



- ⁶¹ Hersbach, H.; Bell, B.; Berrisford, P. et al. The ERA5 Global Reanalysis. *Quarterly Journal of the Royal Meteorological Society* **2020**, *146* (730), 1999–2049. <https://doi.org/10.1002/qj.3803>.
- ⁶² Berg, P.; Almén, F.; Bozhinova, D. HydroGFD3.0 (Hydrological Global Forcing Data): A 25 Km Global Precipitation and Temperature Data Set Updated in near-Real Time. *Earth System Science Data* **2021**, *13* (4), 1531–1545. <https://doi.org/10.5194/essd-13-1531-2021>.
- ⁶³ Kobayashi, S.; Ota, Y.; Harada, Y. et al. The JRA-55 Reanalysis: General Specifications and Basic Characteristics. *Journal of the Meteorological Society of Japan. Ser. II* **2015**, *93* (1), 5–48. <https://doi.org/10.2151/jmsj.2015-001>.
- ⁶⁴ Global Runoff Data Centre (GRDC). *WMO Basins and Sub-Basins*; 3rd rev. ext. ed., Federal Institute of Hydrology (BfG): Koblenz, Germany, 2023.
- ⁶⁵ Elmi, O.; Tourian, M. J.; Saemian, P. et al. Remote Sensing-Based Extension of GRDC Discharge Time Series - A Monthly Product with Uncertainty Estimates. *Scientific Data* **2024**, *11* (1), 240. <https://doi.org/10.1038/s41597-024-03078-6>.
- ⁶⁶ van Verseveld, W. J.; Weerts, A. H.; Visser, M. et al. Wflow_sbm v0.6.1, a Spatially Distributed Hydrologic Model: from Global Data to Local Applications. *Geoscientific Model Development Discussions* **2022** [preprint]. <https://doi.org/10.5194/gmd-2022-182>.
- ⁶⁷ Hanazaki, R.; Yamazaki, D.; Yoshimura, K. Development of a Reservoir Flood Control Scheme for Global Flood Models. *Journal of Advances in Modeling Earth Systems* **2022**, *14* (3), e2021MS002944. <https://doi.org/10.1029/2021MS002944>.
- ⁶⁸ Yamazaki, D.; Kanae, S.; Kim, H. et al. A Physically Based Description of Floodplain Inundation Dynamics in a Global River Routing Model. *Water Resources Research* **2011**, *47* (4). <https://doi.org/10.1029/2010WR009726>.
- ⁶⁹ Arheimer, B.; Pimentel, R.; Isberg, K. et al. Global Catchment Modelling Using World-Wide HYPE (WWH), Open Data, and Stepwise Parameter Estimation. *Hydrology and Earth System Sciences* **2020**, *24* (2), 535–559. <https://doi.org/10.5194/hess-24-535-2020>.
- ⁷⁰ Lehner, B.; Reidy Liermann, C.; Revenga, C. et al. *Global Reservoir and Dam Database, Version 1 (GRanDv1): Dams, Revision 01*; NASA Socioeconomic Data and Applications Center (SEDAC), 2011. <https://doi.org/10.7927/H4N877QK>.
- ⁷¹ van Verseveld, W. J.; Weerts, A. H.; Visser, M. et al. Wflow_sbm v0.6.1, a Spatially Distributed Hydrologic Model: from Global Data to Local Applications. *Geoscientific Model Development Discussions* **2022** [preprint]. <https://doi.org/10.5194/gmd-2022-182>.
- ⁷² Yamazaki, D.; Kanae, S.; Kim, H. et al. A Physically Based Description of Floodplain Inundation Dynamics in a Global River Routing Model. *Water Resources Research* **2011**, *47* (4). <https://doi.org/10.1029/2010WR009726>.
- ⁷³ Hanazaki, R.; Yamazaki, D.; Yoshimura, K. Development of a Reservoir Flood Control Scheme for Global Flood Models. *Journal of Advances in Modeling Earth Systems* **2022**, *14* (3), e2021MS002944. <https://doi.org/10.1029/2021MS002944>.
- ⁷⁴ Lehner, B.; Reidy Liermann, C.; Revenga, C. et al. *Global Reservoir and Dam Database, Version 1 (GRanDv1): Dams, Revision 01*; NASA Socioeconomic Data and Applications Center (SEDAC), 2011. <https://doi.org/10.7927/H4N877QK>.
- ⁷⁵ Hanazaki, R.; Yamazaki, D.; Yoshimura, K. Development of a Reservoir Flood Control Scheme for Global Flood Models. *Journal of Advances in Modeling Earth Systems* **2022**, *14* (3), e2021MS002944. <https://doi.org/10.1029/2021MS002944>.
- ⁷⁶ Yamazaki, D.; Ikeshima, D.; Sosa, J. et al. MERIT Hydro: A High-Resolution Global Hydrography Map Based on Latest Topography Dataset. *Water Resources Research* **2019**, *55* (6), 5053–5073. <https://doi.org/10.1029/2019WR024873>.
- ⁷⁷ Muñoz Sabater, J. *ERA5-Land Hourly Data from 1950 to Present*; Copernicus Climate Change Service (C3S) Climate Data Store (CDS), 2019. <https://doi.org/10.24381/cds.e2161bac>.
- ⁷⁸ Hanazaki, R.; Yamazaki, D.; Yoshimura, K. Development of a Reservoir Flood Control Scheme for Global Flood Models. *Journal of Advances in Modeling Earth Systems* **2022**, *14* (3), e2021MS002944. <https://doi.org/10.1029/2021MS002944>.
- ⁷⁹ Nash, J. E., & Sutcliffe, J. V. River flow forecasting through conceptual models Part I—A discussion of principles. *Journal of Hydrology* **1970**, *10* (3), 282–290. [https://doi.org/10.1016/0022-1694\(70\)90255-6](https://doi.org/10.1016/0022-1694(70)90255-6).
- ⁸⁰ Hanazaki, R.; Yamazaki, D.; Yoshimura, K. Development of a Reservoir Flood Control Scheme for Global Flood Models. *Journal of Advances in Modeling Earth Systems* **2022**, *14* (3), e2021MS002944. <https://doi.org/10.1029/2021MS002944>.
- ⁸¹ Arheimer, B.; Pimentel, R.; Isberg, K. et al. Global Catchment Modelling Using World-Wide HYPE (WWH), Open Data, and Stepwise Parameter Estimation. *Hydrology and Earth System Sciences* **2020**, *24* (2), 535–559. <https://doi.org/10.5194/hess-24-535-2020>.



- ⁸² Biswas, N. K.; Hossain, F.; Bonnema, M. et al. Towards a Global Reservoir Assessment Tool for Predicting Hydrologic Impacts and Operating Patterns of Existing and Planned Reservoirs. *Environmental Modelling & Software* **2021**, *140*, 105043. <https://doi.org/10.1016/j.envsoft.2021.105043>.
- ⁸³ Lehner, B.; Döll, P. Development and Validation of a Global Database of Lakes, Reservoirs and Wetlands. *Journal of Hydrology* **2004**, *296*(1), 1–22. <https://doi.org/10.1016/j.jhydrol.2004.03.028>.
- ⁸⁴ Lehner, B.; Reidy Liermann, C.; Revenga, C. et al. *Global Reservoir and Dam Database, Version 1 (GRanDv1): Dams, Revision 01*; NASA Socioeconomic Data and Applications Center (SEDAC), 2011. <https://doi.org/10.7927/H4N877QK>.
- ⁸⁵ Messenger, M. L.; Lehner, B.; Grill, G. et al. Estimating the Volume and Age of Water Stored in Global Lakes Using a Geo-Statistical Approach. *Nature Communications* **2016**, *7*(1), 13603. <https://doi.org/10.1038/ncomms13603>.
- ⁸⁶ Donchyts, G.; Winsemius, H.; Baart, F. et al. High-Resolution Surface Water Dynamics in Earth's Small and Medium-Sized Reservoirs. *Scientific Reports* **2022**, *12*(1), 13776. <https://doi.org/10.1038/s41598-022-17074-6>.
- ⁸⁷ Biswas, N. K.; Hossain, F.; Bonnema, M. et al. Towards a Global Reservoir Assessment Tool for Predicting Hydrologic Impacts and Operating Patterns of Existing and Planned Reservoirs. *Environmental Modelling & Software* **2021**, *140*, 105043. <https://doi.org/10.1016/j.envsoft.2021.105043>.
- ⁸⁸ Donchyts, G.; Winsemius, H.; Baart, F. et al. High-Resolution Surface Water Dynamics in Earth's Small and Medium-Sized Reservoirs. *Scientific Reports* **2022**, *12*(1), 13776. <https://doi.org/10.1038/s41598-022-17074-6>.
- ⁸⁹ Hou, J.; van Dijk, A. I. J. M.; Beck, H. E. et al. Remotely Sensed Reservoir Water Storage Dynamics (1984–2015) and the Influence of Climate Variability and Management at a Global Scale. *Hydrology and Earth System Sciences* **2022**, *26*(14), 3785–3803. <https://doi.org/10.5194/hess-26-3785-2022>.
- ⁹⁰ Hou, J.; Van Dijk, A. I. J. M.; Renzullo, L. J. et al. GloLakes: Water Storage Dynamics for 27 000 Lakes Globally from 1984 to Present Derived from Satellite Altimetry and Optical Imaging. *Earth System Science Data* **2024**, *16*(1), 201–218. <https://doi.org/10.5194/essd-16-201-2024>.
- ⁹¹ Lehner, B.; Verdin, K.; Jarvis, A. New Global Hydrography Derived from Spaceborne Elevation Data. *Eos, Transactions American Geophysical Union* **2008**, *89*(10), 93–94. <https://doi.org/10.1029/2008EO100001>.
- ⁹² Decharme, B.; Barbu, A. *Crocus-ERA5 Daily Snow Product over the Northern Hemisphere at 0.25° Resolution*; version 2023; Zenodo, 2024. <https://doi.org/10.5281/zenodo.10943718>.
- ⁹³ Luoju, K.; Moisander, M.; Pulliainen, J. et al. *ESA Snow Climate Change Initiative (Snow_cci): Snow Water Equivalent (SWE) Level 3C Daily Global Climate Research Data Package (CRDP) (1979–2020), version 2.0*; NERC EDS Centre for Environmental Data Analysis, 2022. <https://doi.org/10.5285/4647cc9ad3c044439d6c643208d3c494>.
- ⁹⁴ Muñoz Sabater, J. *ERA5-Land Hourly Data from 1950 to Present*; Copernicus Climate Change Service (C3S) Climate Data Store (CDS), 2019 <https://doi.org/10.24381/cds.e2161bac>.
- ⁹⁵ Decharme, B.; Barbu, A. *Crocus-ERA5 Daily Snow Product over the Northern Hemisphere at 0.25° Resolution*; version 2023; Zenodo, 2024. <https://doi.org/10.5281/zenodo.10943718>.
- ⁹⁶ Mudryk, L. R.; Elias Chereque, A.; Derksen, C. et al. *NOAA Arctic Report Card 2023: Terrestrial Snow Cover*; NOAA Technical Report OAR ARC; 23-03; National Oceanic and Atmospheric Administration (NOAA): 2023. <https://repository.library.noaa.gov/view/noaa/56613>.
- ⁹⁷ Mudryk, L. R.; Elias Chereque, A.; Derksen, C. et al. Terrestrial Snow Cover [in “State of the Climate in 2023”]. *Bulletin of the American Meteorological Society* **2024**, *105*(8), S307–S310. <https://doi.org/10.1175/BAMS-D-24-0101.1>.
- ⁹⁸ Tapley, B. D.; Watkins, M. M.; Flechtner, F. et al. Contributions of GRACE to Understanding Climate Change. *Nature Climate Change* **2019**, *9*(5), 358–369. <https://doi.org/10.1038/s41558-019-0456-2>.
- ⁹⁹ Landerer, F. W.; Flechtner, F. M.; Save, H. et al. Extending the Global Mass Change Data Record: GRACE Follow-On Instrument and Science Data Performance. *Geophysical Research Letters* **2020**, *47*(12), e2020GL088306. <https://doi.org/10.1029/2020GL088306>.

For more information, please contact:

World Meteorological Organization

7 bis, avenue de la Paix – P.O. Box 2300 – CH 1211 Geneva 2 – Switzerland

Strategic Communications Office

Tel: +41 (0) 22 730 83 14 – Fax: +41 (0) 22 730 80 27

Email: communications@wmo.int

<https://wmo.int/>